International Journal of Engineering (IJE)

ISSN : 1985-2312

VOLUME 4, ISSUE 1

PUBLICATION FREQUENCY: 6 ISSUES PER YEAR

International Journal of Engineering (IJE)

Volume 4, Issue 1, 2010

Edited By
Computer Science Journals
www.cscjournals.org

Editor in Chief Dr. Kouroush Jenab

International Journal of Engineering (IJE)

Book: 2010 Volume 4, Issue 1

Publishing Date: 31-03-2010

Proceedings

ISSN (Online): 1985-2312

IJE Journal is a part of CSC Publishers

http://www.cscjournals.org

Published in Malaysia

Typesetting: Camera-ready by author, data conversation by CSC Publishing Services – CSC Journals, Malaysia

CSC Publishers

Editorial Preface

This is the first issue of volume fourth of International Journal of Engineering (IJE). The Journal is published bi-monthly, with papers being peer reviewed to high international standards. The International Journal of Engineering is not limited to a specific aspect of engineering but it is devoted to the publication of high quality papers on all division of engineering in general. IJE intends to disseminate knowledge in the various disciplines of the engineering field from theoretical, practical and analytical research to physical implications and theoretical or quantitative discussion intended for academic and industrial progress. In order to position IJE as one of the good journal on engineering sciences, a group of highly valuable scholars are serving on the editorial board. The International Editorial Board ensures that significant developments in engineering from around the world are reflected in the Journal. Some important topics covers by journal are nuclear engineering, mechanical engineering, computer engineering, electrical engineering, civil & structural engineering etc.

The coverage of the journal includes all new theoretical and experimental findings in the fields of engineering which enhance the knowledge of scientist, industrials, researchers and all those persons who are coupled with engineering field. IJE objective is to publish articles that are not only technically proficient but also contains information and ideas of fresh interest for International readership. IJE aims to handle submissions courteously and promptly. IJE objectives are to promote and extend the use of all methods in the principal disciplines of Engineering.

IJE editors understand that how much it is important for authors and researchers to have their work published with a minimum delay after submission of their papers. They also strongly believe that the direct communication between the editors and authors are important for the welfare, quality and wellbeing of the Journal and its readers. Therefore, all activities from paper submission to paper publication are controlled through electronic systems that include electronic submission, editorial panel and review system that ensures rapid decision with least delays in the publication processes.

To build its international reputation, we are disseminating the publication information through Google Books, Google Scholar, Directory of Open Access Journals (DOAJ), Open J Gate, ScientificCommons, Docstoc and many more. Our International Editors are working on establishing ISI listing and a good impact factor for IJE. We would like to remind you that the success of our journal depends directly on the number of quality articles submitted for review. Accordingly, we would like to request your participation by submitting quality manuscripts for review and encouraging your colleagues to submit quality manuscripts for review. One of the great benefits we can

provide to our prospective authors is the mentoring nature of our review process. IJE provides authors with high quality, helpful reviews that are shaped to assist authors in improving their manuscripts.

Editorial Board Members
International Journal of Engineering (IJE)

Editorial Board

Editor-in-Chief (EiC)

Associate Editors (AEiCs)

Editorial Board Members (EBMs)

Table of Contents

Volume 4, Issue 1, March 2010.

Pages

A Novel Topology Of Delta Modulation Technique For Improving The Power Factor Of Ac-Dc Converters

Walid Emar Walidemar@yahoo.com
Faculty of Engineering/Electrical Dept./Power electronics and Control, Isra University
Amman, 11622, Jordan

Issam TTrad Issam_161@yahoo.com
Faculty of Engineering/Electrical Dept./Communication
Isra University
Amman, 11622, Jordan

Rateb Al-Issa Ratebissa@yahoo.com
Faculty of Engineering/Electrical Dept./Mechatronics
Al-Balqa Applied University
Amman, Jordan

Abstract

This work presents a new topology of delta modulation technique. This kind of modulation technique is usually used to improve the power factor of Pulse Width Modulation (PWM) converters used for supplying A.C. drives. Many new topologies have been presented trying to obtain a cost-effective solution to reduce the input current harmonic content and to make it sinusoidal and in phase with the input voltage of AC-DC converters. Each one of them has its application range due to the inherent characteristics of the topology (See [2-3]).

Obviously, not every converter is useful for the same application. Hence, this paper tries to show the most appropriate topology of different variants of modulation technique used for power factor correction. This technique which is used to generate the PWM control signals for the main devices of the PWM converter has the advantage of yielding instantaneous current control, resulting in a fast response [3], [4]. However, the switching frequency is not constant and varies over a wide range during each half-cycle of the A.C. input voltage. Furthermore, the frequency is also sensitive to the values of the circuit components, which is also addressed in this paper. This new delta modulation technique topology proves to give great stability performance over other variants of delta modulation or other modulation techniques.

Keywords: AC-DC Converter, Delta Modulation Technique (DMT), New Topology, Power Factor (PF), Simulation and Modulation.

1. INTRODUCTION

It is well known that the input voltage and current waveforms of ideal AC-DC converters are sinusoidal and in phase. However, the current waveforms of practical AC-DC converters are non-sinusoidal and contain certain harmonics. As a result of that, the phase shift between the input current fundamental component and the voltage of AC-DC converter is increased. The power factor (**PF**) which depends on the delay angle of AC-DC converter, the phase shift between the input current and voltage and the circuit component are then reduced [8]. With the aid of modern control technique and the availability of high speed semiconductor devices, the input current can be made sinusoidal and in phase with the input voltage, thereby having an input power factor of approximate unity.

Delta modulation, also known as ripple controller control, maintains the AC-DC converter input current within a defined window above and below a reference sine wave. The greatest benefits of delta control are that it offers fast load transient response and eliminates the need for feedback-loop compensation. The other well-known characteristic is the varying operating frequency.

However, the regulation inaccuracy issue of the delta controlled converter is almost unknown to engineers. Until now, research on delta controllers has mainly focused on transient analysis and transient modeling [1-3]. The first analysis of accuracy was performed on a current mode delta controller specifically designed to power microprocessors [5]. However, the regulation accuracy of the more widely used current-mode delta-controlled controllers is still unknown.

Furthermore, bang-bang technique used in [2] for the same purpose as DMT suffers from certain drawbacks. For example, it does not enable a simple realization of the shifted switching of the bridge converters that are connected in parallel. The shifted switching evidently reduces the ripple of the current derived from the trolley. It also requires a very fast microprocessor since it needs a very short current sampling period.

In this paper a new topology with new algorithms for generating the PWM control signals for the transistors of the converter is introduced to delta modulation technique (DMT). These new algorithms are solved by using high frequency semiconductor devices and suitable control circuitries. The result of using such algorithms is not only improved performance of the converter, and optimal waveform of the current derived from the trolley, but also the shifted switching of the parallel connected converters will be no longer needed [3], [7].

The remainder of the paper is organized as follows: Section II presents the principle of operation and an overview of the algorithms used for switching the transistors of the converter. Different logic algorithms and some simulation obtained as a result of using these algorithms for delta modulation is shown in Section III. Finally, Section IV gives the conclusions to the paper.

2. PRINCIPLE OF OPERATION OF DMT

Figure 1 shows a unity PF circuit that combines a full bridge AC-DC converter and a full bridge voltage inverter (frequency converter). The control circuits of AC-DC converter have two main functions:

- Ensuring a unity PF (sinusoidal current which is in phase with the input voltage).
- Ensuring a constant voltage U_d across the capacitor

The first function 1 can be easily realized, as the boundary values of the hysteresis band I_{w2} and I_{w1} are generated such that the 1^{st} harmonic component of the current derived from the trolley is in phase with the voltage, as will be shown later in the paper. The switching transistors change their state as soon as current I_{sa} reaches the reference boundary value of the hysteresis band.

The second function is obtained by using a voltage controller R_v of voltage U_d which generates a suitable value for the reference current I_{ref} that is derived from the trolley (during motoring regime $I_{ref}>0$, and during braking regime $I_{ref}<0$). From the simulation obtained in the next sections it is clearly evident that there is a certain relationship between the amplitude of current I_a, current I_d, current I_c and consequently with voltage U_d at the output.

The voltage controller R_v regulates the mean value of voltage U_d which is always estimated at the instant of sampling of R_v. With respect to the required current waveform it is good to have I_w constant during each halve cycle of the required current.

This delta method of control keeps the input current I_{sa} within the window hysteresis band around the reference current I_{ref} which leads the sinusoidal value of this current I_a to be in phase with the sinusoidal voltage U_a and without any dc offset. To obtain a sinusoidal current the sampling of the controller must be synchronized with the current waveform and the sampling period must be $TT = 0.01$. A new value of I_{ref} must be estimated exactly at the zero-crossing of current I_a.

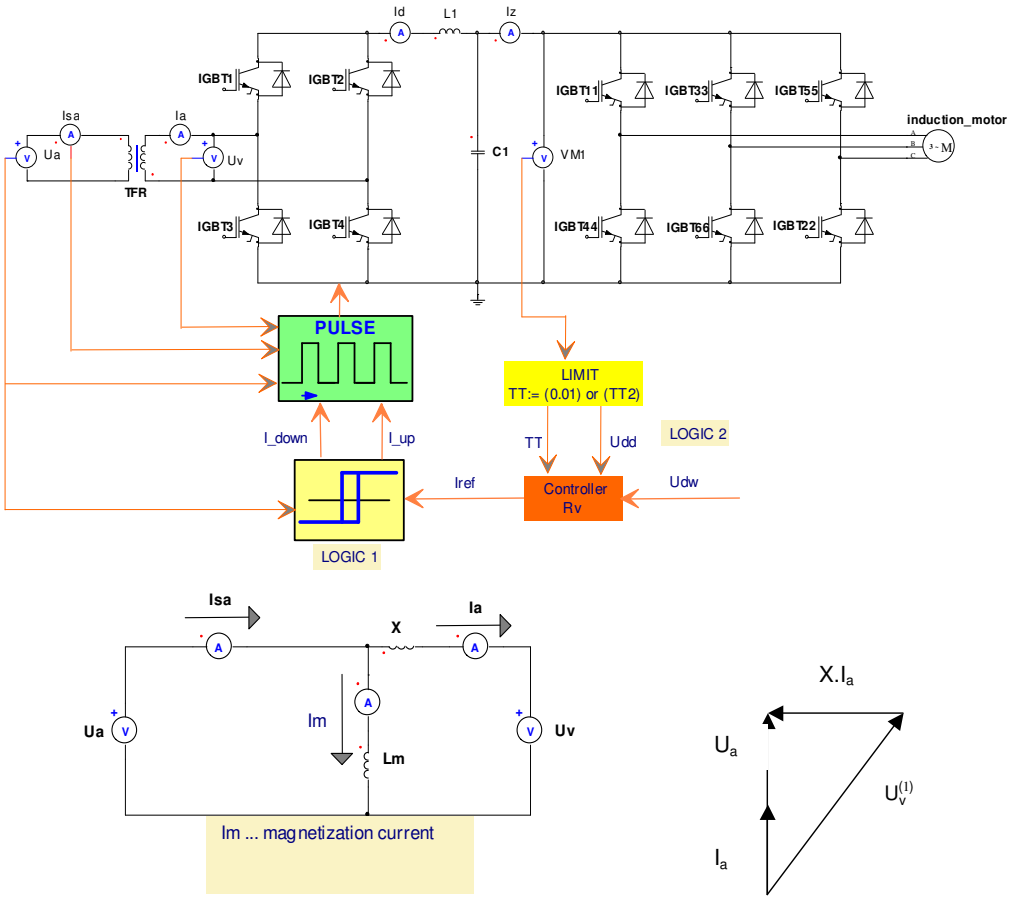

FIGURE 1: FREQUENCY CONVERTER CIRCUIT ARRANGEMENT FOR UNITY PF

This conclusion is based on the assumptions that filter L_1, C_1 at the output of the AC - DC converter is not added into the dc circuit and that all components used are ideal. However, in practical applications, these assumptions have certain types of error. Output voltage ripple also includes output capacitor C_1-caused ripple and L_1-caused ripple. And all components used are not ideal, so there will be delay in the whole control loop. Given these realities, the current waveform I_d then includes a clear harmonic component of frequency $f = 100\,Hz$. This component increases the ripple of current I_d and voltage U_d.

When the controller sampling period is $TT = 0.01s$, then the output of the controller under steady state conditions I_{ref} is purely constant. The sampling period TT of R_v may cause a time delay in the voltage control circuit. Therefore, it is necessary to reduce TT during transients. This therefore will result in a staircase waveform of the current but the dynamic properties of the voltage control loop are improved substantially.

Figure (1) shows clearly how the voltage and current derived from the trolley are measured. It is therefore evident that voltage U_a must be measured at the primary side of the transformer. The current on the other hand, may be measured at the secondary side since current I_a may be obtained as the average value of current I_{sa}.

3. LOGIC 1 USED FOR SWITCHING OF MAIN TRANSISTORS

Figure 2 shows the transistor rectifier circuit with the PWM control signal algorithm of the buck regulator circuit which may be connected at the output of the rectifier. This buck regulator is not considered in this paper. Logic1 demonstrates the algorithms used in delta modulation for generating PWM gating signals for the main transistors of AC-DC converter. The switch state of AC-DC converter is in general determined by comparing U_v with U_0, where U_0 is an arbitrary voltage determined as follows: $0 < U_0 < (U_d)\min$. Around the zero-crossing of voltage U_a, voltages $+U_d$, $-U_d$ are applied alternatively at the ac input terminals of AC-DC converter.

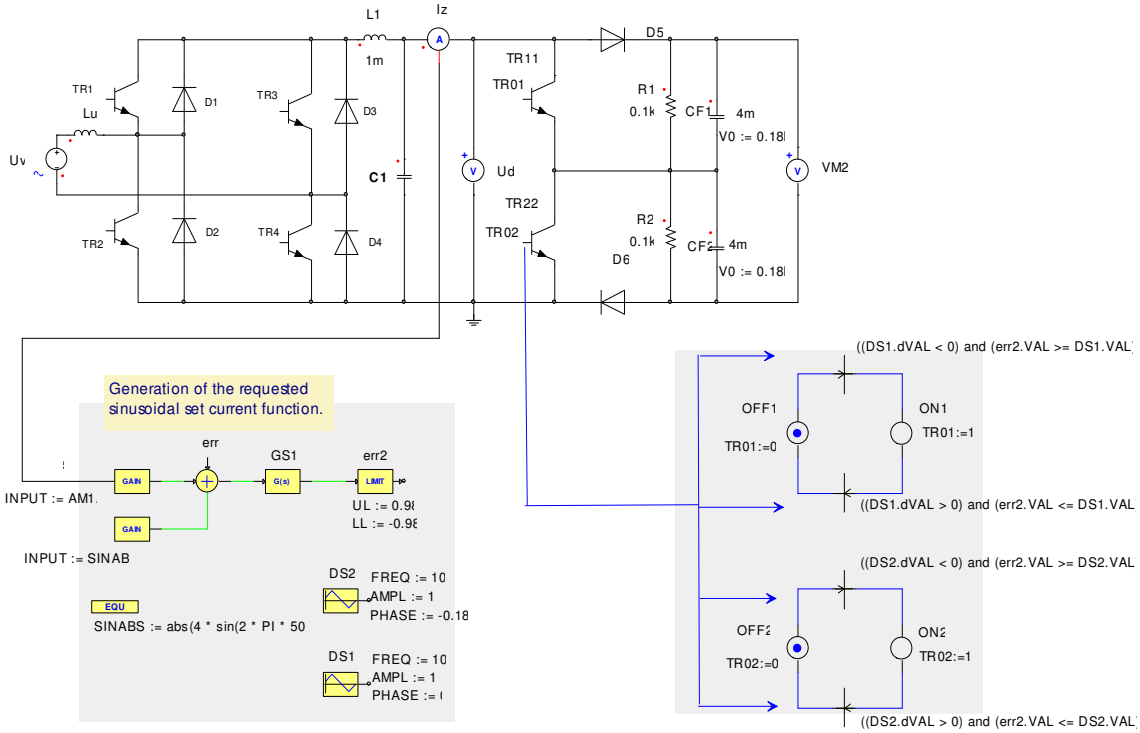

Figure 2: Rectifier circuit with control algorithm of the buck regulator used at the D.C. side of the rectifier

3.1. First variant of Logic 1

The simulation of the rectifier circuit is carried out under the following conditions:

- $I_{sa} < i_{\_down} \ldots U_v = 0$
- $I_{sa} > i_{\_up} \ldots U_v = U_d$
- $i_{\_down} < I_{sa} < i_{\_up}$ … hysteresis effect
- U_0 … arbitrary voltage ($0 < U_0 < U_{d(\min)}$), the switching state of the converter is determined by comparing U_v with U_o.

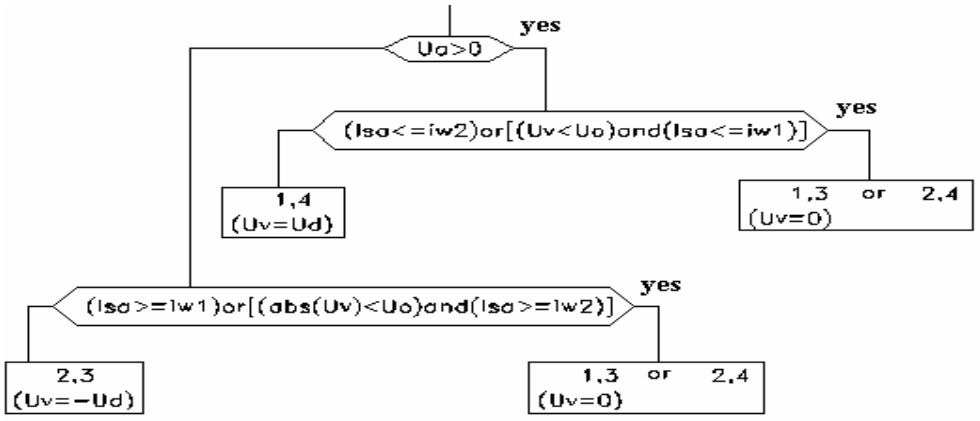

Figure 2a: Variant 1 of Logic 1

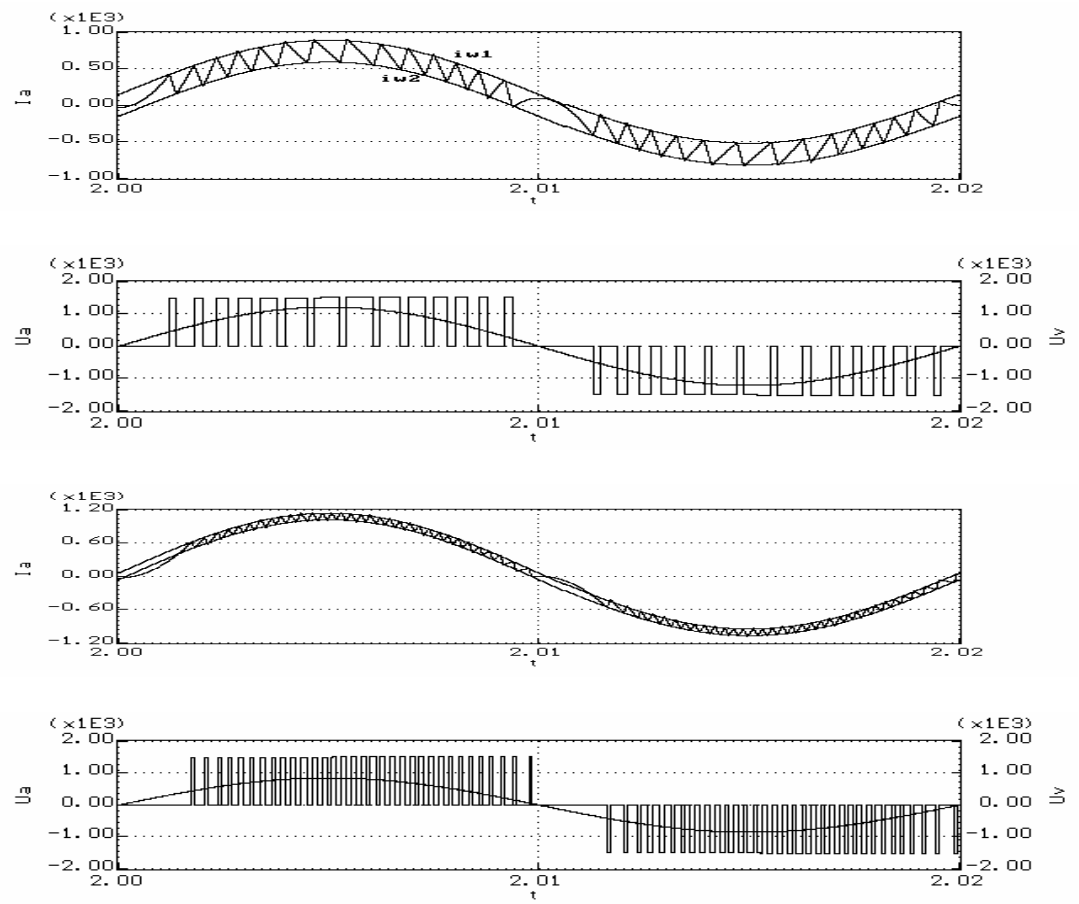

$$\Delta I = 60A\text{, } U_a = 70\%\ of\ U_{an}$$

Figure 2b: Simulation results of variant 1

Note: Concerning this variant of Logic 1, as it is seen of the above simulation, current I_a leaves the window limits around the zero-crossing of U_a which adds a certain drawback to this variant. Current I_a also increases very slowly when U_a is so small.

3.2. Second variant of Logic 1

To force current I_a to stay within the given hysteresis window limits I_{w1}, I_{w2}, then in accordance with the required current, voltage U_d must be applied instead of a zero voltage across the a.c. terminals of the converter. The algorithm with the results obtained is illustrated in figure 3 shown below.

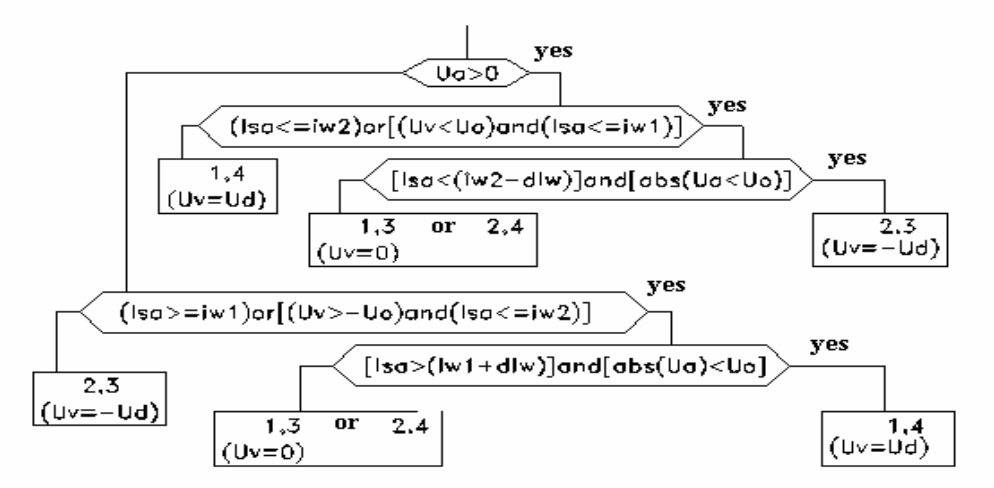

dI_w … tolerance current ripple

U_0 … arbitrary voltage ($0<U_0<(U_d)_{\min}$) (comparing U_v with U_0 determines the switching state of the converter)

Figure 3a: Variant 2 of Logic 1

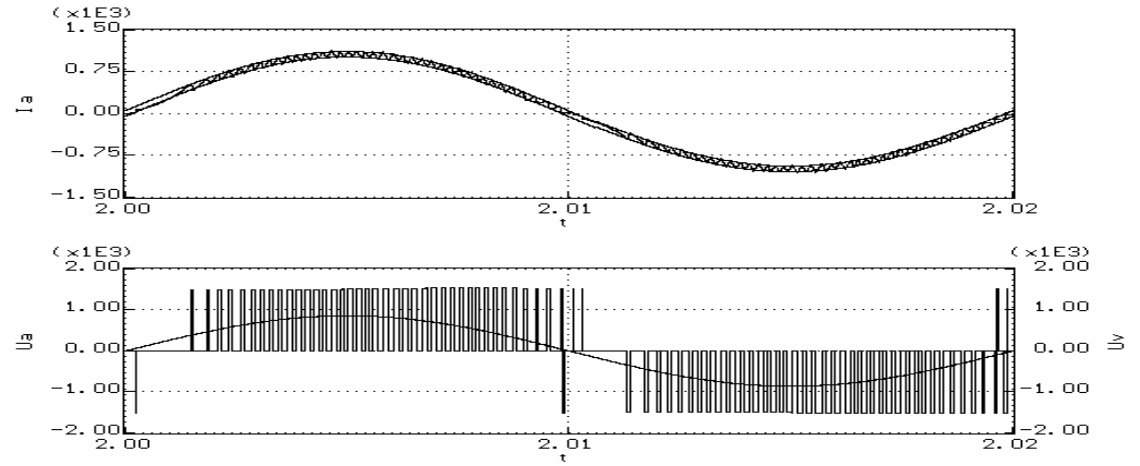

Figure 3b: simulation results of variant 2

3.3. Third variant of Logic 1

To improve the voltage waveform around zero-crossing shown in figure 2b, voltages $+U_d$ and $-U_d$ are applied alternatively at the a.c. terminals of the converters. Variant 3 of Logic 1 and the simulation results of this variant are shown in figure 4.

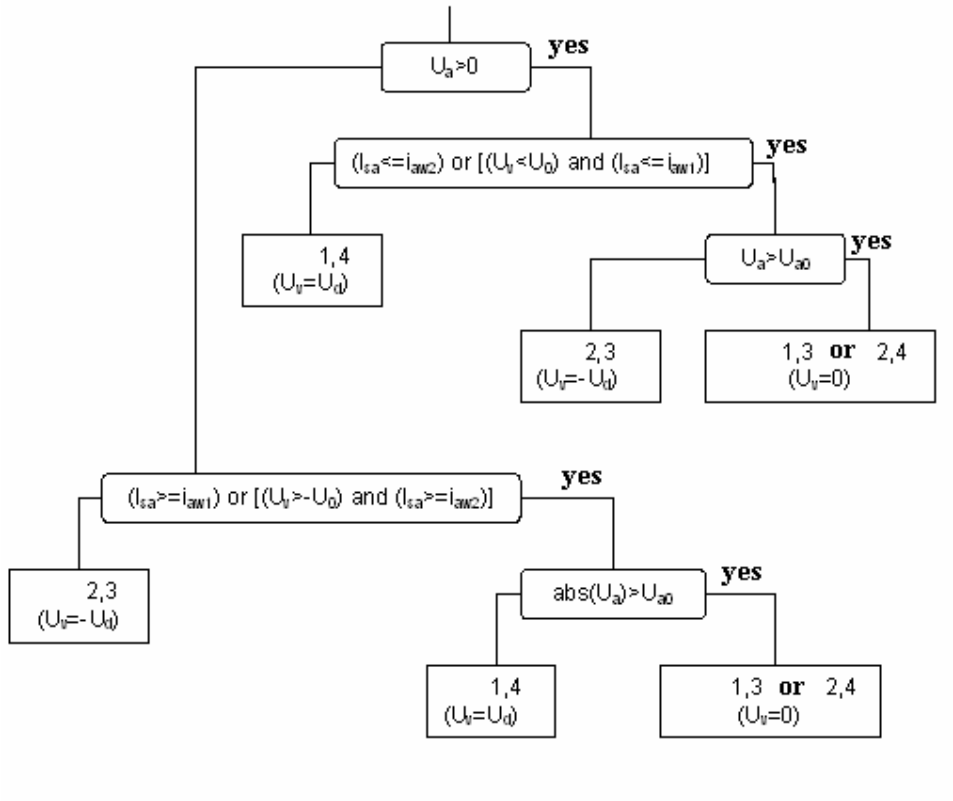

U_0 … arbitrary voltage, ($0<U_0<(U_d)_{\min}$) and again comparing U_v with U_0 determines the switching state of the converter.

If $U_a<U_{a0}$, then the function of Logic 1 is changed.

Figure 4a: Variant 3 of Logic 1

4. LOGIC 2 FOR DETERMINING THE SAMPLING PERIOD TT OF CONTROLLER RV

Logic 2 in Figure (5) explains the algorithm used to test the sampling period TT of R_v. The operating period of the voltage controller R_v is divided into samples. If the deviation between the mean value of the voltage across the capacitor U_{dd} during the sampling period TT and the given dc reference is greater than ΔUd, a shorter period TT2 is then applied. In our simulation example we consider the dc reference voltage to be 1500V. Using this technique, the output voltage U_d is always forced to remain within a fixed given value, and this exactly what is needed.

- TT is the sampling period of R_v.
- TU is the sampling period of voltage U_d.
- U_{dd} is the mean value of voltage U_d over period TT

5. VARIANT 3 OF LOGIC 1 - BEST SIMULATION RESULTS

A demonstration of delta modulation using the above mentioned algorithms is prepared using Matlab 6.5 and software programming language "Pascal". Such work was carried out under the condition of negligible magnetization current. This current is shifted by 90° with respect to voltage U_a because of the prevailing leakage flux at the secondary side of the transformer. The current I_a is forced to remain between the upper and the lower limit of reference window band. To achieve this result, the primary

current I_{sa} is compared with I_{w1} and I_{w2}. For the same purpose voltage U_v is compared with an arbitrary voltage U_0 whose value must be greater than zero and smaller than the minimum value of U_d (as depicted in figure 3). The results of using different algorithm variants for implementing delta modulation technique is current I_a and voltage U_a as it is shown in figures 2, 3, 4. The fundamental components are in phase and therefore, by deploying this means of control, the target of improving the power factor of AC-DC converter is achieved. However, variants 3 gives better results than variant 1 and 2 as it is shown in figure 5, 6 and 7.

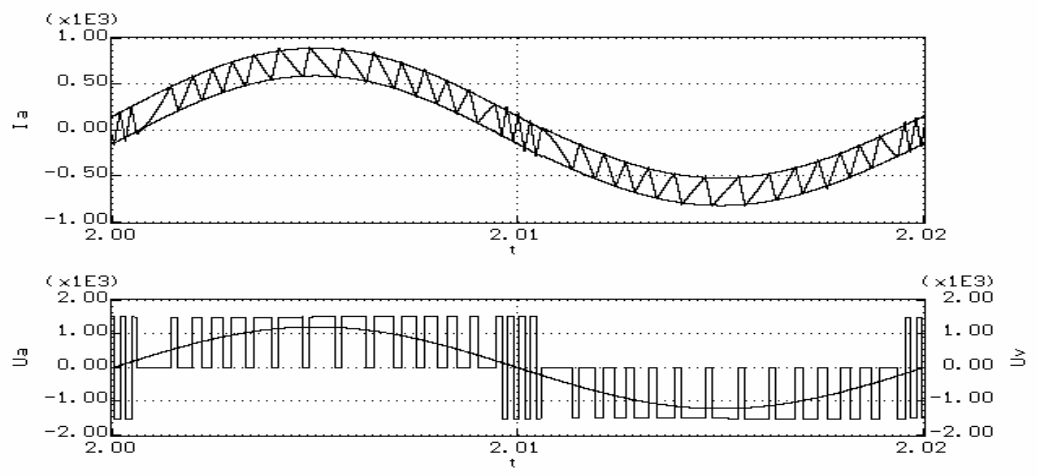

$$\Delta I = 150\,A, U_{a0} = 200V$$

Figure 4b: Simulation results of variant 3

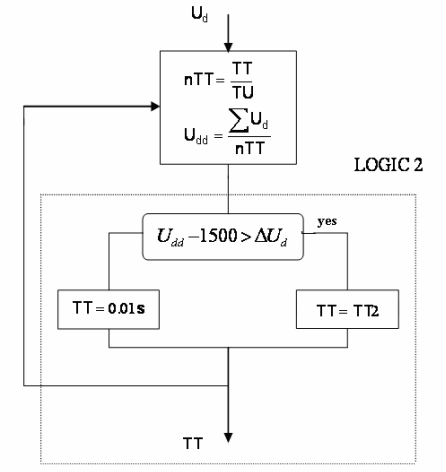

Figure 5: Logic 2 used for testing TT of R_v

Figures (5, 6 & 7) below are graphical representations of variant 3 - Logic 1 and Logic 2. These figures are obtained under the conditions of disconnected and connected filter at the output. The aim of logic 2 is to obtain a constant voltage at the output of AC-DC converter and the input of the voltage inverter.

6. CONCLUSION

Many new modulation techniques have been developed to improve the performance of the AC-DC converters. It can be concluded that, by controlling the input current of a bridge AC-DC converter with the aid of a suitable control technique, the input current of AC-DC converter can be made sinusoidal and in phase with the input voltage, thereby having an input PF of approximate unity, resulting of a more stable performance of the system. This paper presents a new topology (logic variant) of delta modulation technique used for this purpose. Variant 3 introduced in this paper gives better simulation results compared to variant 1 and variant 2.

The reference dc voltage value for U_{dd} was considered in this paper to be 1500-V. Concerning the filter used at the output of AC-DC converter to filter out the high harmonics generated there it may badly affect the dynamic properties of the motor. The simulation however shows that the parameters considered as optimal for the motor without a filter are suitable even for a motor with a filter.

On the other hand the converter can be combined with a high frequency single phase buck-boost converter to reduce the size of the filter. This combination will allow the use of the filter, reduce its bad effect on the motor and make the power factor at the input of the converter more closed to unity.

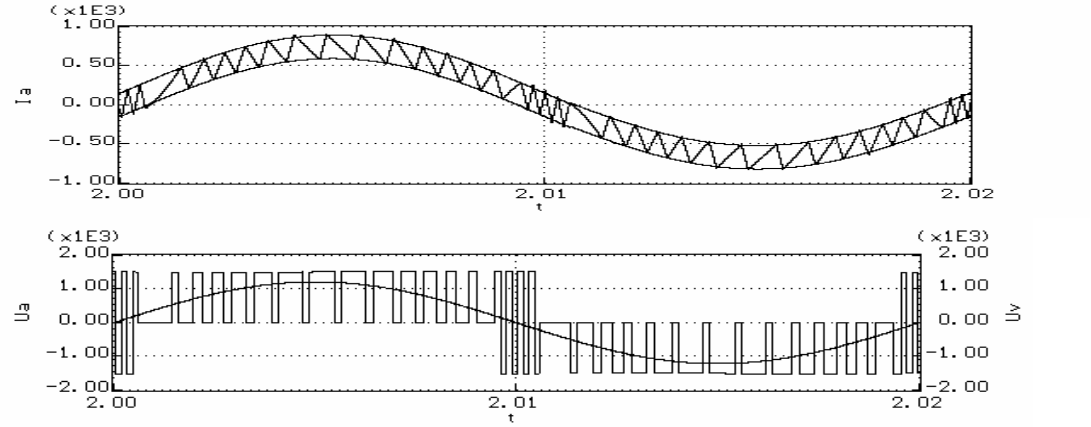

ΔI = 150 A, U_{a0} = 200 V

Figure 5: Input voltage and current waveforms

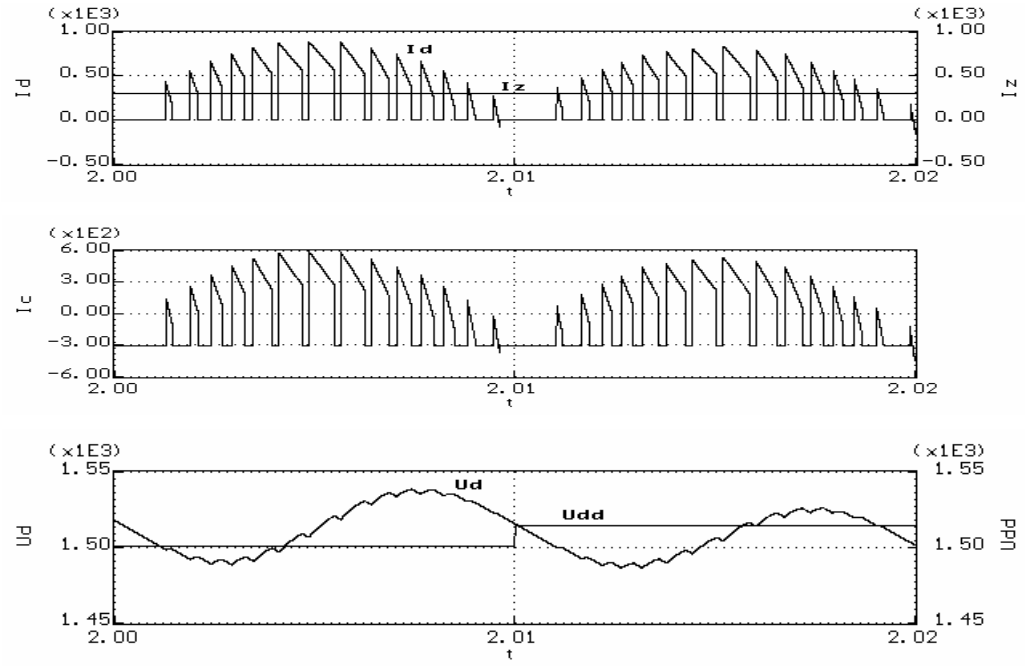

Figure 6: Output voltage waveforms obtained for a disconnected output filter L1, C1.

- $TT = 0.01s, T1 = 1/50000\,s, \Delta I = 150\,A$
- $measuring\ period\ of\ voltage\ U_d\ is TU = 1/1000\,s$
- $Operating\ period\ of\ voltage\ regulator\ R_v\ is\ \mathrm{var}iable$
- $Transformer\ \mathrm{sec}ondary\ voltage\ U_{an} = 860V$
- $No\ \mathrm{min}al\ \mathrm{sec}ondary\ current\ I_{an} = 663\,A$
- $Short-circuit\ volatge\ of\ a\ transformer\ e_k = 30\%$

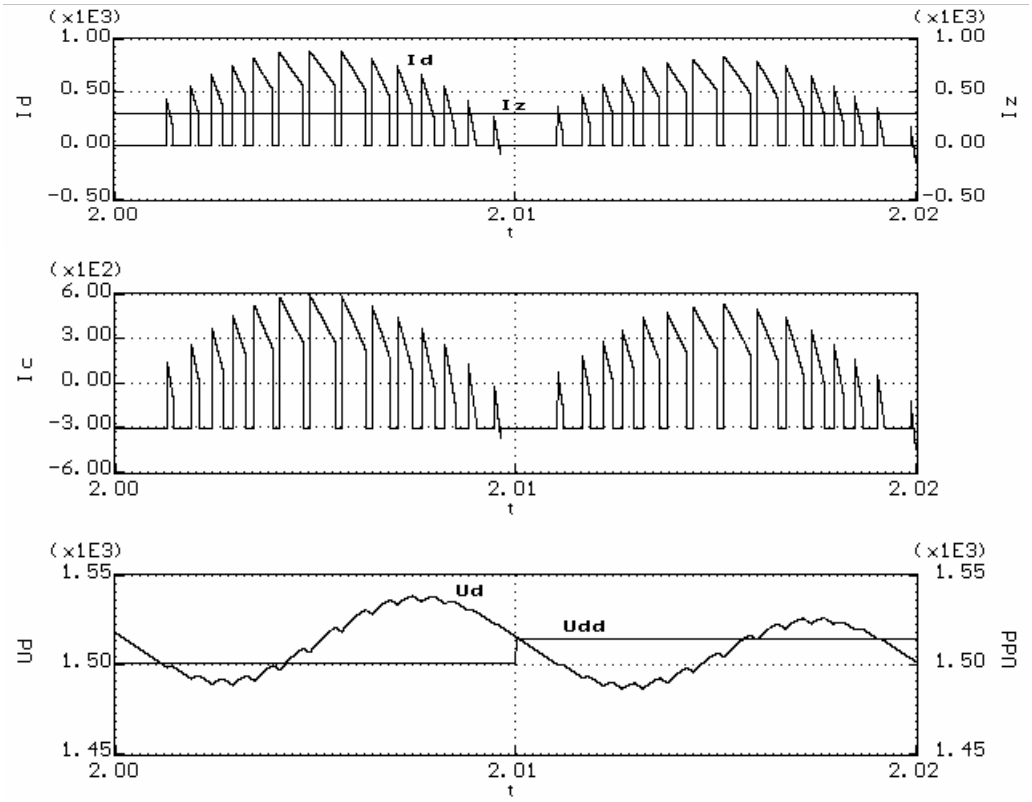

Figure 7: Output voltage waveforms obtained with a connected output filter L_1, C_1, filtr $C_1 = 8\,\text{mF},\ L_1 = 0.316\,\text{mH}$.

- $TT = 0.01s,\ T1 = 1/50000\,s,\ \Delta I = 150\,A$
- *measuring period of voltage* U_d *is* $TU = 1/1000\,s$
- *Operating period of voltage regulator* R_v *is* variable
- *Transformer secondary voltage* $U_{an} = 860V$
- *No minal secondary current* $I_{an} = 663\,A$
- *Short – circuit voltage of a transformer* $e_k = 30\%$

LIST OF ABREVIATIONS	
I_{sa}	Transformer primary current, derived from the trolley at the A.C. side of AC-DC converter.
I_a	Transformer secondary current, at the A.C. side of AC-DC converter
U_a	Primary voltage at the A.C. side of AC-DC converter
U_v	Secondary voltage at the a.c. terminals of AC-DC converter
I_d	Current flowing into the d.c. circuit of AC-DC converter
I_{c1}	Current flowing into filter L_1, C_1
I_z	Current derived by the inverter
U_{dw}	Desired voltage of the capacitor
U_d	Voltage across capacitor C_1
U_{dd}	Average value of the voltage across the capacitor during TT
TU	Sampling period of voltage U_d
TT	Sampling period of voltage controller R_v
T1	Current sampling period
nTT=TT/TU	Number of voltage samples during TT
I_{ref}	Desired amplitude of the current derived from the trolley
$I_{\_down}$, $I_{\_up}$	Window band Limits
ΔI	$I_{\_up} - I_{\_down} = 2.\ \Delta I$

U_0	$0 < U_0 < (U_d)_{min}$. U_0 is an arbitrary voltage used by logic 1 to test the state of the converter
U_{a0}	$U_a < U_{a0}$ … function of logic 2 is then changed
ΔU_d	Voltage deviation on which Logic 2 reacts (from the average value of the voltage across the capacitor)

7. REFERENCES

1. P. D. Ziogas, L. Morán, G. Joos, and D. Vincenti, "A refined PWM scheme for voltage and current source converters," IEEE-IAS Annual Meeting, 1990, PP. 997-983.

2. A. Musbah, E. Walid, and E. Ibrahim, "Modeling and Simulation of a Modified Bang- Bang Hysteresis Control Technique for a Three Phase PWM Converter," European Journal of Scientific Research, Vol.23 No.2 (2008), pp.261-267.

3. R. Wu, S. B. Dewan, and G. R. Slemon, "Analysis of an AC-to-DC voltage source converter using PWM with phase and amplitude control," IEEE Transactions on industry Applications, vol. 27, No. 2, March/April 1991, pp. 355-364.

4. X. Ruan, L. Zhou, and Y. Yan, "Soft-switching PWM three-level converters," IEEE Transactions on Power Electronics, Vol. 6, No. 5, September 2001, pp. 612-622.

5. M. H. Rashid, Power Electronics, Circuits, Devices and applications, Third edition, 2004, Pearson Education, Prentice Hall, Upper Saddle River, NJ 07458.

6. Miftakhutdinov, R. "An Analytical Comparison of Alternative Control Techniques for Powering Next Generation Microprocessors," TI Seminar, 2002.

7. G. Moschopoulos, P. Jain, "Single-phase single-stage power-factor-corrected converter topologies," IEEE Trans. on Industrial Electronics, vol. 52, no. 1, pp. 23- 35, Feb 2005.

8. J.-C. Crebier, B. Revol, J.P. Ferrieux, "Boost-chopper-derived PFC rectifiers: interest and reality," IEEE Trans. on Industrial Electronics, vol. 52, no. 1, pp. 36- 45, Feb 2005.

9. F.J. Azcondo, C. Branas, R. Casanueva, S. Bracho, "Power-mode-controlled power-factor corrector for electronic ballast," IEEE Trans. on Industrial Electronics, vol. 52, no. 1, pp. 56-65, Feb 2005.

10. E. Figueres, J.-M. Benavent, G. Garcera, M. Pascual, "Robust control of power-factor-correction rectifiers with fast dynamic response," IEEE Trans. on Industrial Electronics, vol. 52, no. 1, pp. 66- 76, Feb 2005.

11. J. W. Dixon, and B.-T. Ooi, "Indirect current control of a unity power factor sinusoidal current boost type three-phase rectifier," IEEE Transactions on Industrial Electronics, Vol. 35, No. 4, November 1988, pp. 508-515.

12. P. D. Ziogas, "Optimum voltage and harmonic control PWM techniques for 3-phase static UPS systems," IEEE Transactions on industry Applications, Vol. IA-16, No. 4, 1980, pp. 542-546
13. Miftakhutdinov, R. "An Analytical Comparison of Alternative Control Techniques for Powering Next Generation Microprocessors," TI Seminar, 2002.

14. Song, C., and Nilles, J. "Accuracy Analysis of Hysteretic Current-Mode Voltage Controller," Proc. IEEE APEC, 2005, pp. 276-280.

15. H. Inose, Y. Yasuda and J. Marakami, "A telemetering system by code modulation, delta-sigma modulation," IRE Trans. on Space, Electronics and Telemetry, SET-8, pp. 204-209, Sept. 1962.

16. H. Nyquist, "Certain topics in telegraph transmission theory," AIEE Trans., pp. 617-644, 1928.
17. M. Armstrong, et al, "A COMS programmable self-calibrating 13b eight-channel analog interface processor," ISSCC Dig. Tech. Paper, pp. 44-45, Feb. 1987.

18. K. Lakshmikumar, R. Hadaway, and M. Copeland, “Characterization and modeling of mismatch in MOS transistors for precision analog design,” IEEE J. Solid-State Circuits, Vol. SC-21, pp. 1057-1066, Dec. 1986.

19. N. Ahmed and T. Natarajan, Discrete-Time Signals and Systems, Prentice-Hall, Englewood Cliffs, NJ, 1983.

20. R. Steele, Delta Modulation Systems, Pentech Press, London, England, 1975.
21. N. Scheinberg and D. Schilling, “Techniques for correcting transmission error in video adaptive delta-modulation channels,” IEEE Trans. Commun., pp. 1064-1070, Sept. 1977.

22. J. C. Candy, “A use of double integration in Sigma-Delta modulation,” IEEE Trans. On Communications, Vol. COM-33, No. 3, pp. 249-258, March 1985.

23. R. Koch, et al, “A 12-bit Sigma-Delta analogto- digital converter with a 15-MHz clock rate,” IEEE J. of Solid-State Circuits, Vol. SC-21, No. 6, pp. 1003-1010, Dec. 1986.

24. B. Boser and B. Wooley, “Quantization error spectrum of Sigma-Delta modulators,” Proc. International Symposium on Circuits and Systems, pp. 2331-2334, June, 1988.

Radiation, Chemical Reaction, Double Dispersion effects on Heat and mass transfer in Non-Newtonian fluids

Dr. A.S.N. Murti Asn2005@rediffmail.com
Professor, Department of Engineering Mathematics A.U.College of Engineering Andhra University Visakhapatnam-530003,India

P.K.Kameswaran K_kameswaran@yahoo.com
Research Scholar, Department of Engineering Mathematics A.U.College of Engineering Andhra University Visakhapatnam-530003,India

T.Poorna Kantha tpurnakanta@rediffmail.com
Research Scholar, Department of Engineering Mathematics A.U.College of Engineering Andhra University Visakhapatnam-530003,India

Abstract

Radiation and chemical reaction effects on heat and mass transfer in non-Darcy non-Newtonian fluid over a vertical surface is considered. In this article we have maintained the constant temperature. A mathematical model is developed taking into the account the new elements introduced. Numerical solutions for the governing nonlinear momemtum, energy and concentration are obtained.The governing boundary layer equations and boundary conditions are simplified by using similarity transformations. The governing equations are solved numerically by means of Fourth-order Runge-Kutta method coupled with double-shooting technique. The influence of viscosity index n, thermal and solute dispersion, velocity, temperature, concentration, Heat and mass transfer rates are discussed.

Keywords: Radiation, Chemical reaction, double dispersion, free convection, heat and mass transfer.

1. INTRODUCTION

Transport processes in porous media play significant roles in various applications such as geothermal engineering, thermal insulation, energy conservation, petroleum industries solid matrix heat exchangers, chemical catalytic reactor, underground disposal of nuclear waste materials and many others. Convective heat transfer from impermeable surfaces embedded in

porous media has numerous thermal engineering applications such as geothermal systems, crude oil extraction, thermal insulating and ground water pollution.Nield and Bejan [1] and Pop and Ingham [2] have made comprehensive reviews of the studies of heat transfer in relation to the above applications. Radiation effects on convection can be quite important in the context of many industrial applications involving high temperatures such as nuclear power plant, gas turbines and various propulsions engines for aircraft technology.Ali et.al [3] studied the natural convection-radiation interaction in boundary layer flow over a horizontal surfaces.Hossain and Pop [4] considered the effect of radiation on free convection of an optically dense viscous incompressible fluid along a heated inclined flat surface maintained at uniform temperature placed in a saturated porous medium .Yih [5] investigated the radiation effect on the mixed convection flow of an optically dense viscous fluid adjacent to an isothermal cone embedded in a saturated porous medium. Bakier [6] analyzed the effect of radiation on mixed convection from a vertical plate in a saturated medium.Cheng and Minkowycz [7] presented similarity solutions for free convective heat and mass transfer from a vertical plate in a fluid saturated porous medium. Chen and Chen [8] studied free convection from a vertical wall in a non-Newtonian fluid saturated porous medium. Mehta and Rao [9] studied the free convection heat transfer in a porous medium past a vertical flat plate with non-uniform surface heat flux at the wall. Nakayama and Koyama [10] analyzed the more general case of free convection over a non-isothermal body of arbitrary shape embedded in a porous medium. Anjalidevi and Kandasamy [11] studied the effects caused by the chemical-diffusion mechanisms and the inclusion of a general chemical reaction of order n on the combined forced and natural convection flows over a semi-infinite vertical plate immersed in an ambient fluid. They stated that the presence of pure air or water is impossible in nature and some foreign mass may present either naturally or mixed with air or water.El-Amin [12] studied the effects of chemical reaction and double dispersion on non-Darcy free convective heat and mass transfer in porous medium. The effects of double dispersion on natural convection heat and mass transfer in a non-Newtonian fluid saturated non-Darcy porous medium has been investigated by Murthy et.al [13]. Murti and Kameswaran [14] analyzed the effects of Radiation, chemical reaction and double dispersion on heat and mass transfer in non-Darcy free convective flow. The study by Chamka [15] of MHD flow over a uniformly stretched vertical permeable surface used similar assumptions for the chemical reaction.

The objective of this paper is to study the effects of double dispersion on natural convection heat and mass transfer in non-Darcy, non-Newtonian fluid with Radiation and chemical reaction along the vertical surface.

2. NOMENCLATURE

C Concentration
d Pore diameter
D Mass diffusivity
f Dimensionless stream function
g Gravitational acceleration
Gc Modified Grashof number
k Molecular thermal conductivity
K Permeability of the porous medium
K_0 Chemical reaction parameter
k_d Dispersion thermal conductivity
k_e Effective thermal conductivity
Le Lewis number
m Order of reaction
N Buoyancy ratio
Nu_x Local Nusselt number

$\Pr$ Prandtl number
q Heat transfer rate
Ra Ralyleigh number
Re_x Local Reynolds number
Sc Schmidt number
w Surface conditions
μ^* Fluid consistency of the in elastic non-Newtonian power law fluid
Gr^* Non-Darcy parameter
ε Porosity of the saturated porous medium
m Order of reaction
j_w Local mass flux
T Temperature
u, v Velocity components in the x and y directions
u_r Reference velocity
x , y Axes along and normal to the plate
α Molecular thermal diffusivity
σ Electrical conductivity. mho
α_d Dispersion diffusivity
α_x, α_y Components of the thermal diffusivity in x and y directions
β Thermal expansion coefficient
β^* Solutal expansion coefficient
χ Non-dimensional chemical reaction-porous media parameter
ϕ Dimensionless concentration
γ Mechanical thermal-dispersion coefficient
η Similarity space variable
R Radiation parameter $\dfrac{16av\sigma_R T_\infty^2}{\rho C_p U_\infty^2}$
λ Non-dimensional chemical reaction parameter
μ Fluid dynamic viscosity
υ Fluid kinematic viscosity
θ Dimension less temperature
ρ Fluid density
ψ Stream function
ζ Mechanical solutal-dispersion coefficient
∞ Conditions away form the surface
k^* Intrinsic permeability of the porous medium for flow of power law fluid
b Coefficient of Forchheimer term
σ_0 Stefan-Boltzman constant
k_1^* Mean absorption coefficient

3. MATHEMATICAL FORMULATION

The chemical reaction of order m on natural convective heat and mass transfer in a non-Darcian porous medium saturated with a non-Newtonian fluid adjacent to a vertical surface is considered. The co-ordinate system $x \to y$ is attached to the vertical surface as shown in Fig.1.

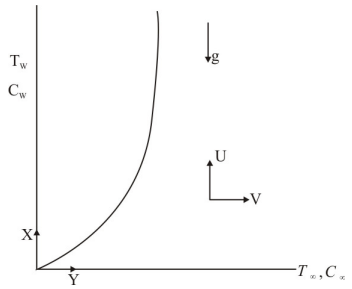

Figure 1. Schematic diagram of the problem

The x axis is taken along the plate and y axis is normal to it. The wall is maintained at constant temperature T_w and concentration C_w respectively. Taking into account the effects of thermal dispersion, the governing equations for steady non-Darcy flow in a saturated porous medium can be written as follows.

Continuity Equation:

$$\frac{\partial u}{\partial x}+\frac{\partial u}{\partial y}=0 \tag{1}$$

Momentum Equation:

$$\frac{\partial u^n}{\partial y}+\rho_\infty \frac{bk^*}{\mu^*}\frac{\partial u^2}{\partial y}=\frac{\rho_\infty g k^*}{\mu^*}\left(\beta_T \frac{\partial T}{\partial y}+\beta_C \frac{\partial C}{\partial y}\right) \tag{2}$$

Energy Equation :

$$u.\frac{\partial T}{\partial x}+v.\frac{\partial T}{\partial y}=\frac{\partial}{\partial y}\left(\alpha_y \frac{\partial T}{\partial y}\right)-\frac{1}{\rho C_p}\frac{\partial q}{\partial y} \tag{3}$$

where $\frac{\partial q}{\partial y}=-16a\sigma R T_\infty^3\left(T_\infty - T\right)$

Concentration Equation:

$$u.\frac{\partial C}{\partial x}+v.\frac{\partial C}{\partial y}=\frac{\partial}{\partial y}\left(D_y \frac{\partial C}{\partial y}\right)-K_0\left(C-C_\infty\right)^m \tag{4}$$

$$\rho=\rho_\infty\left[1-\beta\left(T-T_\infty\right)-\beta^*\left(C-C_\infty\right)\right] \tag{5}$$

where u and v are velocities in the $x-y$ directions respectively, T is the temperature in the thermal boundary layer, K is the permeability constant. β_T and β_C are the coefficients of thermal and solutal expansions, ρ_∞ is the density at some reference point, g is the acceleration due to gravity. The energy equation includes radiation heat transfer effect with Jowl heating. The radiative heat flux term q is written using the Rosseland approximation as $q=-\frac{4\sigma_0}{3k_1^*}\frac{\partial T^4}{\partial y}$, where σ_0 and k_1^* are Stefan-Boltzman constant and the mean absorption coefficient respectively. The chemical reaction effect is added as the last-term in the right hand side of equation (4) where the power m is the order of reaction. It is assumed that the normal component of the velocity near the boundary is small compared with the other components of the velocity and the

derivatives of any quantity in the normal direction are large compared with derivatives of the quantity in the direction of the wall.

The necessary boundary conditions for this problem are

$$\left.\begin{array}{l} y=0\ ;\ v=0,\ T=T_w\ ,C=C_w \\ y\to\infty;u=u_\infty,T=T_\infty,C=C_\infty \end{array}\right\} \tag{6}$$

The quantities of α_y and D_y are variables defined as $\alpha_y=\alpha+\gamma d\left|\mathbf{v}\right|$ and $D_y=D+\zeta\, d\left|\mathbf{v}\right|$ represent thermal dispersion and solutal diffusivity, respectively (Telles and Trevisan [16]).The value of these quantities lies between $\frac{1}{7}$ and $\frac{1}{3}$, Also b is the empirical constant associated with the Forchheimer porous inertia term and μ^* is the consistency index, the modified permeability of the flow k^* of the non-Newtonian power law fluid is defined as

$$k^*=\frac{1}{2c_t}\left(\frac{n\varepsilon}{3n+1}\right)^n\left(\frac{50K}{3\varepsilon}\right)^{\frac{n+1}{2}} \tag{7}$$

where

$$K=\frac{\varepsilon^3 d^2}{150\left(1-\varepsilon\right)^2} \quad \text{and}$$

$$c_t=\begin{cases}\dfrac{25}{12} \\ \dfrac{2}{3}\left(\dfrac{8n}{9n+3}\right)^n\left(\dfrac{10n-3}{6n+1}\right)\left(\dfrac{75}{16}\right)^{\frac{3(10n-3)}{10n+11}}\end{cases}$$

and for $n=1, c_t=\frac{25}{12}$

Introducing the stream function ψ such that $u=\frac{\partial\psi}{\partial y}$ and $v=-\frac{\partial\psi}{\partial x}$.

we introduce similarity variables as

$$\psi=f\left(\eta\right)\alpha\sqrt{Ra_x}\ ,\eta=Ra_x^{\frac{1}{2}}.\frac{y}{x}\ ,\ \theta\left(\eta\right)=\frac{T-T_w}{T_w-T_\infty},\ \phi\left(\eta\right)=\frac{C-C_w}{C_w-C_\infty}$$

where $Ra_x=\frac{x}{\alpha}\left[\frac{\rho_\infty k^* g\beta_T\left(T_w-T_\infty\right)}{\mu^*}\right]^{\frac{1}{n}}$

The above transformation reduces the system of partial differential equations in to the system of ordinary differential equations

$$\left(n\,f^{'n-1}+2Gr^*f^{'}\right)f^{''}=\theta^{'}+N\phi^{'} \tag{8}$$

$$\theta^{''}+\frac{1}{2}f\theta^{'}+\gamma Ra_d\left(f^{'}\theta^{''}+f^{''}\theta^{'}\right)+\frac{4R}{3}\left[3\theta^{'2}\left(\theta+c_r\right)^2+\theta^{''}\left(\theta+c_r\right)^3\right]=0 \tag{9}$$

$$\phi^{''}+\frac{1}{2}Lef\phi^{'}+\zeta Ra_d\,Le\left(f^{'}\phi^{''}+f^{''}\phi^{'}\right)-Sc\lambda\frac{Gc}{\mathrm{Re}_x^2}\phi^n=0 \tag{10}$$

where the primes denote the differentiation with respect to the similarity variable η.

$Ra_d = \frac{d}{\alpha}\left(\frac{k^* \rho_\infty g \beta_T \theta_w}{\mu^*}\right)^{\frac{1}{n}}$ is the modified pore-diameter-dependent Ralyleigh number, and $N = \frac{\beta^*\left(C_w - C_\infty\right)}{\beta\left(T_w - T_\infty\right)}$ is the buoyancy ratio parameter, $R = \frac{4\sigma\theta_w^3}{kk_1^*}$ is the conduction radiation parameter. With analogy to Mulolani and Rahman [17]. Aissa and Mohammadein [18], we define Gc to be the modified Grashof number, Re_x is the local Reynolds number, Sc and λ are the Schmidt number and non-dimensional chemical reaction parameter as

$$Gc = \frac{\beta^* g\left(C_w - C_\infty\right)^2 x^3}{\upsilon^2},\ \mathrm{Re}_x = \frac{u_r x}{\upsilon},\ Sc = \frac{\upsilon}{D},\ \lambda = \frac{K_0 \alpha d\left(C_w - C_\infty\right)^{n-3}}{kg\beta^*}$$

$Gr^* = b\left(\frac{k^{*2}\rho_\infty^2\left[g\beta_T\theta_w\right]^{2-n}}{\mu^{*2}}\right)^{\frac{1}{n}}$ is the non-Darcy Parameter or Grashof number based on permeability for power law fluid. where the diffusivity ratio Le is the ratio of Schmidt number and Prandtl number and $u_r = \sqrt{g\beta d\left(T_w - T_\infty\right)}$ is the reference velocity as defined by Elbashbeshy [19]. The equation (10) can be written as

$$\phi'' + \frac{1}{2} Lef\phi' + \zeta Ra_d\, Le\left(f'\phi'' + f''\phi'\right) - \chi\phi^n = 0 \qquad (11)$$

With analogy to Prasad et. al [20], Aissa and Mohammadein [18], the non-dimensional chemical reaction parameter χ is defined as $\chi = \frac{Sc\lambda Gc}{\mathrm{Re}_x^2}$.

and the boundary conditions become

$$\left.\begin{aligned} f(0) = 0,\ \theta(0) = \phi(0) = 1 \\ f'(\infty) = 1, \theta(\infty) = \phi(\infty) = 0 \end{aligned}\right\} \qquad (12)$$

It is noted that $Gr^* = 0$ corresponds to the Darcian free convection, thermal dispersion effect $\gamma = 0$ and the solute-dispersion effects $\zeta = 0$ are neglected. In equation (8) $N > 0$ indicates the aiding buoyancy and $N < 0$ indicates the opposing buoyancy. On the other hand from the definition of stream function, the velocity components become $u = \frac{\alpha Ra_x}{x} f'$ and $v = -\frac{\alpha Ra_x^{\frac{1}{2}}}{2x}\left[f - \eta f'\right]$.

The local heat transfer rate from the surface of the plate is given by

$$q_w = -k_e\left[\frac{\partial T}{\partial y}\right]_{y=0}. \qquad (13)$$

The local Nusselt number

$$Nu_x = \frac{q_w x}{\left(T_w - T_\infty\right)k_e} \qquad (14)$$

where k_e is the effective thermal conductivity of the porous medium which is the sum of the molecular and thermal conductivity k and the dispersion thermal conductivity k_d .Substituting $\theta(\eta)$ and equation (13) in equation (14) the modified Nusselt number is obtained as

$\frac{Nu_x}{(Ra_x)^{\frac{1}{2}}} = -\left[1+\gamma Ra_d f'(0)\right]\theta'(0)$ .Also the local mass flux at the vertical wall is given by $j_w = -D_y\left(\frac{\partial C}{\partial y}\right)_{y=0}$ defines dimensionless variable and the local Sherwood number is $\frac{Sh_x}{(Ra_x)^{\frac{1}{2}}} = -\left[1+\zeta\, Ra_d f'(0)\right]\phi'(0)$.

4. SOLUTION PROCEDURE

The dimensionless equations (8) (9) and (11) together with the boundary conditions (12) are solved numerically by means of the fourth order Runge-Kutta method coupled with double shooting technique. By giving appropriate hypothetical values for $f'(0), \theta'(0)$ and $\phi'(0)$ we get the corresponding boundary conditions at $f'(\infty)$, $\theta(\infty)$, $\phi(\infty)$ respectively. In addition, the boundary condition $\eta \to \infty$ is approximated by $\eta_{\max} = 4$ which is found sufficiently large for the velocity and temperature to approach the relevant free stream properties. This choice of $\eta_{\max}$ helps in comparison of the present results with those of earlier works.

5. RESULTS & DISCUSSION

The chemical reaction Natural convective problem with radiation effect from a vertical plate with constant wall temperature is analyzed considering both buoyancy aiding and opposing flows. The results obtained are prescribed in graphical form for selected non-dimensional groups having chemical reaction effect, radiation and double dispersion through Figures 2-9. Variation of temperature and velocity within the boundary along with heat and mass transfer characteristics are prescribed in sequential order. The heat transfer coefficient values obtained here for various values of power law index with $\gamma = 0, \varsigma = 0, N = 0, Gr^* = 0, \chi = 0, R = 0$ match well with those tabulated values in Chen and Chen [8] .When $R = 0, \chi = 0$ the problem reduces to effect of double dispersion on natural convection heat and mass transfer in Non-Newtonian fluid saturated non-Darcy porous medium. Results obtained here are good in agreement with Chen and Chen [8] and Murthy [13]. The following values for parameters are considered for discussion. $0.5 \le n \le 1.5$, $0 \le Ra_d \le 3$, $\gamma = 0, 0.3$, $\varsigma = 0, 0.3$, $0 \le Le \le 4$, , $0 \le Gr^* \le 0.3$ $0 \le \chi \le 0.08$.

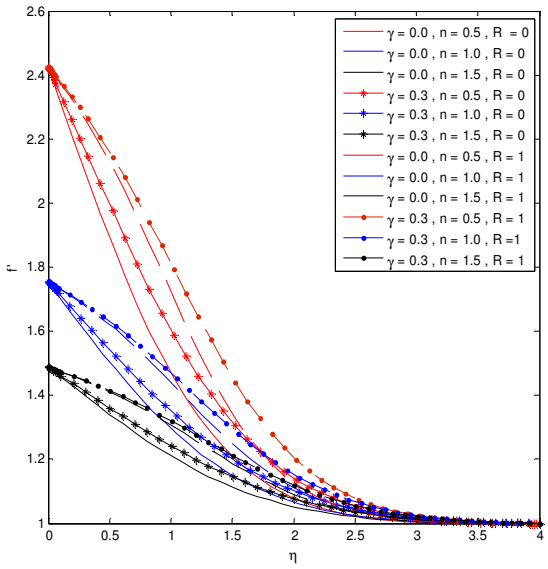

Fig. 2. Variation of velocity with similarity space variable η (opposing)

$$Gr^* = 0.07, N = -0.1, Le = 0.5, Ra_d = 0.7, \xi = 0, \chi = 0.02$$

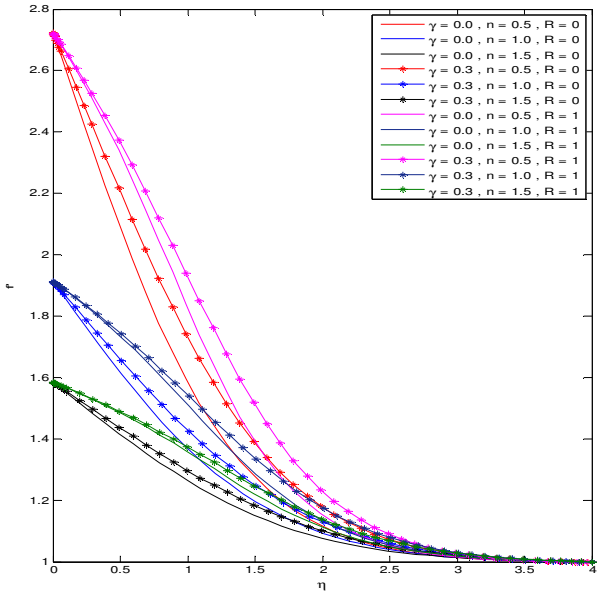

Fig. 3. Variation of velocity with similarity space variable η (aiding)

$$Gr^* = 0.07, N = 0.1, Le = 0.5, Ra_d = 0.7, \xi = 0, \chi = 0.02$$

Figures 2 and 3 describe the velocity variation in the boundary layer with applied chemical reaction and radiation effects. It is found that for a given chemical reaction parameter, with increase in radiation the velocity decreases. However with increase in radiation parameter, the velocity decreases with in the boundary at a given location, velocity decreases with increase in thermal dispersion in presence of radiation. But this decrement is less in presence of Radiation than absence. The same trend is observed in opposing flow also.

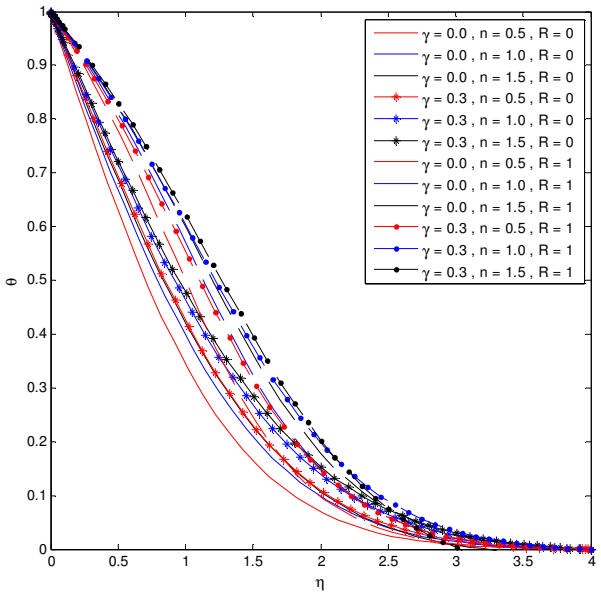

Fig. 4. Effect of temperature with similarity space variable η (opposing)

$$Gr^* = 0.07, N = -0.1, Le = 0.5, Ra_d = 0.7, \xi = 0, \chi = 0.02$$

Figure 4. shows that the effect of non-dimensional temperature profiles for various values of power law index n and γ for fixed values of other parameters in opposing case. It is clearly seen that in the aiding case increasing in power law index tend to increase the boundary layer thickness. With increase in radiation a rise in temperature distribution in the boundary layer is seen.

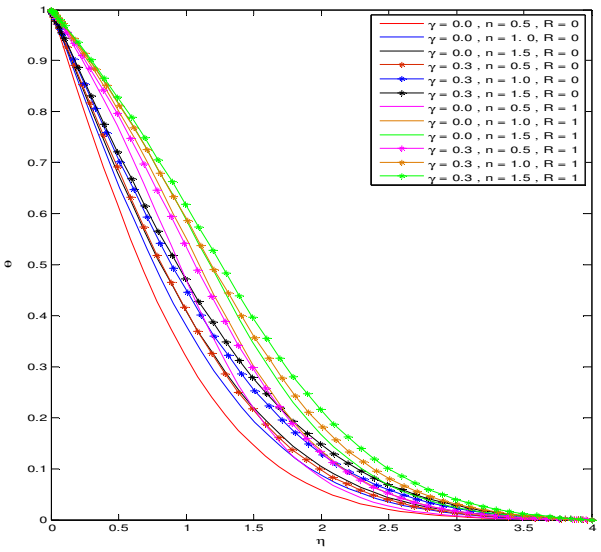

Fig. 5. Effect of temperature with similarity space variable η (aiding)

$$Gr^* = 0.07, N = 0.1, Le = 0.5, Ra_d = 0.7, \xi = 0, \chi = 0.02$$

Figure 5. shows that the effect of non-dimensional temperature profiles for various values of power law index n and γ for fixed values of other parameters in aiding case. With increase in

radiation parameter temperature within the boundary increases. However for a fixed value of radiation parameter temperature increases at a particular location.

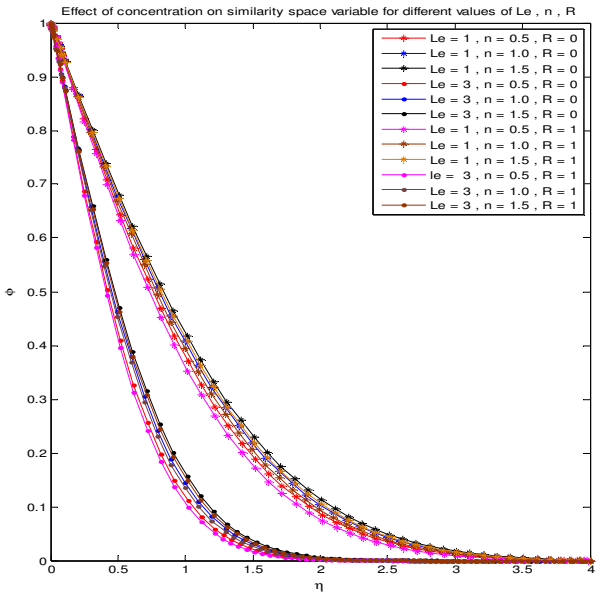

Fig. 6. Effect of concentration with similarity space variable η

$$Gr^* = 0.21, N = -0.1, \gamma = 0, , \xi = 0, \chi = 0.02, Ra_d = 0.7$$

Figure 6.shows that the effect of radiation and natural convection on concentration profile. Concentration with in the boundary decreases with increase in radiation parameter. Further with increase in power law index also the temperature increases. Further it indicates that the effect of radiation parameter on concentration profile is considerable only at the middle of the boundary and negligible at the end of the plate and at the edge of the boundary.

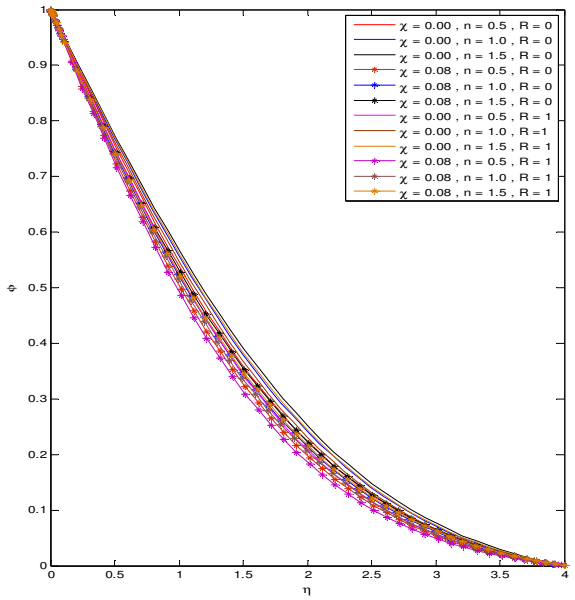

Fig. 7. Effect of concentration with similarity space variable η

$$Gr^* = 0.21, N = -0.1, \gamma = 0, \xi = 0, Le = 0.5, Ra_d = 0.7$$

From Figure 7. we observe that concentration increases with increase in power law index in presence of radiation r. For a fixed value of chemical reaction parameter concentration decreases with increase in radiation parameter.

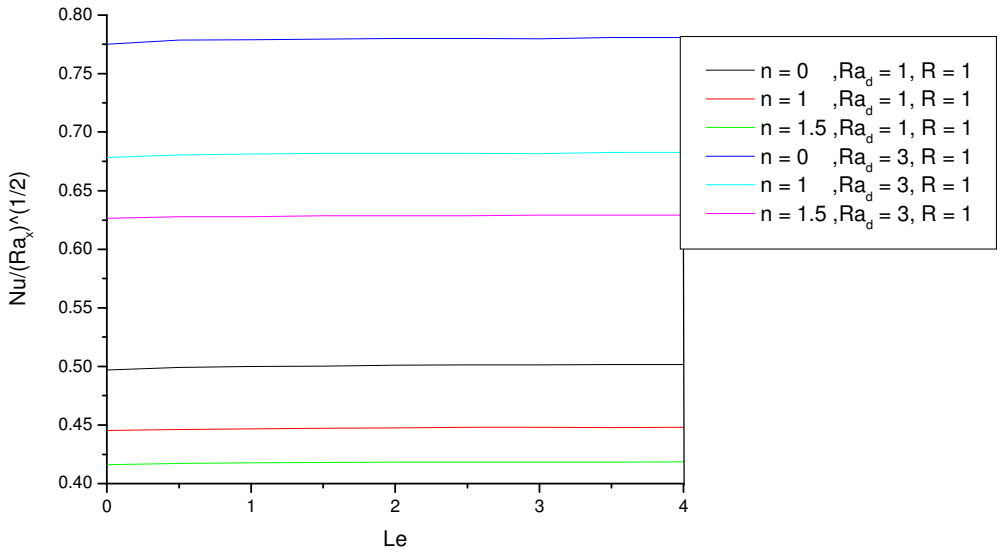

Fig. 8. Effect of Lewis number on Nusselt number

$$Gr^* = 0.21, N = -0.1, \gamma = 0.3, \xi = 0.3, Le = 0.5, \chi = 0.02$$

From Figure 8. we observe that for a fixed value of Ra_d nusselt number decreases with increase in power law index. Increase in Ra_d nusselt number decreases. Hence the heat transfer coefficient decreases with increase in power law index.

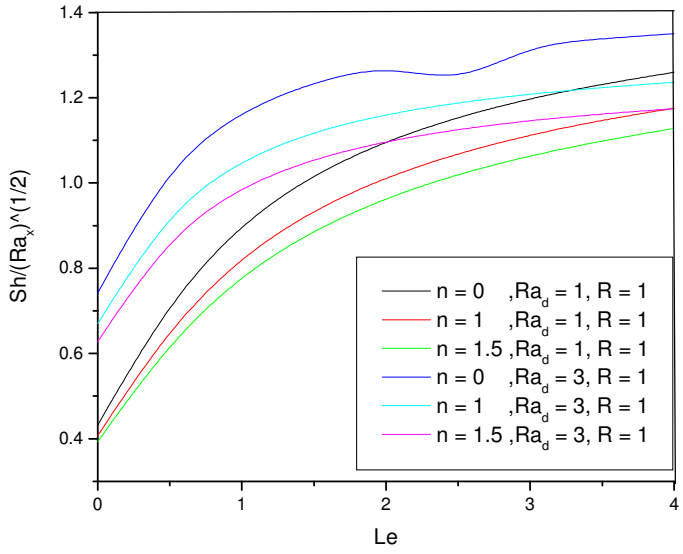

Fig. 9. Effect of Lewis number on Sherwood number

$$Gr^* = 0.21, N = -0.1, \gamma = 0.3, \xi = 0.3, Le = 0.5, \chi = 0.02$$

From Figure 9. we observe that for a fixed value of Ra_d Sherwood number decreases with increase in power law index. Increase in Ra_d Sherwood number decreases. Mass transfer coefficient increases with increase in power law index.

6. CONCLUSIONS

Increase in radiation parameter, the velocity decreases with in the boundary. Increase in radiation a rise in temperature distribution in the boundary layer. Concentration increases with increase in power law index in presence of radiation parameter.Nusselt number decreases with increase in Ra_d parameter. Mass transfer coefficient increases and the heat transfer coefficient decreases with increase in power law index.

7. REFERENCES

[1] D.A. Nield, A. Bejan. "Convection in porous media", Springer-verlag, New York.(1999)

[2] I. Pop, DB. Ingham. "Convection heat transfer "Mathematical and computational modeling of Viscous fluids and porous media" ,Pergamon,Oxford (2001).

[3] MM. Ali ,TS.Chen and BF. Armaly. "Natural convection-radiation interaction in boundary layer flow Over a horizontal surfaces", AIAA J, 22, pp.1797-1803,1984

[4] MA.Hossain ,I. Pop. "Radiation effect on Darcy free convection flow along an inclined surface placed in porous media", Heat and mass transfer, 32(4),pp.223-227,1997.

[5] KA.Yih ."Radiation effect on Mixed convection over an isothermal cone in porous media", Heat mass transfer,37(1),pp.53-57,2001

[6] AY.Bakier. "Thermal radiation effect on mixed convection from vertical surfaces in saturated porous media".Int Commun Heat mass transfer 28(1):119-126, 2001.

[7] P.Cheng ,W.J. Minkowycz . "Free convection about a vertical a plate embedded in a porous medium with application to heat transfer from a dike". *Journal of Geophysical Research* 82, 2040 – 2049,1997.

[8] H.T.Chen , C.K.Chen ."Free convection of non-Newtonian fluids along a vertical plate embedded in a porous medium", *Trans. ASME, J. Heat Transfer* 110, 257–260,1998

[9] K.N. Mehta K.N. Rao."Buoyancy-induced flow of non-Newtonian fluids in a porous medium past a vertical plate with non uniform surface heat flux", *Int. J. Engng Sci.* 32, 297–302,1994

[10] A.Nakayama ,H. Koyama."Buoyancy-induced flow of non-Newtonian fluids over a non isothermal body of arbitrary shape in a fluid-saturated porous medium", *Appl. Scientific Res.* 48, 55–70,1991

[11] S.P.Anjalidevi, P.Kandasamy. "Effects of Chemical reaction, heat and mass transfer on laminar flow along a semi infinite horizontal plate". *Heat mass transfer*.35,465-467,1999

[12] M.F. El-Amin . "Double dispersion effects on natural convection heat and mass transfer in non-Darcy porous medium".*Appl.Math.Comput*.156,1-7,2004

[13] R.R.Kairi,P.V.S.N Murthy. "The effects of double dispersion on natural convection heat and mass transfer in a non-Newtonian fluid saturated non-Darcy porous medium".*Transp Porous Med*,2008

[14] A.S.N.Murti , P.K.Kameswaran .“ Effect of Radiation, Chemical reaction and double dispersion on heat and mass transfer in non-Darcy free convective flow”. *Proceedings of the ASME International Mechanical Engineering congress & Exposition.* Lake Buena vista, Florida, U.S.A.2009.

[15] AJ.Chamka . “ MHD flow of a uniformly stretched vertical permeable surface in the presence of heat generation / absorption and a chemical reaction”. Int Comm Heat Mass Transf 30, 413–422, 2003

[16] Telles R.S, Trevisan O.V , “ Dispersion in heat and mass transfer natural convection along vertical boundaries in porous media ”. *Int.J.Heat mass transf.* 36,1357-1365,1903.

[17] I.Mulolani I, M.Rahman. “Similarity analysis for natural convection from a vertical plate with distributed wall concentration” *Int.J.Math.MathSci*.23, 319-334,2008.

[18] W.A.Aissa,A.A. Mohammadein. “Chemical reaction effects on combined forced and free convection flow of water at 4^0C past a semi-infinite vertical plate”, *J.Eng.Sci.Assiut Univ*. 34, 1225-1237,2006.

[19] E.M.A .Elbashbery.“Heat and mass transfer along a vertical plate with variable surface tension and concentration in the presence of magnetic field”.*Int.J, Eng.Sci.Math.Sci*.4,515-522.1997.

[20] K.V.Prasad ,S. Abel S and P.S. Datti. “Diffusion of chemically reactive species of non-Newtonian fluid immersed in a porous medium over a stretched sheet” .*Int.J.Non-linear Mech*, 38,651-657.

Optimizing PID Tuning Parameters Using Grey Prediction Algorithm

Ala Eldin Abdallah Awouda *ala_awouda@yahoo.com*
Department of Mechatronics and Robotics,
Faculty of Electrical Engineering,
Universiti Teknologi Malaysia,
Johor, 83100, Malaysia
rosbi@fke.utm.my

Rosbi Bin Mamat *rosbi@fke.utm.my*
Department of Mechatronics and Robotics,
Faculty of Electrical Engineering,
Universiti Teknologi Malaysia,
Johor, 83100, Malaysia

ABSTRACT

This paper considered a new way to tune the PID controller parameters using the optimization method and grey prediction algorithm. The grey prediction algorithm has the ability to predict the output or the error of the system depending on a small amount of data. In this paper the grey prediction algorithm is used to predict and estimate the errors of the system for a defined period of time and then the average of the estimated error is calculated. A mat lab program is developed using simulink to find the average of the estimated error for the system whose process is modeled in first order lag plus dead time (FOLPD) form. In the other hand optimization method with mat lab software program was used to find the optimum value for the PID controller gain (K_c (opt)) which minimizes specific performance criteria (ITAE performance criteria). The main goal of the optimization method is to achieve most of the systems requirements such as reducing the overshoot, maintaining a high system response, achieving a good load disturbances rejection and maintaining robustness. Those two parameters (the average of the estimated error and the PID controller gain (K_c (opt))) were used to calculate the PID controller parameters (gain of the controller (K_c), integral time (T_i) and the derivative time (T_d)). Simulations for the proposed algorithm had been done for different process models. A comparison between the proposed tuning rule and a well performance tuning rule is done through the Matlab software to show the efficiency of the new tuning rule.

Keywords: ITAE criteria; Grey prediction; AMIGO tuning rule; PID

1. INTRODUCTION

Since it was appear for the first time in 1922, the PID controller shows the ability of to compensate most practical industrial processes which have led to their wide acceptance in industrial applications. It has been stated, for example, that 98% of control loops in the pulp and paper industries are controlled by PI controllers (Bialkowski, 1996) and that, in more general process control applications, more than 95% of the controllers are

of PID type (Åström and Hägglund, 1995). In order for the PID controller to work probably it has to be tuned which mean a selection of the PID controller parameters has to be made [2, 7]. The requirement to choose either two or three controller parameters has meant that the use of tuning rules to determine these parameters is popular. There are many tuning rules for the PID controller as it has been noted that 219 such tuning rules in the literature to specify the PI controller terms, with 381 tuning rules defined to specify the PID controller parameters (O'Dwyer, 2003), Though the use of tuning rules is practically important [9]. Even though, recent surveys indicate, 30 % of installed controllers operate in manual, 30 % of loops increase variability, 25 % of loops use default settings and 30 % of loops have equipment problems [1]. Most PID tuning rules are based on first-order plus time delay assumption of the plant hence cannot ensure the best control performance. Using modern optimization techniques, it is possible to tune a PID controller based on the actual transfer function of the plant to optimize the closed-loop performance. In this paper optimization method is being used to obtain only one of the PID controller parameter which is controller gain (K_c (opt)). A search of one parameter to be optimized lead to select the Integral of Time multiply by Absolute Error (ITAE) index performance criterion, since it can provide controllers with a high load disturbance rejection and minimize the system overshoot while maintain the robustness of the system. The Integral of Time multiply by Absolute Error (ITAE) index is a popular performance criterion used for control system design. The index was proposed by Graham and Lathrop (1953), who derived a set of normalized transfer function coefficients from 2nd-order to 8th-order to minimize the ITAE criterion for a step input [8]. The grey prediction algorithm had been used for several applications and it proves its ability to forecast the output accurately. In this paper the grey algorithm had been used to estimate the error of the system which will be used to obtain the PID controller parameters. This paper is organized as follows: - The grey prediction algorithm is discussed in section 2. An overview of the traditional and a best performance tuning rule is covered in section 3. The proposed tuning rule which derived from optimization method along with the grey prediction algorithm is outlined in section 4. In section 5 and section 6 graphical results showing the performance and robustness of FOLPD processes, compensated with the proposed PID tuning rule. The process is modeled as a first order lag plus time delay (FOLPD) model, and compensated by PID controllers whose parameters are specified using the proposed tuning rule. The results of the proposed tuning rule are plotted and are used to be compared in the face of the performance, robustness and load disturbance rejection against a well performance tuning rule. Conclusions of the work are drawn in Section 7.

2. GREY PREDICTION ALGORITHM

Grey theory was introduced in 1982. The Grey theory is able to deal with indeterminate and incomplete data to analyze and establish the systematic relations

and a prediction model. Unlike conventional stochastic forecasting theory, Grey prediction simply requires as few as four lagged inputs to construct a Grey differential equation [5]. The Grey prediction has been widely used in studies of social sciences, agriculture, procreation, power consumption and management, as well as other fields. In Grey theory, two techniques are adopted to establish the model for applications. They are accumulated generating operation (AGO) and inverse accumulated generating operation (IAGO). The grey prediction model conducts a so called "accumulated generating operation" on the original sequence. The resultant new series is used to establish a difference equation whose coefficients are found via the least-squares method. The accumulated generating series prediction model value is then obtained. The estimated prediction value in the time-domain is calculated by means of an inverse accumulated generating operation. Only a few original sequence elements are needed, and one does not have to assume the distribution of the sequence. The generated value is then used to establish a set of Grey difference equation and Grey pseudo differential equation. The model is called the Grey Model. Generally, there are a few types used in the literature [5, 10]:

1) GM (1, 1): This represents first-order derivative, containing one input variable, generally used for prediction purposes.

2) GM (1, N): This represents first-order derivative, but containing N input variables, for multi-variable analysis.

3) GM (O, N): This represents zero-order derivative, containing N input variables, for prediction purposes.

In this thesis, the GM (1, 1) model is adopted to perform the prediction of system output response. The standard procedure is as follows [14]:

- Step 1: Collecting the original data sequence;

$$x^{(0)} = \{x^{(0)}(1), x^{(0)}(2) \dots x^{(0)}(n)\} \quad n \geq 4 \dots\dots(1)$$

- Step 2: Conducting an accumulated generation operation, AGO, on the original data sequence in order to diminish the effect of data uncertainty;

$$x^{(1)}(k) = \text{AGO of } x^{(0)} = \sum_{i=1}^{k} x^{(0)}(i) \cdots (2) \qquad k = 1, 2, \dots n \quad \text{and } n \geq 4$$

- Step 3: Establishing Grey differential equation and then calculating its background values:-First we define $z^{(1)}$ as the sequence obtained by the MEAN operation to $x^{(0)}$ as follow:-

$$z^{(1)}(k) = \text{MEAN of } x^{(1)}$$
$$= 0.5 * [x^{(1)}(k) + x^{(1)}(k-1)] \quad k = 2, 3, 4 \quad \dots\dots\dots(3)$$

Secondly Grey differential equation can be obtained the as follow:-

$$x^{(0)}(k) + a * z^{(1)}(k) = u_q \dots\dots\dots\dots (4)$$

Where the parameters a, uq are called the development coefficient and the grey input, respectively. Equation (5) is called the whitening equation corresponding to the grey differential equation.

$$\frac{dx^{(1)}}{dt} + a * x^{(1)} = u_q \dots\dots\dots\dots (5)$$

- Step 4: decide the value of a, uq by means of the least –square method as follow:-

$$L^{\wedge} = \begin{bmatrix} a \\ u_q \end{bmatrix} = (B^T * B)^{-1} * B^T * x^N \dots (6)$$

$$B = \begin{bmatrix} -z^{(1)}(2) \dots\dots\dots 1 \\ -z^{(1)}(3) \dots\dots\dots 1 \\ \cdot \\ \cdot \\ \cdot \\ -z^{(1)}(n) \dots\dots\dots 1 \end{bmatrix} \dots\dots\dots (7)$$

$$x^{(N)} = \{x^{(0)}(2)\ x^{(0)}(3) \dots x^{(0)}(n)\}^T \dots (8)$$

- Step 5: Deriving the solution to the Grey difference equation:-

$$x^{(1)\wedge}(n+p) = \left[x^{(0)}(1) - \frac{u_q}{a}\right] * e^{-a(n+p-1)} + \frac{u_q}{a}$$

Where the parameter (p) is the forecasting step size and the up script "^" means the value $x^{(1)\wedge}$ is a forecasting value of x.

- Step 6 conducting the inverse accumulated generation operation (IAGO) on $x^{(1)\wedge}$ to obtain a prediction value as follow:-

$$x^{(0)\wedge}(n+p) = (1 - e^{a})\left[x^{(0)}(1) - \frac{u_q}{a}\right] * e^{-a(n+p-1)}$$

$$x^{(0)\wedge}(k) = \text{IAGO of } x^{(1)} = x^{(1)}(k) - x^{(1)}(k-1) \qquad k = 2, 3 \dots n \quad \dots (9)$$

$$n \geq 4 \text{ for all equations}$$

3. AMIGO TUNING RULE

The objective of AMIGO was to develop tuning rules for the PID controller in varying time-delay systems by analyzing different properties (performance, robustness etc.) of a process test batch. The AMIGO tuning rules are based on the KLT-process model obtained with a step response experiment. AMIOG tuning rule considered controller describe with the following equation:-

$$u(t) = k(by_{sp}(t) - y_f(t)) + k_i \int_0^t [(y_{sp}(\tau) - y_f(\tau)]) dt + k_d \left(C * \frac{dy_{sp}(t)}{dt} + \frac{dy_f(t)}{dt}\right) \ldots (10)$$

Where u is the control variable, ysp the set point, y the process output, and yf is the filtered process variable, i.e. $y_f(s) = G_f(s)y(s)$ The transfer function $G_f(s)$ is a first order filter with time constant T_f , or a second order filter if high frequency roll-off is desired.

$$G(s) = \frac{1}{(1 + sT_f)^2} \ldots\ldots\ldots\ldots (11)$$

Parameters b and c are called set-point weights. They have no influence on the response to disturbances but they have a significant influence on the response to set point changes. Neglecting the filter of the process output the feedback part of the controller has the transfer function.

$$C(s) = K_c \left(1 + \frac{1}{sT_i} + sT_d\right) \ldots\ldots (12)$$

The advantage of feeding the filtered process variable into the controller is that the filter dynamics can be combined with in the process dynamics and the controller can be designed as ideal controller. The AMIGO tuning rules are [3, 6]

$$K_c = \left(0.2 + 0.45 * \frac{T}{L}\right) \ldots\ldots (13)$$

$$T_i = \left(\frac{0.4L + 0.8T}{L + 0.1\,T}\right)L \ldots\ldots (14)$$

$$T_d = 0.\frac{5LT}{0.3L + T} \ldots\ldots\ldots\ldots (15)$$

4. THE PROPOSED TUNING RULE

The proposed algorithm is depending on finding two important parameters which are the optimal PID controller gain and the average estimated error for the process. Using ITAE performance criteria as a factor to be optimized, Matlab program had been used to obtain the optimal value of the controller gain (K_c (opt)). A Matlab m-file is being used to calculate the ITAE index (the objective function) which is mathematically given by:-

$$IATE = \int_0^{\infty} [t\,|\,e(t)dt]\,| \ldots\ldots\ldots\ldots (16)$$

Where t is the time and e (t) is the error which is calculated as the difference between the set point and the output. A function of Matlab optimization toolbox (*f_{min}search*) is called to calculate the minimum of the objective function. Like most optimization problems, the control performance optimization function is needed to be initialized and a

local minimum is required. To do so, the initial controller parameters are set to be determined by one of existing tuning rules. In this way, the controller derived is at least better than that determined by the tuning method. The stability margin based Ziegler-Nichols is used for initial controller parameters. On each evaluation of the objective function, the process model develop in the simulink is executed and the IATE performance index is calculated using multiple application Simpson's 1/3 rule. The simulation repeated with different values of the process parameters (K_P; T; L) and the values are recorded as shown in table (1). For each process parameters value (K_P, L and T) the grey prediction algorithm is then used to obtain the average of the estimated error (E). The average estimated error is computed as follow: - Initial value of the PID controller parameters is used. The selection of the initial values is made depending on the behavior of the system. In this paper the initial value of the PID parameters is K_c = 0.2, K_i = 0.003 and K_d = 0 so as to keep the system behavior under damp. This setting can be used to control different system as long as the system behavior with the initial values of the PI controller will be under damp and the ratio (L/T) is equal or less than 2. The estimated error is computed during the period from the start of the simulation until the steady state reached and then average value is taken from the computed values. The simulation step size is fixed to 0.1 sec so as to make it real time simulation since the suitable sampling time in the real time process can be equal to 0.1 sec. The average of the estimated error produced by grey prediction algorithm and the optimal values of the PID controller gain (K_c (opt)) produced by optimization method is recorded as shown in the table (1). These two parameters are then used to adjust the three parameters of the controller.

5. RSEULTS

Using Matlab simulation tools several processes with different parameters were taken under test. A record of the controller gain (K_c (opt)) that minimize ITAE performance criteria was observed along with the average of the estimated error (E) as shown in table below. The processes under test were first order plus dead time (FOPDT) process.

$$P_{KTL}(S) = \frac{K_P}{Ts+1} * e^{-Ls} \ldots\ldots\ldots (17)$$

Table1: Controller parameters for different Process parameters

E	K_p	L	T	L/T	K_c (opt) Matlab
0.38	0.5	0.1	1	0.1	11.7157
0.381	0.5	0.5	1	0.5	2.1989
0.387	0.5	2	1	2	0.0112
0.3872	0.5	1	2	0.5	2.2008
0.392	0.5	2	2	1	0.009
0.401	0.5	4	2	2	0.0058
0.3881	0.5	0.1	3	0	39.4482
0.3921	0.5	1	3	0.3	0.0115
0.416	0.5	6	3	2	0.0039
0.3942	0.5	0.5	4	0.1	8.8396
0.3963	0.5	1	4	0.3	4.2533
0.4111	0.5	4	4	1	0.0047
0.422	0.5	6	4	1.5	0.0036

0.433	0.5	8	4	2	0.003
0.363	1	1	1	1	0.009
0.37	1	2	1	2	0.0059
0.3701	1	1	2	0.5	0.0069
0.377	1	2	2	1	0.0047
0.3943	1	4	2	2	0.0029
0.378	1	1	3	0.3	0.0057
0.3863	1	2	3	0.7	0.8715
0.4044	1	4	3	1.3	0.0026
0.424	1	6	3	2	0.002
0.3821	1	0.5	4	0.1	4.0914
0.3864	1	1	4	0.3	2.1267
0.3912	1	1.6	4	0.4	1.3568
0.3952	1	2	4	0.5	1.1018
0.437	1	6	4	1.5	0.0018
0.464	1	8	4	2	0.0015
0.344	1.5	1	1	1	0.006
0.348	1.5	0.5	2	0.3	1.3646
0.3531	1.5	1	2	0.5	0.0044
0.3551	1.5	0.1	3	0	9.4915
0.3742	1.5	2	3	0.7	0.0027
0.3703	1.5	0.5	4	0.1	0.0046
0.3751	1.5	1	4	0.3	0.0033
0.45	1.5	6	4	1.5	0.0012
0.497	1.5	8	4	2	0.00099
0.318	2	0.1	1	0.1	0.0174
0.337	2	2	1	2	0.0029
0.3281	2	0.1	2	0.1	4.7457
0.3371	2	1	2	0.5	0.0033
0.3491	2	2	2	1	0.0024
0.3752	2	4	2	2	0.0015
0.3501	2	1	3	0.3	0.0027
0.3621	2	2	3	0.7	0.002
0.3532	2	0.1	4	0	9.4914
0.3642	2	1	4	0.3	1.0633
0.3792	2	2	4	0.5	0.0018
0.4132	2	4	4	1	0.0012

Using carve fitting techniques the tuning rule are found as shown below.
First a parameter (M_T) which describes the relation between the optimum value of the controller gain (K_c (opt)) and the average of the estimated error is found as follow:-

$$M_iT = (0.25502 * EXP((0.0019648/(K_ic * K_iP))) - 0.32209 * K_ic * K_iP))/E \ldots..(18)$$

Second a use of the parameter M_T to obtain the controller parameters is made as follow:-

$$K_c = \frac{0.2 + \frac{0.45}{M_T}}{K_p} \ldots\ldots(19)$$

$$T_i = \frac{\sqrt{E - 0.305}}{\frac{\sqrt{0.00328827}}{4}} \ldots\ldots(20)$$

$$T_d = \frac{\left(\left(\frac{1}{E}\right) + 2.103\right)}{20.414} \ldots\ldots(21)$$

Where $K_i = \frac{K_c}{T_i}$ and $K_d = K_c * T_d$

If the value of $(K_c \geq 50)$ then scale down the parameters value by factor equal to $(K_1(d))$. The new controller parameters will be equal to:-

$$(K_c = \frac{K_c}{K_d}) \quad \text{And} \quad (K_i = \frac{K_i}{K_d}) \quad \text{and} \quad (K_1(d) = 1)$$

6. MATLAB SIMULATION RESULTS

Several processes were taken under test to simulate the efficiency of the proposed tuning rules. All processes were Fist order Plus Dead Time. A reduction procedure is used to modulate the higher order models in the FOPDT model
The processes which are used in the simulation are:-

$$G_1(s) = \frac{1}{(s^2 + 1.4s + 1)} = \frac{0.99 * e^{-0.73s}}{0.885s + 1} \ldots\ldots(22)$$

$$G_2(s) = \frac{10 * e^{-5}}{(s+1)(s+2)(s+3)(s+4)} = \frac{0.4169 * e^{-2.16s}}{1.1696s + 1} \ldots(23)$$

$$G_3(s) = \frac{10}{(s+1)(s+2)(s+3)(s+4)} = \frac{2.941 * e^{-0.76s}}{1.96s + 1} \ldots(24)$$

$$G_4(s) = \frac{0.5 * e^{-0.5s}}{2s + 1} \ldots\ldots(25)$$

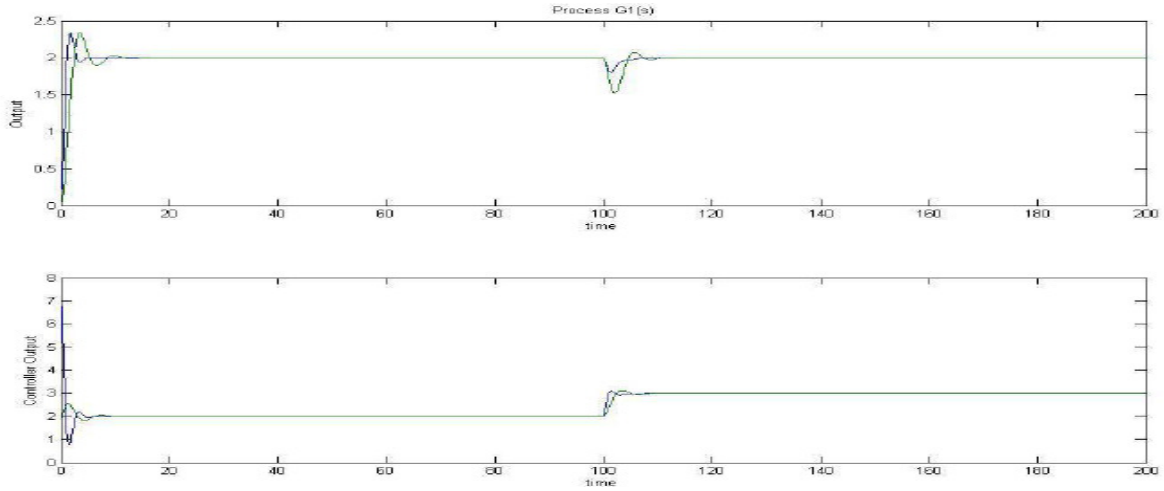

Figure 1: Second order process Step response

Table 2: The response parameters values of AMIGO and Proposed tuning rule for the process $G_1(s)$.

Algorithm	Rise time (s)	Settling Time (s)	Set point overshoot	IAE (disturbance)
AMIGO	2.3	5.00	15.08%	11.8479
Proposed tuning rule	1.1	2.5	16.82%	4.9772

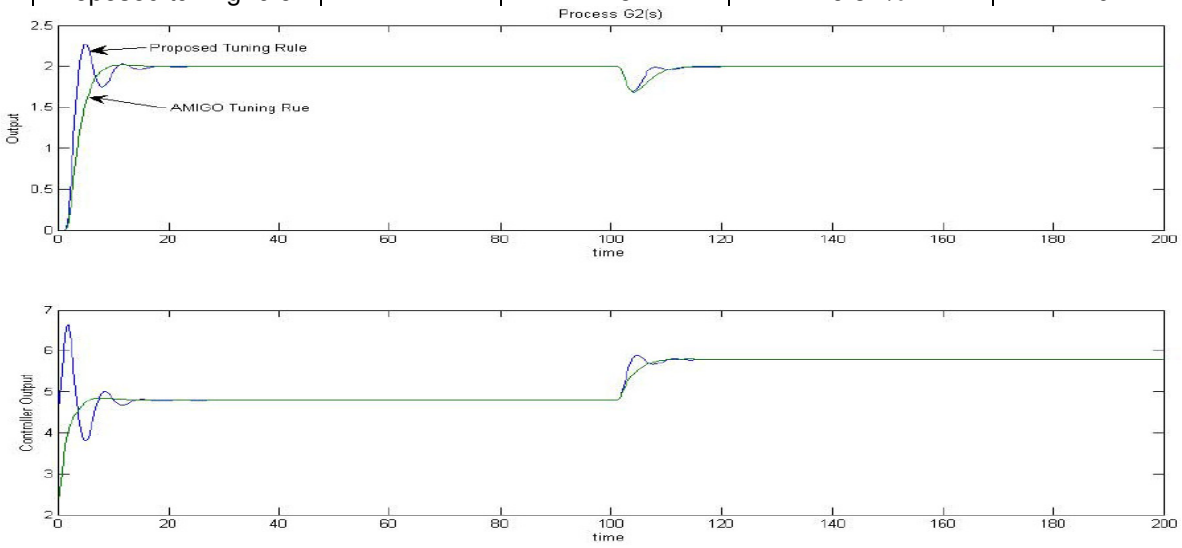

Figure 2: High order process with delay Step response

Table 3: The response parameters values of AMIGO and Proposed tuning rule for the process $G_2(s)$.

Algorithm	Rise time (s)	Settling Time (s)	Set point overshoot	IAE (disturbance)
AMIGO	6.2	7.3	0.9%	11.95
Proposed tuning rule	3.6	9.8	13.6%	16.03

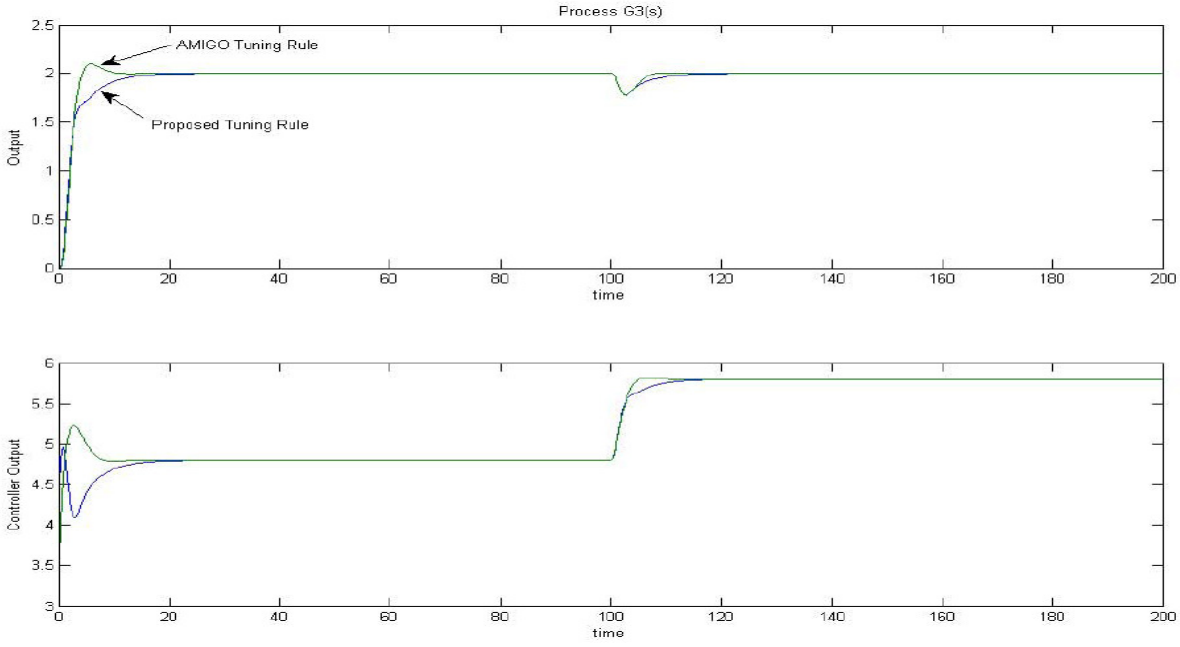

Figure 3: High order process without delay Step response

Table 4: The response parameters values of AMIGO and Proposed tuning rule for the process $G_3(s)$.

Algorithm	Rise time (s)	Settling Time (s)	Set point overshoot	IAE (disturbance)
AMIGO	6.2	3.8	4.9%	7.93
Proposed tuning rule	3.4	9.2	0.0%	11.74

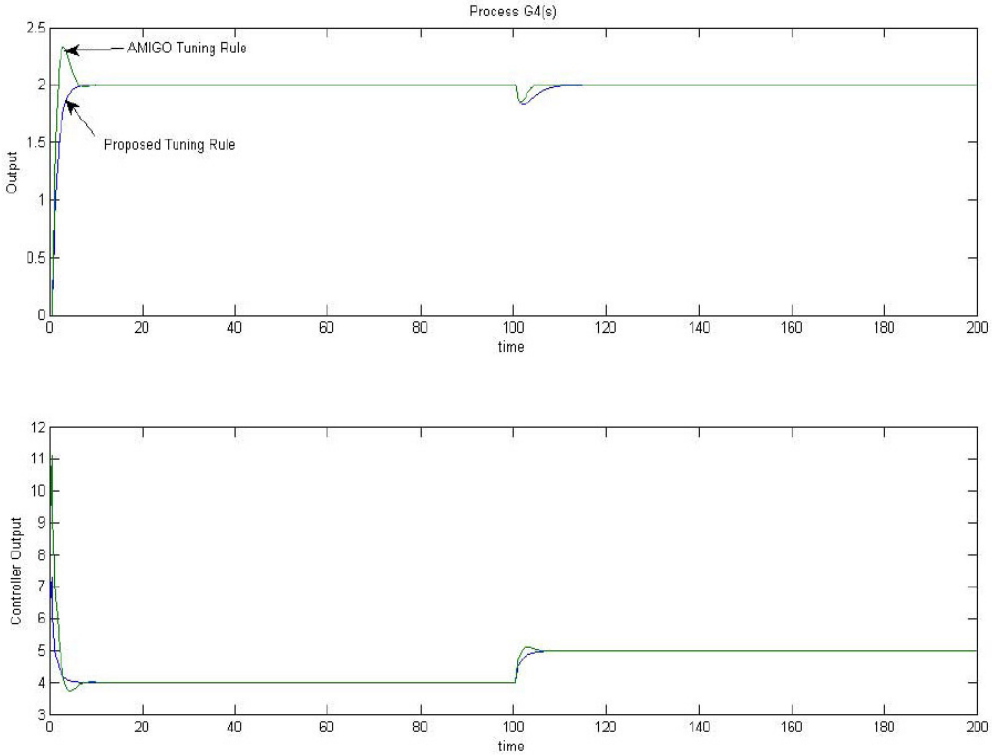

Figure 4: First order process with delay (FOPDT) Step response

Table 5: The response parameters values of AMIGO and Proposed tuning rule for the process $G_4(s)$.

Algorithm	Rise time (s)	Settling Time (s)	Set point overshoot	IAE (disturbance)
AMIGO	1.6	5	16.76%	3.21
Proposed tuning rule	3.0	4	0.0%	8.16

7. CONCLUSION

Based on the results of the simulations for the process models chosen for this analysis, conclusion can be drawn out that the proposed tuning rule may give slow but highly robust and stable response and no overshoot for most processes while it may give a fast response but in the expense of high overshoot and long settling time. The proposed tuning rule is the easiest to apply to find the necessary settings, and is applicable to a wide range of process types. Also, over a range of modified parameters, the proposed tuning rules can be improved slightly, but only by sacrificing stability and robustness. The most important advantage of this design is in the use of the IATE performance criteria index along with the grey prediction algorithm to find the new tuning rule since it can provide the controller with a good performance and also it eliminates the need of knowing the process parameters

since we only need to know the average of the estimated error and the process gain K_c. As it appears from the simulation, the proposed tuning rule is able to deal with the possible variation of system parameters. It is so obvious that the proposed tuning rule has the same or better performance than AMIGO tuning rule. The observation from those results shows that a high overshoot appears in the output of the system for some cases of processes. This overshoot appears as expense of achieving a high response and a better load disturbance rejection. The proposed tuning rule is also able to deal with the process parameters change since the approximation of FOPDT is not accurate. The limitation of this proposed tuning rule is concentrate in the initial value of the PID controller because it must lead the system to behave under damp behavior. The concluded important contributions in this paper regarding the use of the proposed tuning rule are that it proves the ability of the proposed tuning rule in tuning the PID controller probably with only need of small information about the process parameters (only K_p is needed). Also it validates the flexibility of the proposed tuning rule to deal with different modeling systems with different parameters.

II. REFRENCES

[1] Dingyu Xue, YangQuan Chen. Derek P. Atherton. "Linear Feedback Control" Society for Industrial and Applied Mathematics. 2007.

[2] Guillermo J. Silva, Aniruddha Datta. S. P. Bhattacharyya. “PID Controllers for Time-Delay Systems”. Boston. ISBN 0-8176-4266-8.2005.

[3] Hang, C.C, K.J.Astrom and W.K. Ho, “refinement of Ziegler-Nichols Tuning Formula”, IEE Proc. Pt. D, Vol. 138, pp. 111-118 .1991.

[4] J. G. Ziegler and N. B. Nichols, “Optimum Settings for Automatic Controllers,” Trans. ASME, Vol. 64, pp. 759-768, 1942.

[5] J. L. Deng, "Introduction to Grey System Theory," The Journal of Grey System, vol., pp. 1-241, 1989.

[6] K.J.Astrom, T.Hagglund, “Revisiting the Ziegler–Nichols step response method for PID control”, Journal of Process Control 14,635–650, Department of Automatic Control, Lund Institute of Technology. 2004.

[7] Lasse M. Eriksson and Mikael Johansson, “PID Controller Tuning Rules for Varying Time-Delay Systems”, Proceedings of the 2007 American Control Conference ,New York City, USA, July 11-13, 2007.

[8] Panagopoulos H., Astrom K. J., Hagglund T., “Design of PID Controllers Based on Constrained Optimisation”, IEE Proc., Control Theory Appl., Vol. 149, No. 1. – P. 32–40. 2002.

[9] P. Cominos and N. Munro, “PID Controllers: Recent Tuning Methods and Design to Specification,” IEE Proc. D, Control Theory and Applications, Vol. 149, No. 1, pp. 46-53, 2002.

[10] Si-Feng Liu, Member, IEEE, Jeffrey Forrest, “Advances in Grey Systems Theory and Its Applications”, Proceedings of 2007 IEEE International Conference on Grey Systems and Intelligent Services, November 18-20, 2007, Nanjing, China.

Evaluation of Heat Transfer Shear of Different Mechanisms in Subcooled Nucleate Boiling

Mohammadreza Nematollahi nema@shirazu.ac.ir
School of Mechanical Engineering
Shiraz University
Shiraz, 71348-51154, Iran

Mohammad Nazififard mnazifi@shirazu.ac.ir
School of Mechanical Engineering
Shiraz University
Shiraz, 71348-51154, Iran

Abstract

Since the mean characteristic of nucleate boiling is bubble formation and collapse near the heating surface, in this study attempts have been made to investigate heat transfer effects due to the bubbles ebullition and collapse cycle. All possible heat transfer mechanisms are studied qualitatively and quantitatively. For quantitative calculation of the heat transfer portion by each of the introduced mechanisms, a series of bubble parameters was selected from the experimental data provided by the high-speed photography of a heated rod containing nucleate boiling regime on its surface. According to the present results, the portion of the mechanisms such as latent heat transfer, super heated layer mixing and single-phase heat transfer are between 6~15%, 12~17%, and 3~5%, respectively. The results also show that the two mechanisms of the turbulence induced by the bubble formation and collapse and quenching have the main performance in transferring heat from the heating surface to the bulk flow. The shared percentage of these two mechanisms is estimated between 23~58.5% and 20.5~40% respectively.

Keywords: *Bubble, Heat Transfer, Nucleate Boiling, Quenching & Turbulence*

1. INTRODUCTION

The ability of subcooled boiling flow for transferring high heat loading in compact area without a significant void fraction and heating surface temperature increase has caused it to be widely used in industry. Because of the special characteristics of subcooled boiling flow, this technique is used for making compact heat exchangers, or transferring high heat loadings in nuclear plants. Using the subcooled boiling technique, transferring heat fluxes of up to 10^8 W/m^2 are reported to be attainable through high velocities, large subcooling, small diameter channels and short heated lengths [1].

Vandervort et al. (in 1992) have identified all possible mechanisms for subcooled boiling [2]. Their explanation is divided into two different parts of; 1) the bubble growing on the heated surface and 2) the bubble detachment from the heated surface.

In recent studies Nematollahi et al. [3] ,according to their experimental study, addressed the nine mechanisms as the following:

(1) Single-phase forced convection
(2) Local dispersion of the super heated layer around the active cavity due to implosive bubble formation that is referred to as super heated layer
(3) Latent heat transport due to bubble collapse
(4) Vapor/liquid interchange due to the bubble departure that is addressed as quenching
(5) induced micro-convection due to evaporation of the entrapped water from the cavity
(6) induced micro-convection due to the boundary layer motion around the bubble
(7) Micro-convection due to the special manner of the bubble collapse
(8) Transferring of heat and kinetic energy by the stable micro-bubble to the bulk flow
(9) Marangoni-force induced micro-convection

The introduced mechanisms of 5,6,7,8 and 9 could count as a comprehensive mechanism of the *turbulence induced by the bubble formation and collapse* because of their similarity in creation of turbulence by inducing micro-convection.

In the present study an attempt was made to investigate the mechanisms of heat transfer in a subcooled boiling condition by analyzing bubble behavior in subcooled boiling flow on a heated rod using the technique of high-speed photography. The bubble behavior at three locations 1, 25 and 45 cm from the beginning of a heated rod were analyzed at different conditions of subcooling temperature, linear power density and flow rate. For the evaluation of the heat transfer shear of different mechanisms in nucleate boiling, and the quantitative calculation of partial heat transfer by each of the introduced mechanisms, a series of bubble parameters was selected from the experimental data provided by high-speed photography of a heated rod having a nucleate boiling regime on its surface.

2. Experimental apparatus and procedure of the High-Speed Photography

Fig. 1 shows the schematic view of the test loop. The subcooled boiling was performed by Joule heating on the middle part of the stainless steel rod, which has high electrical resistance compared to the rest of the rod made by copper. Flow of distilled water was used as the recirculating coolant in the loop. A power between 0~60 kW was supplied from a voltage regulator and a transformer connected to an electrical power line with 200V and 300A electricity current.

The rod diameter and length of the heated surface of the rod are 10 mm 50 cm, respectively. The outer tube of the test section was made of glass having 30mm inner diameter, which was permitted visual observation. In the present experiment, several different conditions were chosen such as different incoming coolant subcooling temperature 25, 50 and 75K, coolant flow velocities 16, 32, 53 cm/sec and imposed linear power densities 100~600, W/cm for the interracial high-speed photography from the heating surface.

High-speed photography was performed using a KODAK EKTAPRO High-speed Motion Analyzer (model 4540), which contains an imager, a processor and a keypad. By using this system photographic pictures were able to be taken from 30 to 40500 frames per second. This system was connected with three other accessories, a computer, a monitor and a video tape recorder. Fig. 2 shows the experimental setup of the high-speed photography.

The high-speed photography was operated at 13500 frames per second in different conditions of subcooled boiling. The taken pictures would cover the cross-section 2.5mm X 2.5mm of the visible test section. This was achieved by using a 100mm telephoto lens (SMC PENTAX-M MACRO 1:4 100mm) with a 180mm extended tube. The slow motion behaviors (10 frames per second) of the bubble for five minutes were recorded on videotape by the video tape recorder for each condition For each condition a minimum of 200 consequential images of the bubble behaviors have been saved in the computer memory. The bubble behaviors were visualized for four different conditions which were in different heights, inlet subcooled temperatures, linear power densities and flow rates.

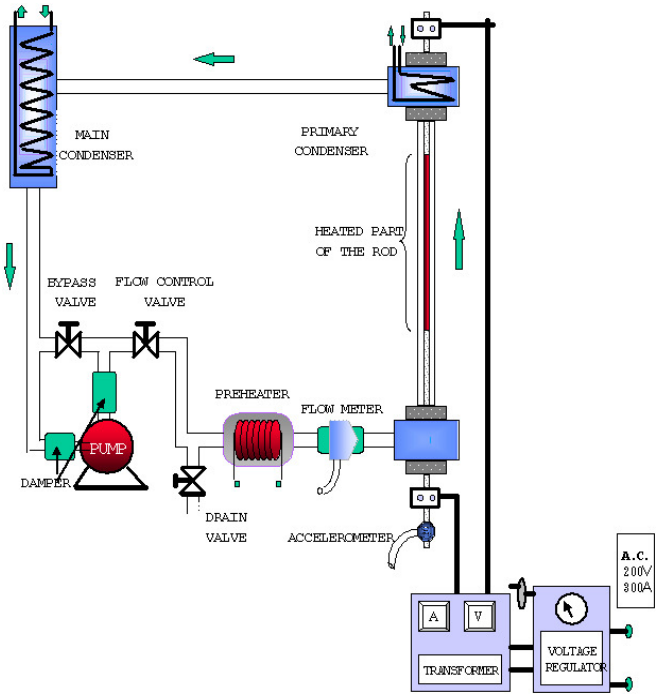

Fig.1: Schematic diagram of the experimental setup

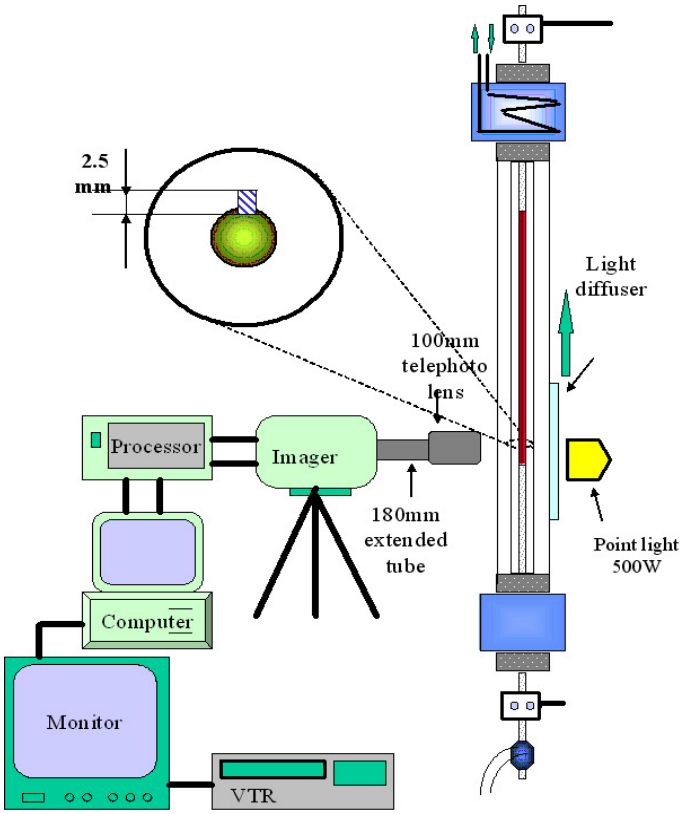

Fig. 4: Experimental setup of high-speed photography

3. Experimental Results

The behavior of bubbles in different conditions of subcooling temperature, linear power density and flow rate was analyzed using high-speed photography. The observed behaviors can be divided into two main categories:
a) General aspects of interfacial behavior of the coolant in subcooled boiling flow
b) Specific aspects of bubble behavior at different subcooled boiling flow conditions.
A brief explanation on the results is presented here.

3.1. General aspects

In all cases in which the bubble formed on the heating surface, a thin shear flow, which looks similar to a dark fluid layer in the photographs, covers the heating surface. The darkness of the thin layer can be explained by the difference in the reflection angle of the back light due to the temperature difference between the subcooled water and the saturated or superheated water. This thin layer disappears in the linear power densities less than that required for the onset of nucleate subcooled boiling flow, and in the low subcooling or in the saturated conditions.
High-speed photography of the bubble ebullition cycle shows that vapor blown from a cavity forms as a bubble with a hemispheric or an elongated hemispheric shape. This process occurs during a short interval between less than 74 μs to around 222 μs, depending on parameters such as linear power density, subcooling, and cavity characteristics. The motion of water in the layer around the bubble causes the bubble to separate from the heating surface. The contact area of the bubble with the wall starts to shrink. This continues until the bubble adheres to the wall at a single point, at which time the bubble becomes similar to a balloon. This process is followed by the ejection of the bubble from the surface. Most of the bubble volume condenses in bulk flow near the surface. The collapse starts from the bottom of the bubble. It appears that the condensation rate from the bottom is much more notable than the bubble top.
Condensation of the bubble and the work due to surface tension cause a balloon type bubble to change into a micro-bubble with a diameter around one fiftieth of that of the original bubble. Immediately after its formation, the micro-bubble escapes very rapidly from its location towards the bulk flow. A micro-bubble has a relatively high kinetic energy. In addition to this, a simple theoretical calculation shows that the inside pressure and temperature of the micro-bubble are both relatively much higher than the original bubbles height. These states can keep micro-bubbles much more stable. Due to this stable characteristic of micro-bubbles, the authors call it "stable micro-bubble" or in brief "SMB". A general bubble behavior in subcooled boiling flow is shown in Fig. 3.

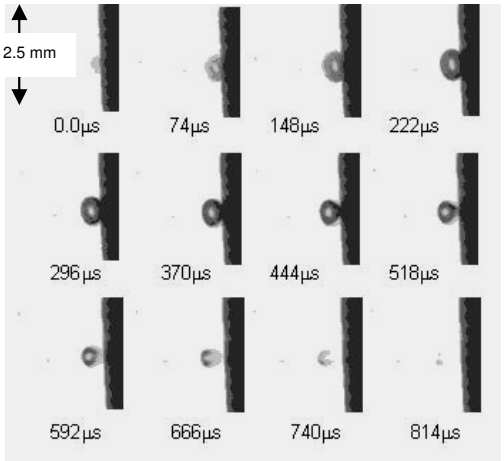

Fig. 3: Typical bubble ebullition cycle in subcooled boiling flow

Table 1: The summery results of the bubble behavior in three subcooled temperatures of the 75, 50 and 25K in fixed LPD 182W/cm at the 1, 25 and 45cm

Degree of Sub-cooling	Attitude	Bubble sites number in 2.5 mm	Bubble growing-time (μs)	Bubble life time (μs)	Bubble max-diameter (μm)	Bubble emission frequency (H z)	Super-Heated-Layer Thickness (μm)
75K	1	3	74~148	148~370	125~435	135~1555	60
	25	4	74~148	148~370	125~280	135~1350	100
	45	5	~148	148~444	156~625	205~540	130
50K	1	4	~148	148~444	94~375	205~945	85
	25	6	~148	148~519	218~500	270~340	115
	45	8	148~222	296~519	155~685	135~475	135
25K	1	6	~148	296~1111	250~685	135~880	55
	25	8	~148	444~889	315~685	205~475	?no
	45	9	148~222	740~1481	440~500	405~610	no

Table 2: The summery results of the bubble behavior in the LPDs of the 182, 290, 430 and 600W/cm in fixed subcooled temperature 75K at the 1, 25 and 45cm

LPDW/cm	Attitude (cm)	Bubble sites number in 2.5 mm	Bubble growing-time (μs)	Bubble lifetime (μs)	Bubble max-diameter (μm)	Bubble emission frequency (Hz)	Super-heated-layer thickness (μm)
600	1	many	? (<<74)	?(<74)	-	-	115
	25	Film Boiling					230~315
	45						285~360
430	1	20	<74	148~222	185	405~880	85
	25	Film Boiling					200~285
	45						215~300
290	1	6	74~148	148~222	125~280	270~1015	70
	25	10(4)	74~148	148~296	95~280	270~945	140~170
	45	12(2)	~74	148~222	65~185	205~610	140~200
182	1	3	74~148	148~370	125~435	135~1555	60
	25	4	74~148	148~370	125~280	135~1350	100
	45	5	~148	148~370	156~625	205~540	130

Table 3: The summery results of the bubble behavior in the flow velocities of the 16, 32 and 53cm/s in fixed LPD of the 182W/cm and subcooling 75K at the 1, 25cm

Flow Rate	Attitude (cm)	Bubble sites number in 2.5 mm	Bubble growing-time (μs)	Bubble lifetime (μs)	Bubble max-diameter (μm)	Bubble emission frequency (Hz)	Super-heated-layer thickness (μm)
53 cm/s	1	3	74~148	148~370	125~435	135~1555	60
	25	4	74~148	148~370	125~280	135~1350	100
32 cm/s	1	4	~148	222~593	~250	135~745	85
	25	6(1)	74~148	~370	80~315	~540	100
16 cm/s	1	4	~148	296~740	59~780	135~745	100
	25	7(1)	~148	~296	80~280	205~475	115

1. The density of active nucleation sites increased with increasing linear power densities and decreasing subcooled temperature.

2. The average bubble maximum diameter decreased with increasing linear power density and subcooled temperature.

3. The bubble emission frequency depends upon the sites.

However, it increased with increasing linear power density and subcooling.

4. Bubble growth time varies between 74μs and 222μs. For large bubbles the results show that increasing boiling length and decreasing linear power density, subcooled temperature or the flow rate will slightly increase bubble growth time.

5. Shorter growth time occurred in lower subcooling temperatures and higher linear power densities.

For a typical bubble the main parameters for linear power density 182 W/cm are listed in Table 4.

Table 4 Typical bubble parameters extracted from the experimental results for linear power density 182 W/cm

Average cavity diameter	Bubble growing time	Bubble life time	Bubble maximum diameter
59 (μm)	148(μs)	500(μs)	555(μm)

3.3. Evaluation of Heat Transfer Shear of Different Mechanisms

In this research the following mechanisms are considered as the most important because of their higher portion in the heat removal from the heating surface:

1. Quenching
2. Super heated layer mixing
3. Latent heat transfer
4. Single-phase heat transfer
5. Turbulent induced by bubble formation and collapse

The quantitative heat transfer portion in percentage for each of the above first four mechanisms was calculated for a typical bubble parameter presented in Table 5. Based on the available models in the literature, there was no exact model for the calculation of the turbulent induced by bubble formation and collapse. Therefore the portion percentage of the turbulent mechanism was calculated by subtracting the summation of the four other mechanisms portion percent from one hundred percent. The evaluated heat transfer shears of the different mechanisms are presented in Table 5.

Table 5. The evaluated heat transfer shear of the different mechanisms

MECHANISMS TYPE	PORTION
Quenching [4,5,6]	(20.5~40)%
Super Heated Layer Mixing [6]	(12~17)%
Latent Heat Transfer [6,7,8,11]	(6~15)%
Single-Phase Heat Transfer [6,9,10,11]	(3~5)%
Turbulent Induced by Bubble Formation And Collapse	(23~58.5)%
Total	100%

As can be seen from Table 5, because of using a different model for calculation of the heat transfer percentage of the four first mechanisms, the portion percentages are expressed in

ranges. The calculated portion percentage for the turbulent induced by the bubble formation and collapse is estimated to be between 23~58%.
The results show that *turbulence induced by the bubble formation and collapse* play a very considerable role in nucleate boiling heat transfer by inducing micro-convection in the different manners of:
(1) induced micro-convection due to evaporation of the entrapped water from the cavity
(2) induced micro-convection due the boundary layer motion around the bubble
(3) Micro-convection due to the special manner of the bubble collapse
(4) Transferring heat and kinetic energy by the stable micro-bubble to the bulk flow
Marangoni-force induced micro-convection

4. Conclusion
The results show that the mechanisms of quenching and turbulent induced by bubble formation and collapse, have between 20.5~40% and 23~58.5% the portion percentage in heat transfers from the heating surface to the bulk flow, respectively. According to the present results, the portion of other mechanisms such as latent heat transfer, super heated layer mixing and single-phase heat transfer are between 6~15%, 12~17%, and 3~5%, respectively. Therefore, it can be concluded that the *quenching* and the *turbulence induced by the bubble formation and collapse* mechanisms play the most important role in nucleate boiling heat transfer by vapor/liquid interchange and inducing micro-convection, respectively.

References

[1] Omatskii A.P. and Vinyarskii L.S., 1965, "Critical Heat Transfer in the Forced Motion of Under Heated Water-Alcohol Mixtures in Tubes of Diameter 0.5mm", Teplofizika Vyskikh Temperatur (High Temperature), Vol. 3, No. 6, pp. 881-3.

[2] Vendervort C., Bergles A. E. and Jensen M. K., "Heat Transfer Mechanisms in Very High Heat Flux Subcooled Boiling", Fundamentals of Subcooled Flow Boiling, 1992, HTD-Vol. 217, pp. 1-9.

[3] Nematollahi M. R., "Doctoral Thesis on Fundamental Study of Vibration Phenomena Induced by Subcooled Flow Boiling." Dept. of Quantum Science and Energy Engineering High Loading Energy Engineering Laboratory.February, 1999.

[4] Maruyama S., shoji M., "Numerical Simulation of Boiling Heat Transfer.", department of mechanical Engineering, faculty of Engineering the University of Tokyo, Tokyo, Japan.

[5] Del Valle M. V. H. and Kenning D. B. R., "Subcooled Flow Boiling at High Heat Flux", Int. J. Heat &Mass Transfer, 1985, Vol.28, pp.1907-1920.

[6] Ebrahimi M. Master thesis on Behaviour of Bubble in Nucleate Boiling, Shiraz University, Shiraz, Iran, June 2002.

[7] Manon E., Mimouni S. "3D Simulations Of Subcooled Boiling Flows with ASTRID, Comparisons with The DEB Experimental Results", 2001.

[8] Giese T., Laurien E.,"A Three Dimensional Numerical Model for The Analysis of Pipe Flow with Cavitation ", Institute of Nuclear Technology and Energy Systems (IKE) University of Stuttgart, Pfaffenwaldring 31, D-70550 Stuttgart, Germany.

[9] Ronald D. and Meng X.," Local subcooled flow boiling model development". Prairie View A&M University, College of Engineering and Architectore Thermal Science Research Center, 1996.

[10]Wolvering, Tube Heat Transfer Data Book."Boiling Heat Transfer", P 255-265.

[11] Das A.K., Das P.K., Saha P. ,"Heat transfer during pool boiling based on evaporation from micro and macrolayer", International Journal of Heat and Mass Transfer 49 (2006) 3487–3499.

Analysis of Unequal Areas Facility Layout Problems

P.Arikaran arivarsini_2006@yahoo.com
Research scholar,
Dept. of Manufacturing, Anna University,
Chennai 600 025 India
Professor & H.O.D.,Dept. of Mechanical Engineering,
M.N.M. Jain Engineering College,
Chennai 600097, phone: 9444154329

Dr. V. Jayabalan jbalan@annauniv.edu
Professor, Dept. of Manufacturing
and Controller of Examinations, Anna University,
Chennai 600 025 India

R. Senthilkumar rskumar1967@yahoo.com
Assistant Professor, Dept.of Mechanical Engineering,
M.N.M. Jain Engineering College,
Chennai 600097, India

Abstract

The facility layout design has been regarded as the key to improve plant productivity, which are relevant to both manufacturing problems; various optimization approaches for small problems and heuristic approaches for the larger problems have been proposed to elucidate the problem. Unequal area facility layout problems comprise a class of extremely difficult and widely applicable optimization problems, arising in many diverse areas. There are many variations on the basic formulation, involving alternative objective functions, side constraints, distance metrics, cost measures, and facility shapes. Various techniques were applied after finding the solution through traditional methods to get much improved optimum solutions. Different heuristics were used to solve the unequal area facility layout problems. Multi-objective approaches are the norm and developing facility layout software using meta-heuristics such as simulated annealing (SA), genetic algorithm (GA), ant colony algorithm (ACO), and concurrent engineering is prevailing nowadays. Sometimes hybrid approaches were used by applying combination of above techniques i.e. combining high level genetic algorithm with simulated annealing or genetic algorithm followed by simulation techniques to get the better solutions. Application of these facility lay out designs includes construction sites, manufacturing industry and service industries.and service sectors. Facility Layout Problems (FLPs) are known to be NP-hard

Keywords—Facility layout, unequal area , Hybrid methods , Genetic Algorithm, Automated layout Manufacturing Industries, construction sites.

1.INTRODUCTION

The static facility layout problem (SFLP) is a well-researched problem of finding positions of departments on the plant floor such that departments do not overlap while some objective is optimized. The most commonly used objective is minimizing material handling cost (i.e., minimizing the sum of the product of the flow of materials, distance, and transportation cost per unit per distance unit for each pair of departments). When material flows between departments change during the planning horizon, the problem becomes the dynamic facility layout problem (DFLP).

A solution to the FLP is a block layout that specifies the relative location and the dimensions of each department. Once a block layout has been achieved, a detailed layout can be designed which specifies department locations, aisle structures and input/output point locations [3, 6, 7]. Two types of approaches for finding provably optimal solutions for the FLP have been proposed in the literature. The first type are graph-theoretic approaches that assume that the desirability of locating each pair of facilities adjacent to each other is known. Initially, the area and shape of the departments are ignored, and each department is simply represented by a node in a graph. Adjacency relationships between departments can now be represented by arcs connecting the corresponding nodes in the graph. The objective is then to construct a graph that maximizes the weight on the adjacencies between nodes. We refer the reader to [4] for more details. The second type are mathematical programming formulations with objective functions based on an appropriately weighted sum of centroid-to-centroid distances between departments. Exact mixed integer programming formulations were proposed for the above type was shown in [8,9].

2. UNEQUAL AREA LAYOUTS

The unequal-areas facility layout problem (FLP) is concerned with finding the optimal arrangement of a given number of non-overlapping indivisible departments with unequal area requirements within a facility. The block layout design problem with unequal areas, which was originally formulated by Armour and Buffa in the early 1960s, is a fundamental optimization problem encountered in many manufacturing and service organizations. Different methods were discussed for solving unequal area problems in Literature. These methods are summarized under the various topics to have a understanding of Unequal area problem.

2.1 Tree structure Model

The facility layout design has been regarded as the key to improve plant productivity, which are relevant to both manufacturing and service sectors. A tree structure model has been proposed for representing the unequal-area facility layout by[10]. Each facility has a different rectangular shape specified by its area and aspect ratio. In this layout problem, based on the assumption that the shop floor has enough space for laying out the facilities, no constraint is considered for a shop floor. Objectives are minimizing total part movement between facilities and total rectangular layout area where all facilities and dead spaces are enclosed. Using the genetic code corresponding to two kinds of information, facility sequence and branching positions in the tree structure model, a genetic algorithm has been applied for finding non-dominated solutions in the two-objective layout problem. [10] used three kinds of crossover (PMX, OX, CX) for the former part of the chromosome and one-point crossover for the latter part. Two kinds of layout problems have been tested by the proposed method. The results demonstrated that the presented algorithm was able to find good solutions in enough short time.

2.2 Genetic Search

[23] used Genetic search for solving construction site-level unequal-area facility layout problems. A construction site represents a conflux of concerns, constantly calling for a broad and multi-criteria approach to solving problems related to site planning and design. As an important part of site planning and design, the objective of site-level facility layout is to allocate appropriate locations and areas for accommodating temporary site-level facilities such as warehouses, job offices, workshops and batch plants. Depending on the size, location and nature of the project, the required temporary facilities may vary. The layout of facilities can influence on the production time and cost in projects. [23]described a construction site-level facility layout problem as allocating a set of predetermined facilities into a set of predetermined places, while satisfying layout constraints and requirements. A genetic algorithm system, which is a computational model of Darwinian evolution theory, was employed to solve the facilities layout problem. A case study was presented to demonstrate the efficiency of the genetic algorithm system in solving the construction site-level facility layout problems

2.3 Hybrid Method

[12] presented the solution of the unequal area problem by hybridizing the meta-heuristic methods i.e. Genetic Algorithm (GA) and Simulated Annealing (SA). (SA) is a related global optimization technique that traverses the search space by testing random mutations on an individual solution. A mutation that increases fitness is always accepted. A mutation that lowers fitness is accepted probabilistically based on the difference in fitness and a decreasing temperature parameter. In SA parlance, one speaks of seeking the lowest energy instead of the maximum fitness. SA can also be used within a standard GA algorithm by starting with a relatively high rate of mutation and decreasing it over time along a given schedule.

[12] could be used in future as a reference for those researchers interested in tackling this challenging unequal facility layout problem. A mathematical model was developed for the unequal size facility layout problem with fixed flow between departments. The orientations of the departments with various sizes were considered to minimize the distance traveled by people, material, and other supporting services in the safest and most effective manner. Some of the constraints considered in the modeling were the restricted areas, reserved department locations, and also the irregularity of the shapes of manufacturing layout. This paper has also presented the use of hybrid algorithm (GA - SA) as a general methodology to solve the facility layout problem under consideration.

A hybrid optimization approach was presented in [21] for the layout design of unequal-area facilities. Simulated annealing was used to optimize a randomly generated initial placement on an “extended plane” considering the unequal-area facilities enclosed in magnified envelop blocks. An analytical method was then applied to obtain the optimum placement of each envelop block in the direction of steepest descent. Stepwise reduction of the sizes of the envelop blocks allowed controlled convergence in a multi-phase optimization process. The presented test problems include two large size benchmark problems of 50 and 100 facilities of unequal areas. The results indicated a significant improvement over previously published techniques for unequal-area facilities and could yield solutions of the same quality as obtained by PLANOPT, a general-purpose layout optimization program based on pseudo-exhaustive search.

2.4 Convex Optimization Framework

[13] presented a convex-optimization-based framework for efficiently finding competitive solutions for this problem. The framework is based on the combination of two mathematical programming models. The first model is a convex relaxation of the layout problem that establishes the relative position of the departments within the facility, and the second model uses semi-definite optimization to determine the final layout. Aspect ratio constraints, frequently used in facility layout methods to restrict the occurrence of overly long and narrow departments

in the computed layouts, are taken into account by both models. It suggested that using ellipsoids instead of circles to approximate the initial positions of departments could provide better results and Ellipsoids would likely provide more realistic estimations of department positions, since departments in real-world applications are not square-shaped. Further work also included adjusting the φ (the parameter that can control what the desired smallest length or width should be in each department's layout) and potentially using a different value φi for each department. Finally, different combinations of first stage and second stage models from past papers tested to get the over all results.

2.5 Tabu search Method

Tabu search (TS) is similar to simulated annealing in that both traverse the solution space by testing mutations of an individual solution. While simulated annealing generates only one mutated solution, tabu search generates many mutated solutions and moves to the solution with the lowest energy of those generated. In order to prevent cycling and encourage greater movement through the solution space, a tabu list is maintained of partial or complete solutions. It is forbidden to move to a solution that contains elements of the tabu list, which is updated as the solution traverses the solution space.

[14] discussed a slicing tree based tabu search heuristic for the rectangular, continual plane facility layout problem by incorporation of facilities with unequal areas and integrated the possibility to specify various requirements regarding (rectangular) shape and dimensions of each individual facility by using bounding curves which made possible to solve problems containing facilities of fixed and facilities of flexible shapes at the same time. This paper presented a procedure that calculated the layout corresponding to a given slicing tree on the basis of bounding curves and integrated the tabu search to find the better results. [19] proposed a heuristics for the dynamic facility layout problem with unequal-area departments. The solution is improved using a tabu search heuristic. The heuristics were tested on some instances from the DFLP and static facility layout problem (SFLP) literature. The results obtained demonstrated the effectiveness of the heuristics.

2.6 Genetic Algorithm

[15] presented a genetic algorithm-based model for facility layout problems with unequal departmental areas and different geometric shape constraints. Gene structures of the genetic algorithm are used to represent layout of departments. The algorithm involved deriving an initial assignment of departments to the given floor plan and then, possibly, improving the solution quality through genetic algorithm mechanisms (i.e., exchange parts of layout). Since genetic algorithm is parameter sensitive, the experiments indicated that crossover type, mutation type, mutation probability, and population size which are the main parameters that designers need to consider while designing facility layout with genetic algorithm. Guidelines for such parameters were also given.

[11] presented a heuristic search methodology, based on genetic algorithms (GA), for unequal area layout. this methodology was applied to several standard test problems from the literature, and was showed that the GA method gave solutions which were much better than the best previously reported solutions.[11] used penalty-directed search to find very good solutions to problems with difficult-to-satisfy side constraints, and to perform multi-criterion optimization with respect to cost measures that have been considered incommensurable in the past. The methodology presented in [11] is not intrinsically restricted to layout problems, but could be extended to other hard combinatorial problems. The GA/penalty method's ability to find improved solutions to known problems, together with the ability to address problems with ill-behaved cost functions, multiple objectives, and/or side constraints, constitutes a significant contribution to the state of the art in facility layout. Furthermore, GA could be implemented to

take advantage of parallel hardware to an extent not possible for other heuristic optimization methods.

[18] outlined a GA based algorithm for solving the single-floor facility layout problem with departments of both equal and unequal sizes. The GA performance was evaluated using several test problems available in the literature. The results indicated that GA may provide a better alternative in a realistic environment where the objective is to find a number of "reasonably good" layouts. The implementation also provided the flexibility of having fixed departments and to interactively modify the layouts produced.

[24] gave a solution to the unequal area facilities layout problem by genetic algorithm. The majority of the issued facilities layout problems (FLPs) minimize the material handling cost and ignore other factors, such as area utilization, department shape and site shape size. These factors, however, might influence greatly the objective function and should give consideration. The research range of [24] was focused on the unequal areas department facilities layout problem, and implement analysis of variance (ANOVA) of statistics to find out the best site size of layout by genetic algorithm. The proposed module took the minimum total layout cost (TLC) into account. TLC was an objective function combining material flow factor cost (MFFC), shape ratio factor (SRF) and area utilization factor (AUF). In addition, a rule-based of expert system was implemented to create space-filling curve for connecting each unequal area department to be continuously placed without disjoint (partition). In this manner, there was no gap between each unequal area department. The experimental results showed that the proposed approach is more feasible in dealing with the facilities layout problems in the real world.

2.7 Swarm Optimisation

Layout of temporary facilities on a construction site is essential to enhancing productivity and safety, and is a complex issue due to the unique nature of construction. [16] proposed a particle swarm optimization (PSO)-based methodology to solve the construction site unequal-area facility layout problem. A priority-based particle representation of the candidate solutions to the layout problem was proposed. The particle-represented solution in terms of priorities should be transformed to the specific layout plan with consideration of non-overlap and geometric constraints. In addition, a modified solution space boundary handling approach was proposed for controlling particle updating with regard to the priority value range. Computational experiments were carried out to justify the efficiency of the proposed method and to investigate its underlying performances. This paper claimed to provide an alternative and effective means for solving the construction site unequal-area layout problem by utilizing the PSO algorithm.

2.8 Space Partitioning

[17] proposed a space partitioning method for facility layout problems with shape constraints A heuristic algorithm was developed for the problems with the objective of minimizing the sum of rectilinear distances weighted by flow amounts between the facilities. The suggested algorithm was a simulated annealing algorithm in which a solution is encoded as a matrix that has information about relative locations of the facilities on the floor. A block layout was constructed by partitioning the floor into a set of rectangular blocks according to the information while satisfying the areas of the facilities. [17] suggested three methods for the partitioning.

2.9 Ant System

Ant Colony Optimization (ACO) is a young metaheuristic algorithm which has shown promising results in solving many optimization problems. To date, a formal ACO-based metaheuristic has not been applied for solving Unequal Area Facility Layout Problems (UA-FLPs). [20] proposed an Ant System (AS) (one of the ACO variants) to solve them. As a discrete optimization algorithm, the proposed algorithm used slicing tree representation to easily represent the

problems without too restricting the solution space. It used several types of local search to improve its search performance. It is then tested using several case problems with different size and setting. Overall, the proposed algorithm showed encouraging results in solving UA-FLPs.

2.10 MILP and MINLP optimization methods

[22]presented a new modelling framework for effectively finding global optimal solutions for the block layout design problem with unequal areas. The most fundamental aspect of the framework consists of an exact representation of the underlying area restrictions. Our computational results consistently yield optimal solutions on several well-known test problems from the published literature. Furthermore, different mixed-integer linear and mixed-integer nonlinear optimization methods are compared. Our study indicates that the new modeling framework together with simple constraints to avoid symmetric layout solutions can be successfully used to find optimal layout solutions; therefore, seriously challenging other optimization methods on this important class of hard, fundamental problems. The new modeling framework may easily be applied in the context of the process plant layout and piping design problems.

2.11 automated layout

[25] generated Automated layout of facilities of unequal areas. Common to the analytical techniques for automated layout of rectangular facilities of unequal areas is the problem of too rapid movement of the representative blocks to form a cluster. This phenomenon made the converged designs too dependent on the initial layout and the order of movement of the blocks. A concept of “controlled convergence” was introduced to solve this problem. Convergence is controlled by carrying out the optimization with the “envelop blocks” of sizes much larger than the actual facilities. The sizes of the envelop blocks were gradually reduced to the actual sizes of the facilities through the optimization cycles. Test results were given to demonstrate the effectiveness of the presented technique.

2.12 Mixed Integer Programming method

[26] proposed an ε-accurate model for optimal unequal-area block layout design by developing a mixed-integer linear programming model for the block layout design problem with unequal areas that satisfies the area requirements with a given accuracy. The basic aspect of the model consists of an ε-accurate representation of the underlying non-convex and hyperbolic area restrictions using cutting planes. The use of such a representation of the area restrictions gave way to solve several challenging test problems to optimality with a guarantee that the final area of each department was within an ε% error of the required area. Numerical results indicated that the proposed model seriously challenge other optimization approaches on this important class of hard, fundamental problems

2.13 Graph Theory method

[27] developed Graph theoretic heuristics for unequal-sized facility layout problem. It considered the unequal-sized facility layout problem with the objective of minimizing total transportation distance. The total transportation distance was defined as the sum of products of flow amounts and rectilinear distances between facilities, where flow amount represents the number of trips per time period between facilities. In the layout problem, it was assumed that shapes of facilities are not fixed and that there was no empty space between facilities in the layout. It proposed new graph theoretic heuristics for the problem. In the heuristics, an initial layout was obtained by constructing a planar adjacency graph and then the solution was improved by changing the adjacency graph (not the physical layout). Therefore, these heuristics did not need an initial layout in advance, and sizes and locations of facilities did not

have to be considered in the improvement procedure. Computational results showed that the proposed algorithms gave better solutions than those from CRAFT, which is one of the most popular algorithms for unequal-sized facility layout problems.

3. SUMMARY

The various techniques such as simulated annealing (SA), genetic algorithm (GA), ant colony algorithm (ACO), and concurrent engineering is prevailing nowadays. Sometimes hybrid approaches were used by applying combination of above techniques i.e. combining high level genetic algorithm with simulated annealing or genetic algorithm followed by simulation techniques to get the better solutions. Application of these facility lay out designs includes construction sites, manufacturing industry and service industries. Out of these techniques, most commonly used techniques were discussed briefly to highlight the growth in unequal area facility layout. There is a vast scope to improve the facility layout design to fulfill the dynamic needs of Manufacturing and construction industries.

REFERENCES

[1] Armour, G.C. and E.S. Buffa, "A heuristic algorithm and simulation approach to relative allocation of facilities." *Management Science*, 1963, 9, 294-309

[2] K. Anstreicher, N. Brixius, J.-P. Goux, and J. Linderoth. Solving large quadratic assignment problems on computational grids. *Math. Program.*, 91(3, Ser. B):563–588, 2002.

[3] Tam, K.Y., "Genetic algorithms, function optimization, and facility layout design." *European Journal of Operational Research*, 1992 63, 322-346.

[4] Chutima, P., and Yiangkamolsing, C., Genetic Algorithms with Improvement Heuristic for Plant Layout Problems. Research and Development Journal of the Engineering Institute of Thailand,Vol.l0,No.2. 62-12. 1999.

[5] FrenchS, .,Sequencing and Scheduling: An Introduction to the Mathematics of the Job-Shop. Ellis Horwood Ltd,1982.

[6l Sule, D.R., Manufacturing Facilities: Location, Planning, and Design. PWS Publishing Company. 1994.

[7] Gen, M., and Chen, R., Genetic Algorithm and Engineering Design .John Wiley & Sons I.n c. 1997.

[8] R.D. Meller, V. Narayanan, and P.H. Vance. Optimal facility layout design. *Oper. Res. Lett.*, 23:117–127, 1999.

[9] B. Montreuil. A modeling framework for integrating layout design and flow network design. *Proceedings of the material handling research colloquium*, pages 43–58, 1990.

[10] Terushige Honiden, Tree Structure Modeling and Genetic Algorithm-based Approach to Unequal-area Facility Layout Problem by IEMS Vol. 3, No. 2, pp. 123-128, December 2004

[11]] David M. Tate, Senior Member IIE and Alice E. Smith, Senior Member IIE1, Unequal Area Facility Layout Using Genetic Search by Department of Industrial Engineering, University of Pittsburgh--Accepted to *IIE Transactions*, April 1994

[12] Nurul Nadia Nordin, Zaitul Marlizawati Zainuddin, Sutinah Salim and Raja Rajeswari d/o Ponnusamy, Mathematical Modeling and Hybrid Heuristic for Unequal Size Facility Layout Problem *Journal of Fundamental Sciences 5 (2009) 79-87*

[13]Tam, K.Y., "Genetic algorithms, function optimization, and facility layout design." *European Journal of Operational Research*, 1992 63, 322-346.

[14]Tam, K.Y., "A simulated annealing algorithm for allocating space to manufacturing cells." *International Journal of Production Research*,1992 30, 63-87.

[15]Tate, D.M. and A.E. Smith, "Unequal-area facility layout by genetic search." *IIE Transactions*, 1995 27, 465-472.

[16] Hong Zhang, and Jia Yuan Wang--Particle Swarm Optimization for Construction Site Unequal-Area Layout *Journal of Construction Engineering and Management*, Vol. 134, No. 9, September 2008, pp. 739-748

[17] KIM, JAE-GON; KIM, YEONG-DAE-A space partitioning method for facility layout problems with shape constraints.by -IIE Transactions ,October 1, 1998

[18]] Kochhar, J.S., Heragu, S.S. and Foster, B., "HOPE: A Genetic Algorithm for Unequal Area Facility Layout Problem," Computers and Operations Research, 25, 583-594, 1998
[19] Alan R. McKendall Jr., Artak Hakobyan,Heuristics for the dynamic facility layout problem with unequal-area departments *European Journal of Operational Research*, *Volume 201, Issue 1*, *16 February 2010*, *Pages 171-182*
[20] Komarudin, Kuan Yew Wong, Applying Ant System for solving Unequal Area Facility Layout Problems *European Journal of Operational Research*, *Volume 202, Issue 3*, *1 May 2010*, *Pages 730-746*
[21] M. Mir, M. H. Imam, A hybrid optimization approach for layout design of unequal-area facilities *Computers & Industrial Engineering*, *Volume 39, Issues 1-2*, *February 2001*, *Pages 49-63*
[22] Ignacio Castillo, Joakim Westerlund, Stefan Emet, Tapio Westerlund Optimization of block layout design problems with unequal areas: A comparison of MILP and MINLP optimization methods, *Computers & Chemical Engineering*, *Volume 30, Issue 1*, *15 November 2005*, *Pages 54-69,*
[23] Heng Li, Peter E. D. Love, Genetic search for solving construction site-level unequal-area facility layout problems *Automation in Construction*, *Volume 9, Issue 2*, *March 2000*, *Pages 217-226*
[24] Ming-Jaan Wang, Michael H. Hu, Meei-Yuh Ku, A solution to the unequal area facilities layout problem by genetic algorithm *Computers in Industry*, *Volume 56, Issue 2*, *February 2005*, *Pages 207-220*
[25] M.Hasan Imam, Mustahsan Mir ,Automated layout of facilities of unequal areas Comp*uters & Industrial Engineering*, *Volume 24, Issue 3*, *July 1993*, *Pages 355-366*
[26] Ignacio Castillo, Tapio Westerlund, An -accurate model for optimal unequal-area block layout design *Computers & Operations Research*, *Volume 32, Issue 3*, *March 2005*, *Pages 429-447*
[27] J. -Y. Kim, Y. -D. Kim Graph theoretic heuristics for unequal-sized facility layout problems , *Omega*, *Volume 23, Issue 4*, *August 1995*, *Pages 391-401*
[28] S. Bock and K. Hoberg. Detailed layout planning for irregularly-shaped machines with transportation
path design. *Eur. J. Oper. Res.*, 177:693–718, 2007.
[29] L.R. Foulds. *Graph Theory Applications*. Springer-Verlag, New York, 1991.
[30] J.G. Kim and Y.D Kim. A space partitioning method for facility layout problems with shape constraints. *IIE Trans.*, 30(10):947–957, 1998.
[31] J.G. Kim and Y.D Kim. Branch and bound algorithm for locating input and output points of departments on the block layout. *J. Oper. Res. Soc.*, 50(5):517–525, 1999.
[32] K.Y. Lee, M.I. Rohb, and H.S. Jeong. An improved genetic algorithm for multi-floor facility layout problems having inner structure walls and passages. *Comput. Oper. Res.*, 32:879–899, 2005.
[33] Ibolya Jankovits; Chaomin Luo; M.F. Anjos; Anthony Vannelli, A Convex Optimisation Framework for the Unequal-Areas Facility Layout Problem April 15, 2007, Manuscript Draft for European Journal of Operational Research
[34] Scholz, Daniel Petrick, Anita Domschke, Wolfgang , A Slicing Tree and Tabu Search based heuristic for the unequal area facility layout problem European Journal of Operational Research. , 197 (August 2009,1) p-166-178
[35] Parames Chutima,J. ,Genetic Algorithm for Facility Layout Design with Unequal Departmental Areas and Different Geometric Shape Constraints. Thammasa Itn Sc.Tech.,V o1.6,N o.2, May-August 2001
[36] Ashwani Dhingra; Pankaj Chandra Hybrid Genetic algorithm for Multicriteria Scheduling with sequence dependent set up time International Journal of Engineering Vol.3(5) Nov 2009 p-520-530
[37] Science and Technology encyclopedia from internet

Failure Mode and Effect Analysis: A Tool to Enhance Quality in Engineering Education

Veeranna.D.Kenchakkanavar, vdk_mtech@yahoo.com

Asst.Professor,
Sambhram Institute of Technology, Bangalore-560097

Dr.Anand.K.Joshi dranandkjoshi@gmail.com

Professor & Dean,
Wellingakar Institute of Management Studies and Research, Bangalore-560100.

Abstract

It is very important to change or make improvement in engineering education, How long an institute or university can survive? If it is just passing the students for B.E certificates and not able to improve students quality. Improving and sustaining quality in technical education is a growing concern among stakeholders of the system. The quality journey which focuses on continuous improvement of processes, products and services through well planned and efficient management of technical education.

In this paper an attempt has been made to assess the reasons behind the failures in some subjects of the mechanical engineering course. Failure Mode and Effect Analysis (FMEA) is a tool used to detect the reasons and finally the recommendations were made to solve the problems occurred in the course.

Key words: FMEA, Occurrence, Detection, Severity, Risk Priority Number, Quality

1. INTRODUCTION

Continually measuring the reliability of a machine, product or process is an essential part of Total Quality Management. When acquiring new machines, creating a new product or even modifying an existing product, it is always necessary to determine reliability of the product or process. Then what is Reliability? The reliability may be defined as the probability of the product to perform as expected for a certain period of time, under the given operating conditions and at a given set of product performance characteristics. Reliability is also an important aspect when dealing with customer satisfaction. Whether the customer is internal or external. The reliability is not only applicable to production but also to service.

Failure Mode and Effect Analysis (FMEA) is an *analytical technique* that combines the technology and experience of people in identifying foreseeable failure modes of a process and planning for its elimination. In other words FMEA can be explained as a group of activities intended to "*Recognize and evaluate the potential failure of a product or process and its effects. Identify actions that could eliminate or reduce the chance of potential failures [1] "*

FMEA attempts to detect the potential product/process related failure modes. The technique is used to anticipate causes of failure and prevent them from happening. FMEA uses Occurrence of failure and Detection probability

criteria in conjunction with Severity criteria to develop Risk Prioritization Number for the prioritization of corrective action considerations.

2. TERMINOLOGY

The following terms are used in the FMEA.

2.1. Potential failure mode: It may be one of two things; first it may be the method in which the item being analyzed may fail to meet the design criteria. Second, it may be method that may cause potential failure in higher- level system or may be the result of failure of lower-level system.

2.2. Severity(S): It is the assessment of the seriousness of the effect of potential failure mode to the next system or customers if it occurs. It is important to realize that the severity applies only to the effect of the failure, not the potential failure mode. Reduction in severity ranking must not come from any reasoning except for a direct change in design of the system.

The severity be rated on 1 to 4 scale with a 1 being no harm, 2 being minor harm, 3 being low harm and 4 being high harm

2.3. Occurrence (O): It is the chance that one of the specific cause/mechanism leads to failure. The reduction or removal on occurrence ranking must not come from any reasoning except for a direct change in the design.

Like severity criteria the likely hood of occurrence of failure is based on 1 to 4 scale with a 1 being not at all, 2 being rare occurrence,3 being some times and 4 being always occurrence.

2.4. Detection (D): It is the relative measure of the assessment of the ability of the design control to detect a potential cause/ mechanism or the subsequent failure mode during the system operation.

Like other two criteria the detection also based on 1 to 4 scale with a 1 being highly detectable , 2 being very easy to

Detect, 3 being moderately detectable and 4 being uncertain detection

2.5. Risk Priority Number (RPN): It is the product of Severity(S), Occurrence (O) and Detection (D)

RPN = S*O*D

The product may be viewed as a relative measure of the risk. Here values for RPN can range from 1 to 64 with 1 being smallest risk and 64 is the highest risk. For parameters with highest RPN make efforts to take corrective action to reduce RPN [2]. The purpose of the RPN is to rank the various parameters; concern should be given for every method available to reduce the RPN.

3. CASE STUDY:

We have seen more number of failures in some subjects of Mechanical Engineering course, A research has been taken up to know the reasons for the same from students, faculties and the subject experts with different sets of questionnaire to make one cycle.

The survey has been conducted in the Department of Mechanical Engineering, Sambhram Institute of Technology, Bangalore, the responses were collected apprehensively by students, faculty and subject expert on questionnaires comprising different criteria's . About 54 students of VI Semester were asked to give response to the subject "MECHANICAL VIBRATION" with the given questionnaire. The questionnaire comprises the questions regarding the fear about the subject/faculty, individual care, syllabus coverage, opportunity for creativity, usefulness of notes for exams, cleanliness of classrooms, availability of good books in the library, input quality of the student, poor in basic science fundamentals, valuators competency, variation in the scheme of the valuation among the valuators, present examination system. The questions were close ended type with options **Always/ some times/ rarely/ not at all.** The respondents were asked to select any one appropriate answer from the given options.

The following Table1 shows the responses from the students in the subject called Mechanical Vibrations.

Table 1. Analysis of student's responses:

SL. No.	DETAILS	Subject: Mechanical Vibrations				
		Occurrence (O)	Severity (S)	Detection (D)	(RPN)	Ranking
1	Fear about the subject & fear about the faculty	3.34	3.43	2.0	23.53	**V**
2	Contextualization of the subject with practical application	3.0	3.0	3.0	27.00	**IV**
3	Individual care of students	4.43	4.43	3.0	58.87	**I**
4	Syllabus coverage	2.33	2.33	1.0	5.43	**X**
5	Opportunities for self learning, confidence building and creative thinking	3.22	3.22	3.22	33.39	**III**
6	Student's problems solving	2.33	2.33	2.33	12.65	**VII**
7	Usefulness of notes to the examination	3.43	3.43	3.43	40.35	**II**
8	Concurrency of lectures with pattern of question paper	3.43	3.43	1.0	11.76	**IX**
9	Availability of text books and reference books	4.0	4.0	1.0	16.00	**VI**
10	Cleanliness of classrooms	3.44	3.44	1.0	11.84	**VIII**

3.1. Findings:

3.1.1. It is seen that the serial number 3 carries highest RPN, where students expressed that they have not given the individual care and attention.

3.1.2. The notes issued by the faculty are not useful for the examination purpose.

3.1.3 The self confidence building and encouragement for creative thinking is very less.

3.1.4 There is no contextualization of the subject and topics with practical applications.

3.1.5 The students have inbuilt fear about the subject

3.1.6 There is no availability of good text books in the library.

3.1.7 The Faculty is unable to solve the problems raised by the students

3.1.8 The class rooms are not clean for the sessions.

3.1.9 The class lecture is not in line with the question paper pattern.

3.1.10 There is no cent percent syllabus coverage.

3.2. Recommendations:

3.2.1 The individual care and attention should be given to each student. The proctor scheme can be introduced.

3.2.2 The faculty is informed to provide good notes to the students.

3.2.3 The students are given chance for development of creativity, by conducting seminars, debates, group discussions and mini projects.

3.2.4 The faculty members are advised to correlate their subject with the practical applications.

3.2.5 The students are motivated and encouraged to remove the inherent fear about the subject.

3.2.6 Good text books and reference books are recommended to the library.

3.2.7 Faculty should be informed to be prepared to face the questions.

3.2.8 House keeping department is informed to keep clean the class rooms before the session starts.

3.2.9 Faculty informed to solve the previous year question papers after each chapter completion.

3.2.10 The faculty is monitored to cover the cent percent syllabus.

The following Table 2. Shows the responses from the faculty of the subject called Mechanical Vibrations.

Table 2. Analysis of faculty response:

SL. No.	DETAILS	Subject: Mechanical Vibrations				
		Occurrence (O)	Severity (S)	Detection (D)	(RPN)	Ranking
1	choice of the subject	1.0	1.0	1.0	1.0	**VI**
2	input quality of the student to the course	3.0	3.0	1.0	9.0	**V**
3	some topics are above the understanding level of students	3.0	3.0	3.0	27.0	**III**
4	students are poor in basic science fundamentals	3.0	3.0	3.0	27.0	**III**
5	Syllabus coverage	3.0	3.0	1.0	9.0	**V**
6	Availability of text books and reference books	3.0	3.0	1.0	9.0	**V**
7	Fear about the subject	4.0	4.0	4.0	64.0	**I**
8	students read for the exam purpose only and not for knowledge	4.0	4.0	3.0	48.0	**II**
9	class room compatibility	4.0	4.0	1.0	16.0	**IV**
10	pattern of question paper on performance	4.0	4.0	3.0	48.0	**II**

3.3. Findings:

3.3.1. It is seen that the serial number 7 carries highest RPN; Students have inherent fear about the subject

3.3.2. a) Students read only for exam purpose not knowledge.

3.3.2. b) The question paper pattern matters on the performance

3.3.3. Students are poor in basic science fundamentals.

3.3.4. Class rooms are not compatible for teaching

3.3.5. a) There no availability of good text books in the library.

3.3.5. b) The in put quality of the students is low to the course.

3.3.6. There is no choice of the subject on there wishes

3.4. Recommendations:

3.4.1. The students are motivated and encouraged to gain confidence over the subject.

3.4.2. a) The students are encouraged for knowledge oriented study.

3.4.2. b) Students are given sufficient number of tests with wide variety of questions to get ready to face the final exam.

3.4.3. Students are given a bridge course to learn basic science fundamentals.

3.4.4. House keeping department is informed to keep the class rooms clean before the session starts. The concerned authority is informed to equip the rooms with essential infrastructure.

3.4.5. a) Good text books and reference books are recommended to the library.

3.4.5. b) All admitted students are made to undergo special training programs to improve their knowledge.

3.4.6. The subject allotment should be made on the choice of the faculty.

The following Table 2. Shows the responses from the subject expert of the subject called Mechanical Vibrations

TABLE 3. Analysis of Subject expert's response:

SL. No.	DETAILS	Subject: Mechanical Vibrations				
		Occurrence (O)	Severity (S)	Detection (D)	(RPN)	Ranking
1	Relevance of some topics in the subject	1.0	1.0	1.0	1.0	**VI**
2	Communication gap between faculty and subject experts	3.0	3.0	1.0	9.0	**III**
3	High standard Syllabus	1.0	1.0	3.0	3.0	**V**
4	input quality of the student to the course	3.0	3.0	3.0	27.0	**I**
5	Deviation from guidelines in paper setting	3.0	3.0	1.0	9.0	**III**
6	Valuators competency	2.0	2.0	1.0	4.0	**IV**
7	Scheme variation among valuators	2.0	2.0	4.0	16.0	**II**
8	Marks variation among valuators	3.0	3.0	3.0	27.0	**I**
9	Action against non serious valuators	3.0	3.0	1.0	9.0	**III**
10	Wheat her the Present examination is the best?	1.0	1.0	3.0	3.0	**V**

3.5. Findings:

1. It is seen that the serial number 4 & 8 carries highest RPN; a) Input quality of the student to the course it self is low b) It is found that there is marks variation among the valuators.
2. There is a variation in the valuation scheme among valuators.
3. a) The paper setters deviate from guidelines while paper setting
   b) There is no action against non-serious valuators.

c) There communication gap between the paper setter and the faculties engaging the subject.
4. The valuators may not be engaging the subject but they go for valuation.
5. Some topics are above the understanding level of the students.

3.6. Recommendations:

1. a) All admitted students are made to undergo special training programs to improve their knowledge.
   b) The moderator of the valuation should observe the extreme variation and take necessary action.
2. The valuators are informed to adhere to the valuation scheme.
3. a) The paper setters are given with the guidelines while preparing the question papers
   b) Examination authority is asked to take actions against the non-serious valuators.
   c) The communication should be encouraged between the paper setter and the faculties engaging the subject
4. The strict observation should be made by the college authority to send the faculties to the valuation only who deal with the subject.
5. The syllabus framing committee should observe topic relevance and understanding level of the student.

4. CONCLUSION

The application of the tool Failure Mode and Effect Analysis (FMEA) in the technical education yields better results. The highest RPN number is given highest priority to solve the problems. The recommendations for the system will reduce the risk of failures in the system. By the proper understanding and application of Total Quality Management tools leads to the better quality in the education system.

4. REFERENCES:

1. Dale H Bester field, “Total Quality Management”.5th edition Pearson Edition Education.Inc, PP377-393.
2. L.Suganthi, Anand A Samuel, “Total Quality Management”, Prentice Hall of India Pvt. Ltd, New Delhi,PP 193-197

Synchronization in the Genesio-Tesi and Coullet Systems Using the Sliding Mode Control

Jamal Ghasemi jghasemi@stu.nit.ac.ir
Faculty of Electrical and Computer Engineering,
Signal Processing Laboratory
Babol Noshirvani University of Technology
Babol, P.O. Box 47135-484, IRAN

A. Ranjbar N. a.ranjbar@nit.ac.ir
Faculty of Electrical and Computer Engineering,
Babol Noshirvani University of Technology
Babol, P.O. Box 47135-484, IRAN

Amard Afzalian a.afzalian@gmail.com
Islamic Azad University, Science
and Research,Tehran, IRAN.

Abstract

Chaotic behavior and control of Genesio-Tesi and Coullet is studied, in this paper. The Sliding Mode Control is proposed for synchronization in a pair of topologically inequivalent systems, the Genesio-Tesi and Coullet systems. The simulation result verifies the effectiveness of the proposed method.

Keywords: Chaos, Sliding Mode, Synchronization, Genesio-Tesi System, Coullet System

1. INTRODUCTION

Chaotic systems have recently been much considered due to their potential usage in different fields of science and technology particularly in electronic systems [17], secure communication [22] and computer [1]. Sensitive dependence on initial conditions is an important characteristic of chaotic systems. For this reason, chaotic systems are difficult to be controlled or synchronized. Control of these systems has been considered as an important and challenging problem [12]. Control of chaotic systems would have been supposed impossible with uncontrollable and unpredictable dynamic. The imagination was changed when three researchers (Ott, Grebogi, Yorke) have shown in [13] other vice. The effort has been progressed to control a chaos in great different areas, e.g. feedback linearization [2, 7, 20], Delay feedback control [3], OPF [9] and TDFC [16]. Over last two decades, due to the pioneering work of Ott et al. 1990, synchronization of chaotic systems has become more and more interesting in different areas. A very important case in chaotic systems is synchronizing the two identical systems with unequal initial conditions, but in these years, more and more applications of chaos synchronization in secure communications make it much more important to synchronize two different chaotic systems [4, 10, 14]. The problem of designing a system, whose behavior mimics that of another chaotic system, is called synchronization. Two chaotic systems are usually called drive (master) and response (slave) systems respectively. Different control technique e.g. a chattering-free fuzzy sliding-mode control (FSMC) strategy for synchronization of chaotic systems even in presence of uncertainty has been proposed in [5]. In [6] authors have proposed an active sliding mode control to synchronize two chaotic systems with parametric uncertainty. An algorithm to determine

parameters of active sliding mode controller in synchronizing different chaotic systems has been studied in [11]. In [19] an adaptive sliding mode controller has also been presented for a class of master–slave chaotic synchronization systems with uncertainties. In [15], a backstepping control was proposed to synchronize these systems. Genesio-Tesi and Coullet systems are topologically inequivalent [8]. It is difficult to synchronize two topologically inequivalent systems. In [8], a backstepping approach was proposed to synchronize these systems. In this paper a controller designed via Sliding Mode control to synchronize such systems. The organization of this paper is as follows: In Section 2, chaotic behaviors of two systems is studied. In Section 3, a controller is designed via Sliding Mode Control to synchronize Coullet and Genesio-Tesi systems. In Section 4, numerical simulations verify the effectiveness of the proposed method. Finally the paper will be concluded in section 5.

2. CHAOS IN GENESIO-TESI AND COULLET SYSTEMS

It is assumed that Genesio-Tesi system drives Coullet system. Thus, the master and slave systems are considered as follows:

$$\text{Master}: \begin{cases} \dot{x}_1 = x_2 \\ \dot{x}_2 = x_3 \\ \dot{x}_3 = a_3 x_3 + a_2 x_2 + a_1 x_1 + x_1^2 \end{cases} \quad (1)$$

And

$$\text{Slave}: \begin{cases} \dot{y}_1 = y_2 \\ \dot{y}_2 = y_3 \\ \dot{y}_3 = b_3 y_3 + b_2 y_2 + b_1 y_1 - y_1^3 \end{cases} \quad (2)$$

If we select the parameters of the systems as $(a_1, a_2, a_3) = (-1, -1.1, -0.45)$ and $(b_1, b_2, b_3) = (-0.8, -1.1, -0.45)$ the two systems chaotic behaviors will be occurred. Their chaotic attractors are shown in Fig.1 and Fig.2 respectively.

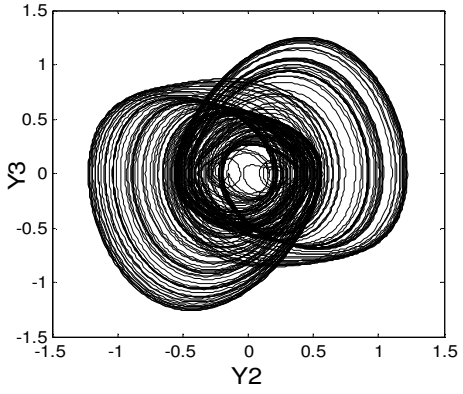

Fig.1: Chaotic attractors Y2-Y3 of Genesio-Tesi System

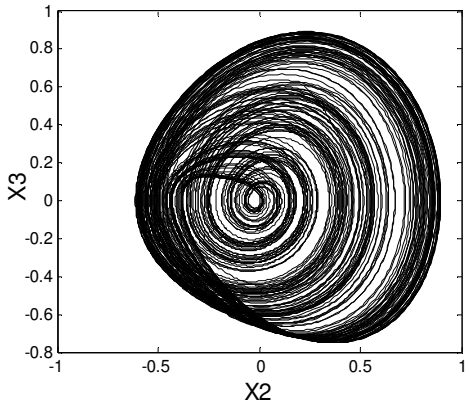

Fig.2: Chaotic attractors X2-X3 of Coullet system

3. SLIDING MODE CONTROLLER DESIGNATION

The aim in this section is to design a Sliding Mode Controller to achieve synchronization between two systems. The procedure of designing will be briefly shown here. The controller has a duty to synchronization between two inequivalent systems. In general in the sliding mode control terminology, a controller is designed such that states approach to zero in finite time [21],

Thereafter states have to stay in the location for the rest of time. To gain the benefit of sliding mode control, a sliding surface has to be defined first. This surface introduces a desired dynamic and the route of approaching the states towards a stable point. This also defines the switching of the sliding control (as a compliment of control law) in the surface. Any outside state in a finite time approaches to the surface.

In this work this surface defines based on the error of stats two inequivalent systems. Choosing $a_3x_3+a_2x_2+a_1x_1+x_1^2=F(x)$, the equation of Genesio-Tesi system, Eq. (1) will be rewritten as:

$$\begin{cases}\dot{x}_1=x_2\\ \dot{x}_2=x_3\\ \dot{x}_3=F(X)\end{cases} \tag{3}$$

Choosing $b_3y_3+b_2y_2+b_1y_1-y_1^3=G(Y)$, the Eq. (2) can be rewritten as:

$$\begin{cases}\dot{y}_1=y_2\\ \dot{y}_2=y_3\\ \dot{y}_3=G(Y)+U_c\end{cases} \tag{4}$$

Where U_c is controller which will be designed via Sliding Mode Control to synchronize the Coullet system and Genesio-Tesi system. The design of the Controller for this system will be completed in two stages:

1- Design of surface that explanatory dynamics of system
2- Compietion of control law until states of system slide upon to the surface

The essential work in this procedure is to determine control law, so the error of states between two systems and sliding surface are defined as follow:

$$e_i=Y_i-X_i \tag{5}$$

And

$$S(t)=\sum_{i=1}^{n}c_ie_i(t) \tag{6}$$

Where n is the number of stats and c_i will be chosen according to the sliding dynamics. When any state reaches the surface, it is told the sliding mode is taken place. At this time, the state dynamics will be controlled via sliding mode dynamics, so selection of c_i is important [18]. After the reaching, the state must stay in the surface. The sliding mode control needs two stages of:

Approaching phase to the surface $S(t)\neq 0$

A sliding phase to $S(t)=0$

To verify the stability requirements function $V=\frac{1}{2}s^2$ is candidate as a Lyapunov function, where S is the sliding surface. To guarantee the stability the differentiation of Lyapunov function has to be negative definite. A sufficient condition of transition from the first phase to the second will be defined by the sliding condition as Differentiation of V when approaches to:

$$\dot{V}=s\dot{s}<0 \tag{7}$$

Differentiation of (6) yields:

$$\begin{aligned}\dot{S}(t) = c_1\dot{e}_1 + c_2\dot{e}_2 + c_3\dot{e}_3 &= c_1(y_2 - x_2) \\ &+ c_2(y_3 - x_3) \\ &+ c_3[G(Y) - F(X) + U]\end{aligned} \tag{8}$$

Replacing Eq. (8) into (7) achieves:

$$\begin{aligned}\dot{V}(t) = s(t)\{&c_1(y_2 - x_2) \\ &+ c_2(y_3 - x_3) \\ &+ c_3[G(Y) - F(X) + U]\}\end{aligned} \tag{9}$$

The selection $\dot{s} = -K\,\mathrm{sgn}(s)$ meets the sliding condition and yields the control law in the following form:

$$\begin{aligned}U_1 = &-\frac{K}{c_3}.\mathrm{sgn}(S(t)) \\ &-\frac{c_1}{c_3}(y_2 - x_2) \\ &-\frac{c_2}{c_3}(y_3 - x_3) - [G(Y) - F(X)]\end{aligned} \tag{10}$$

Where

$$u_c = -\frac{K}{c_3}.\mathrm{sgn}(S(t)) \tag{11}$$

And

$$u_{eq} = -\frac{c_1}{c_3}(y_2 - x_2) - \frac{c_2}{c_3}(y_3 - x_3) - [G(Y) - F(X)] \tag{12}$$

u_c and u_{eq} are the corrective control law and the equivalent control law, respectively, whereas $K > 0$ is the switching coefficient. An equivalent control $u_{eq}(t)$ causes the system dynamics to approach to the sliding surface and u_c is corrective control law which completes the control law in $u_{eq}(t)$.

4. SIMULATION RESULTS

To verify the capability of the proposed method the Genesio-Tesi and Coullet systems with unequal initial condition is selected as:

$$X(0) = \begin{bmatrix}0.21\\0.22\\0.61\end{bmatrix}, \quad \mathrm{Y}(0) = \begin{bmatrix}0.1\\0.41\\0.31\end{bmatrix} \tag{13}$$

The simulation is performed by MATLAB software. To avoid occurrence of chattering, saturation function is gained instead of the signum function in Eq. (10). This will be defined as:

$$sat(S) = \begin{cases}+1 & S(t) > \varepsilon \\ t & -\varepsilon \le S(t) \le \varepsilon \\ -1 & S(t) < -\varepsilon\end{cases} \tag{13}$$

The simulation results are shown in Fig. (3)-(5). Synchronization results and error of tracking are shown in Fig. (3) and Fig (4), respectively. The control input is shown in Fig. (5). It should be noted that the control is triggered at t=100s. These verify the performance of the sliding mode to stabilize the chaos and synchronize two inequivalent systems.

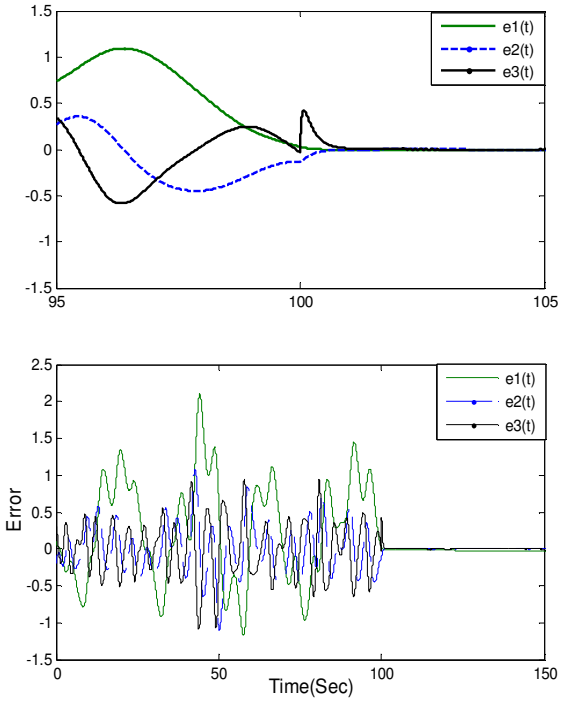

Fig. 4(a): The States Synchronization Error of Cuollet system and Genesti Tesi system

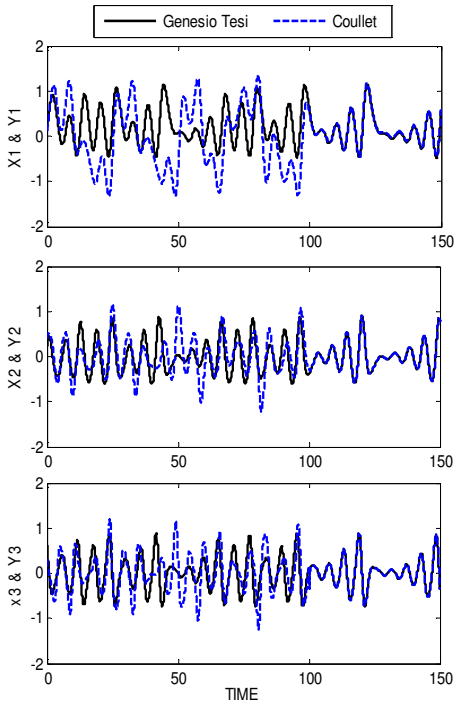

Fig. 3: Synchronization states of Collet system with Genesio-Tesi system

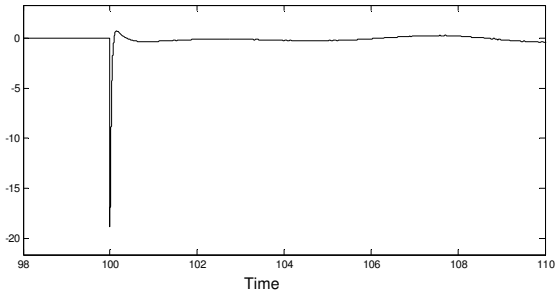

Fig. 5: The Signal Control Designed By Sliding Mode Controller

5. CONCLUSION

In this paper the synchronization between two different chaotic systems, i.e. Genesio-Tesi and Coullet systems is studied via Sliding Mode Controller. Although, different dynamics made more difficulty in synchronization control, a controller is designed based on Sliding Mode Control and Lyapunov stability theory which efficiently synchronized the Genesio-Tesi and Coullet systems.

6. REFERENCES

[1] Abdous F., A. Ranjbar, S.H. Hossein-Nia, Stabilizing the Hopf Bifurcation Using Time-delay Feedback Control in the Network Congestion, IEEE conference, WOSPA, 2008.

[2] Abdous F., A. Ranjbar N., S.H. Hosein Nia, A. Sheikhol Eslami, B. Abdous, The Hopf Bifurcation control in Internet Congestion Control System, Second International Conference on Electrical Engineering (ICEE), Lahore (Pakistan), 2008.

[3] Abdous, F. ,A. Ranjbar N., S.H. Hosein Nia, A. Sheikhol Eslami, Chaos Control of Voltage Fluctuations in DC Arc Furnaces Using Time Delay Feedback Control, Second International Conference on Electrical Engineering (ICEE) ,Lahore (Pakistan), 2008.

[4] Chua L. O., M. Itah, L. Kosarev and K. Eckert, Chaos synchronization in Chua's Circuits, J. Circuits, Syst. And Comp., 3 93-108, 1993.

[5] Deng W., C.P. Li, Chaos synchronization of the fractional Lu system, Phys., 353: 61–72, 2005.

[6] Deng W., C. Li, Synchronization of chaotic fractional Chen system, J. Phys.Soc. 74 (6):1645–1648, 2005.

[7] Gallegos JA., Nonlinear regulation of a Lorenz system by feedback linearization techniques. Dyn. Control 1994; 4: 277–98, 1994.

[8] Hu J. B., Y. Han, L. D Zhao, Synchronization in the Genesio-Tesi and Coullet systems using the Backstepping Approach", International Symposium on Nonlinear Dynamics (2007 ISND), Journal of Physics:Conference Series 96 012150 doi:10.1088/1742-6596/96/1/012150, 2007.

[9] Hunt E. R., Stabilization High-Period Orbits in a Chaos System, Phys. Rev. Lett. 1991; 67: 1953-55, 1991.

[10] Li D., J. A. Lu and X. Wu, Linearly coupled synchronization of the unified chaotic systems and the Lorenz systems, Chaos, Solitons & Fractals, Vol 23, Issue 1, Pages 79-85, January 2005

[11] Li C.P., W.H. Deng, D. Xu, Chaos synchronization of the Chua system with a fractional order, Phys. A 2006;360:171–185, 2006.

[12] Liu Shu-Yong, Xiang Yu and Shi-Jian Zhu, Study on the chaos anti-control technology in nonlinear vibration isolation system, Journal of Sound and Vibration, 310(4-5): 855-864, 2008.

[13] Ott. E., Grebogi, C., York, J. A, Controlling Chaos, Phys. Rev. Lett. ; 64: 1196-99, 1990.

[14] Park J. H., Stability criterion for synchronization of linearly coupled unified chaotic systems, Chaos, Solitons & Fractals, Vol. 23, Issue 4, Pages 1319-1325, February 2005.

[15] Phuah J., J. Lu, and T. Yahagi, Chattering free sliding mode control in magnetic levitation system, IEEJ Trans. EIS, 125(4):600–606, 2005.

[16] Pyragas K., Continuous control of chaos by self controlling feedback, Phys. Rev. Let. 67: 1953-55, 1991.

[17] Roy R., T. W. Murphy، T. D. Maier، Z. Gillis and E. R. Hunt, Dynamical Control of a chaotic Layser: Experimental stabilization of a Globally Coupled System, Physc. Rev. Lett, vol. 68، pp. 1259-1262, 2000.

[18] Slotine J. E., S. S. Sastry, Tracking control of nonlinear systems using sliding surface with application to robotic manipulators, Int. J.Contr. ,vol. 38, pp. 465 492, 1983.

[19] Utkin V. I., Variable structure systems with sliding mode, IEEE Trans.Automat. Contr., 22: 212–222, 1977.

[20] Yassen MT., Controlling chaos and synchronization for new chaotic system using linear feedback control, Chaos Solitons Fractal, 26: 913–20, 2005.

[21] L.-C. Yao, J.-S. Chen, C,-Y, Hsu, A Mode Switching Sliding-mode Controller with Observer based State-Dependent Boundary Layer and Its Application, International Journal of Engineering, vol. 1(1), pp. 39:53, 2007 .

[22] Yang T., "A survey of chaotic secure communication systems", Int. Journal of Compational Cognition, vol. 2. No. 2. pp. 81-130, 2004.

Second Law Analysis of Super Critical Cycle

I.Satyanarayana *sindigibilli@gmail.com*
Research Scholar
Dept. of Mechanical Engg.
JNTUH College of Engineering
Kukatpally.
HYDERABAD-500 085,INDIA

Dr.A.V.S.S.K.S. Gupta *avs_gupta@rediffmail.com*
Associate Professor
Dept. of Mechanical Engg.
JNTUH College of Engineering
Kukatpally
HYDERABAD-500 085,INDIA

Dr. K.Govinda Rajulu *govindjntu@gmail.com*
Professor
Dept. of Mechanical Engg.
JNTUA College of Engineering
ANANTAPUR-515001
Andhra Pradesh
INDIA

Abstract

Coal is the key fuel for power generation in the Supercritical Rankine cycle. Exergy, a universal measure has the work potential or quality of different forms of energy of energy in relation to a given environment. In this paper, an exergy analysis has carried out to the supercritical power plant tells us how much useful work potential or exergy, supplied to the input to the system under consideration has been consumed by the process. A computer code has developed for exergy to analyses the supercritical cycle without reheat as well as with single reheat. The temperature and pressure inlet to the turbine and exhaust pressure from the turbine are identified as key parameters in this analysis. Both first law efficiency and exergetical efficiency have studied at various temperature and pressure inlet to the turbine. Irreversibility as well as Fractional exergy loss of all the components has also been studied. To decrease exergy loss of supercritical power plant, effects of pump discharge pressure increases, effects of steam turbine discharge pressure decreases and effects of steam temperature increases. First law efficiency is increases with increase in temperature at a given pressure. Exergy efficiency is increases with increase in temperature and pressure. It is found that both the efficiencies increases more in temperature rise than the pressure rise in the turbine inlet. Both Irreversibility and Fractional exergy losses in the boiler is reducing with increase in temperature.

Keywords: Supercritical cycle, reheat, cycle efficiency, exergy efficiency and Fractional exergy loss

1. INTRODUCTION

Advanced Coal fired electric power plants that are cleaner, more efficient and less costly than the current fleet of coal fired power plants. The efficiency of power plants in developing countries like India and China are still around 32-35% lower heating value, modern sub critical cycles have attained efficiencies close to 40%. Further improvement in efficiency can be achieved by using supercritical steam conditions. Current supercritical coal fired power plants have efficiencies above 45%. Presently, there are more than 450 supercritical power plants are available in operation. Coal based thermal power plants are the main source of power generation in India. Energy is an important ingredient of economic development. Economic growth is directly or indirectly related to energy consumption. The total installed capacity of Indian power plants is 104,917 MW, nearly 74,420MW are accounted by thermal power generation and of this about 71% of electricity generation is coal based. The need today is to have low emission with high efficiency of operation; hence it is necessary that the sub critical operation limit have to go supercritical ranges, which is beyond 221.2bar steam pressure. Supercritical units has around 3 percent higher efficiency resulting in 8 to 10 percent savings in fuel than the sub critical units, since the fuel fired is reduced, hence the emissions are also less.

The cycle originally taken from the Rankine cycle. The basic thermodynamic principles and exergy methods are taken from the Bejan, A [1]. Nag, P.K., and Gupta are analyzed Exergy analysis of Kalina cycle [2]. EI-sayed, and M.Tribus, made a Theoretical Comparison of Rankine with Kalina cycle. T.J.Kotas made description of the exergy as well as Enthalpy of the flue gas inlet and outlet of the boiler [3]. The Supercritical Rankine cycle comparison with the Rankine cycle working with same temperature limits. The area between the line of heat source and the line of representing the working fluid corresponds to the exergy loss in the process of heat transfer in HRSG. These losses are less in the supercritical cycle compared with Rankine cycle.

There are two ways usually considered for increasing the efficiency of the Supercritical Rankine Cycle utilizing variable-temperature heat sources. One is the use of a multi pressure boiler, and the other is the implementation of the so-called “supercritical cycle”. The use of a multi pressure boiler is widely accepted in the industry, but results in only moderate improvement unless the number of such boiling steps is very large. However, a significant increase in the number of boiling steps is technically and economically unfeasible and, as a result, the number of such steps does not exceed three. The use of supercritical cycle, especially with organic and exotic working fluids, can theoretically achieve a triangular shape of the cycle, and thus high efficiency, but requires extremely high pressure in the boiler, which in turn has an adverse effect on turbine performance [4]. S.L.Milora and J.W.Tester have presented a very complete study of potential of supercritical cycle [5]. As follows from their data, such a cycle has one more setback, i.e., if the working fluid is heated to a higher temperature on a turbine inlet, the temperature in the turbine outlet is relatively high, and the remaining heat cannot be properly utilized in the cycle. EI-sayed, and M. Tribus, made a Theoretical Comparision of Rankine with Kalina cycle [6]. The exergy method is the best-known member of a class of techniques of thermodynamic analyses, which are, collectively referred to as second law analysis. An account of the historical development of second law analysis can be found in a paper by Haywood. Fratzscher and Beyer have given a critical examination of the developments in exergy analysis with special reference to the decade 1970-80. Kotas, Mayhew and Raichura made nomenclature for exergy analysis [7]. In this paper, complete analysis is given only for the supercritical cycle with single reheat.

2. REHEAT SUPECRITICAL CYCLE

Figures 1 and 2 are the schematic and T-s diagrams for the supercritical reheat power cycle. It is triangular in shape because there is no latent heat of vaporization during the boiling process. The temperature profile is well matched with flue gas temperature line; hence there would not be much of exergy loss during heat exchange process in the boiler. The steam may be reheated to a high temperature after it has partially expanded through the turbine. A significant portion of the work by the steam is accomplished when the pressure is such that the steam is saturated or nearly saturated. This is the correct place for the vapor to be re-superheated. The steam reenters the turbine and expands to condenser pressure. The steam expands through the turbine until state 2 is reached, then it removed and reheated (P_1= 0.2 x P_{rh}) at a constant pressure to state 3. The steam reenters the turbine at state 3 and

expands the condenser at state 4. The steam is condensed (state point 4-5) and pumped (state point 6-1) back to the steam generator, completing the cycle.

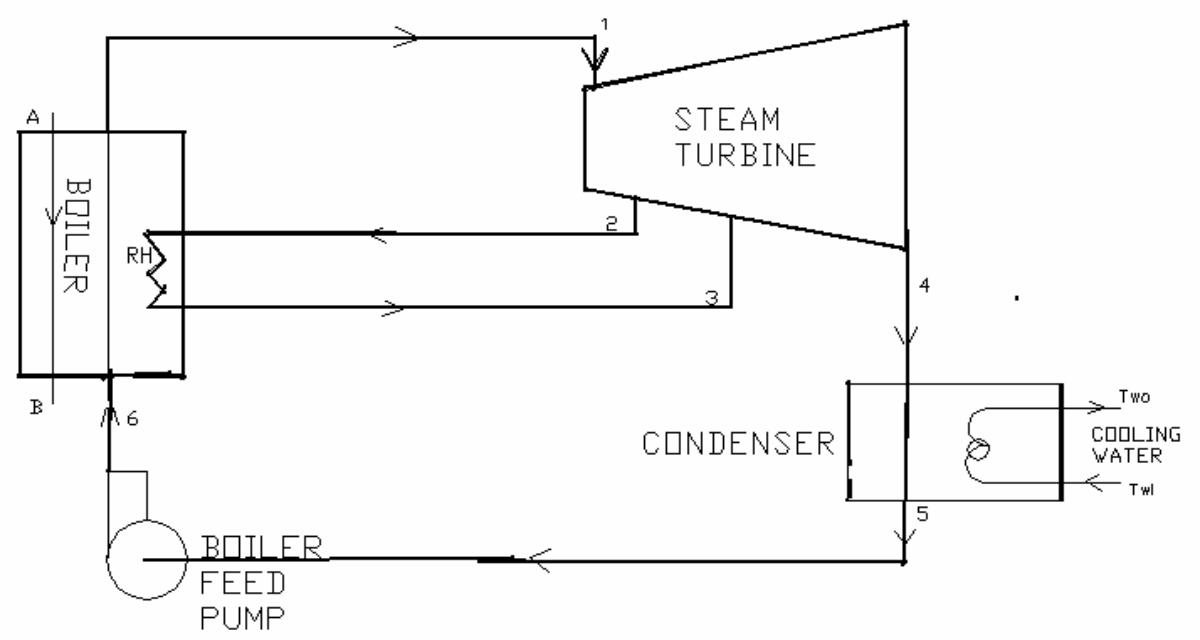

Fig1. Schematic diagram of Supercritical cycle with reheat

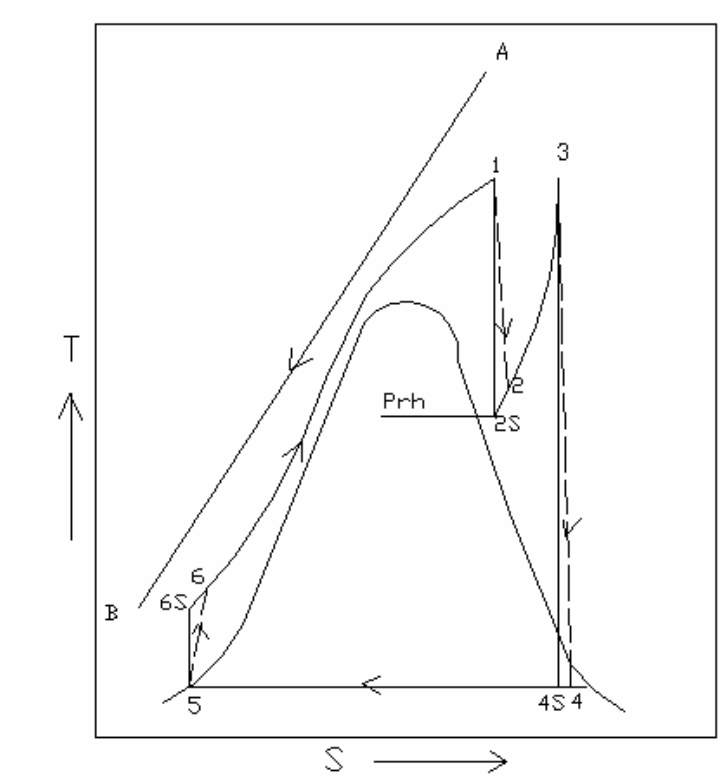

Fig 2. T-S diagram of Supercritical cycle with reheat

3. EXERGY ANALYSIS OF THE CYCLE:

3.1 ASSUMPTIONS:

1. Capacity of the power plant = 660 MW
2. Reheat pressure = 0.2 times the initial pressure
3. No heat losses and no pressure losses
4. The isentropic efficiency of the steam turbine is 90%.
5. The pump efficiency is assumed to be 80%.
6. Flue gas entering into the boiler is 970^0C and leaving is 210^0C.
7. The pinch point temperature difference for the heat exchanges in the condenser is 5^0C.
8. Condenser pressure P_c= 0.06 bar
9. Cooling water temperature inlet to the condenser $T_{wi}=25^0$C

ANALYSIS

3.2 CYCLE EFFICIENCY:

To calculate the cycle efficiency for the supercritical reheat cycle, the work and heat added terms must be found. An energy balance equation on the turbine yields,

The work done per kg of steam supplied to the turbine,

$$W_{turbine} = ((h_1 - h_2) + (h_3 - h4)) \quad kJ/kg \qquad (1)$$

Boiler pump work per kg of steam supplied,

$$W_{pump} = h_6 - h_5 \quad kJ/kg \qquad (2)$$

Heat supplied to steam boiler,

$$H.S = h_1 - h_6 \quad kJ/kg \qquad (3)$$

$$W_{net} = W_{turbine} - W_{pump} \qquad (4)$$

The cycle efficiency or first law in the efficiency is defined as the ratio of output energy to the input energy,

$$\text{Cycle efficiency} = (W_{turbine} - W_{pump}) / H.S \qquad (5)$$

3.3 EXERGY EFFICIENCY:

The method of exergy analysis aims at the quantitative evaluation of the exergy destructions and losses (irreversibilities) associated with a system. Hence it is required to calculating the irreversibility in all the components of the power cycle for the estimation of exergy efficiency.

The irreversibility or exergy losses in each of the components are calculated for the specified dead state.

Let $P_{0,}$ T_0 are the pressure and temperature of the system when it is in the dead state.

3.3.1 Boiler:

The coal used is anthracite of the chemical composition of the power plant has taken form T.J.Kotas [3] are as:

	CO_2	H_2O	N_2	O_2	SO_2	Total
n_k[kmol/ 100kgfuel]	6.51	1.634	35.32	9.324	0.047	57.735

$$H_A = \left(\theta_A - \theta^0\right)\sum_k n_k \tilde{c}_{pk}^{\,h} \quad \text{kJ} \quad (6)$$

$$H_B = \left(\theta_B - \theta^0\right)\sum_k n_k \tilde{c}_{ph}^{\,h} \quad \text{kJ} \quad (7)$$

$$E_A = \left(\theta_A - \theta^0\right)\sum_k n_k \tilde{c}_{pk}^{\,\varepsilon} \quad \text{kJ} \quad (8)$$

$$E_B = \left(\theta_B - \theta^0\right)\sum_k n_k \tilde{c}_{pk}^{\,\varepsilon} \quad \text{kJ} \quad (9)$$

Where mean isobaric heat capacity for evaluating enthalpy changes is

$$\bar{c}_p^{\,h} = \left[\frac{\bar{h} - \bar{h}^0}{T - T_0}\right] = \frac{1}{T - T_0}\int_{T_0}^{T} \bar{c}_p dT \quad \text{and} \quad (10)$$

Mean molar isobaric exergy capacity for evaluating changes in physical exergy is

$$\bar{c}_p^{\,\varepsilon} = \left[\frac{\bar{\varepsilon}^{\Delta T}}{T - T_0}\right] = \frac{1}{T - T_0}\left[\int_{T_0}^{T} \bar{c}_p dT - T_0 \int_{T_0}^{T} \frac{\bar{c}_p dT}{T}\right] \quad (11)$$

Where H_A = Enthalpy of flue gases entering The boiler,

H_B = Enthalpy of flue gases leaving the boiler
Ex_A = Exergy in the flue gas at the entering the boiler
Ex_B = Exergy in the flue gas at the exiting from the boiler

Mass of stream generated for the given flow rate of flue gases obtained from the energy balance.
The mass of the steam is calculated from the capacity of the power plant.

$m_s(W_{net})$ = 660 MW

m_s= 660x1000 kW/ W_{net} kg/sec (12)

Energy balance equation for obtaining the number of flue gases (m_g) is,
Heat gained by the steam = Heat lost by the flue gases.

$$m_s((h_1 - h_6) - (h_3 - h_2)) = m_g(H_A - H_B)$$

$$m_g = ((h_1 - h_6) - (h_3 - h_2)) / (H_A - H_B) \quad (13)$$

The irreversibility or exergy loss in the boiler is obtained as decrease in availability function across the component. Exergy of the flue gas entering the Boiler, for the given temperature θ_A = 970°C and θ^0 =25 °C .the composition of the flue gas has been calculated and enthalpy and exergy of the flue gas entering in to the boiler and leaving the boiler are as,

Exergy in the flue gas at the entering the boiler is $Ex_{in} = Ex_A$ = 958953.69 kJ

Enthalpy of the flue gas entering is H_A =1711969.25 kJ

Exergy in the flue gas at the exit the boiler is $Ex_{out} = Ex_B$ =68474.05 kJ.

Enthalpy of the flue gas at exit of the boiler is H_B = 304951.47 kJ.

Availability or Gibbs function of steam at state point 1

$$G_1 = Es_1 = m_s (h_1 - T_o s_1) \text{ kJ} \quad (14)$$

Availability or Gibbs function of steam at state point 6 $G_6 = Ew_6 = m_s (h_6-T_os_6)$ kJ (15)

Irreversibility in the boiler is $I_{boiler} = Ex_A-Ex_B – (Es_1 – Ew_6)$ kJ (16)

3.3.2 Steam Turbine:

The irreversibility rate in the steam turbine given by Gouy-Stodola equation is

$$I_{turbine}=T_0.m_s((s_2-s_1)+(s_4-s_3)) \text{ kW} \quad (17)$$

3.3.3 Condenser:

Mass of cooling water circulated to condense ms kg of steam is obtained from the energy balance is

C_{pw}= 4.1868 kJ/kg.K.

$m_{cw} C_{pw} (T_f-T_d)= m_s (h_2-h_3)$ (18)

$m_{cw}= m_s(h_2-h_3)/ C_{pw} (T_f-T_d)$ is 154735.2 kg.

Irreversibility in the condenser,

$I_{condenser}=T_0[m_{cw}C_{pw}\ln(T_f/T_d)–m_s(s_2-s_3)]$ kW (19)

3.3.4 Pump :

Irreversibility rate in the boiler feed pump,

$I_{pump}=m_s T_0(s_6-s_5)$ kW (20)

3.3.5 Exhaust:

Irreversibility or exergy loss through the exhaust

$I_{exhaust} = Ex_B$ =103041.92 kJ.

Total Irreversibility is

$\Sigma I = I_{boiler} + I_{turbine} + I_{pump} + I_{condenser} + I_{exhaust}$ kW (21)

Exergy efficiency is defined as the ratio of exergy output to the exergy input. Exergy output depends on the degree of Irreversibility of the cycle.

Exergy efficiency, $\eta_{II} = \frac{\left(Ex_A - \sum I\right)*100}{Ex_A}$ (22)

4. FRACTIONAL EXERGY LOSS:

The definition of the fractional exergy loss of the component is the ratio of irreversibility of the individual component to the total irreversibility of the cycle. Its value is estimated for all the components of the cycle. It gives the information regarding the loss of useful energy in all the component has been studied with different operating variables. The Fractional exergy formulas of each component are as follows.

Fractional exergy loss in the boiler is,

$$\frac{I_{boiler}}{\sum I} * 100 \quad (23)$$

Fractional exergy loss in the turbine is,

$$\frac{I_{turbine}}{\sum I} * 100 \quad (24)$$

Fractional exergy loss in the condenser is,

$$\frac{I_{condenser}}{\sum I} * 100 \quad (25)$$

Fractional exergy loss in the Pump is,

$$\frac{I_{pump}}{\sum I} * 100 \quad (26)$$

Fractional exergy loss in the exhaust is,

$$\frac{I_{exhaust}}{\sum I} * 100 \quad (27)$$

5. RESULTS AND DISCUSSION:

All the dashed lines in the following graphs are related to single reheat where as other is without reheat. It is observed from figure 3 that with the increase in pressure for a particular temperature cycle efficiency increases for a supercritical cycle with no reheat. Also with the consideration of a single reheating, the cycle efficiency is increasing with the increase in pressure, but the increase in efficiency is high when compared to a supercritical cycle without reheating. The cycle efficiency at a pressure of 200 bar is 44.02% and for a pressure of 425 bar the efficiency is 44.94%. It is also observed that the increase in cycle efficiency is very less when compared to the increase in turbine inlet pressure limits. It is observed from figure 4, the cycle efficiency increases with the increase in turbine inlet temperature at a particular pressure for a supercritical cycle without reheating. The cycle efficiency also increases with increase in inlet temperature at a particular pressure by considering the reheating, but the increase in efficiency is high when compared to a supercritical cycle without reheating.

Fig 5 shows the variation of exergy efficiency with increase in pressure at different turbine inlet temperature. It is obvious that exergy efficiency increases with increase in pressure at a particular turbine inlet temperature for a supercritical cycle without reheating. The exergy efficiency also increases for a supercritical cycle with reheating and the increase in efficiency is high when compared to a cycle without reheating.

Figure 6 shows the variation of exergy efficiency with temperature at different turbine inlet pressures. Exergy efficiency increases with increase in temperature at different turbine inlet pressures with and without reheating. The increase in exergy efficiency is high for a cycle with reheating when compared to a cycle without reheating.

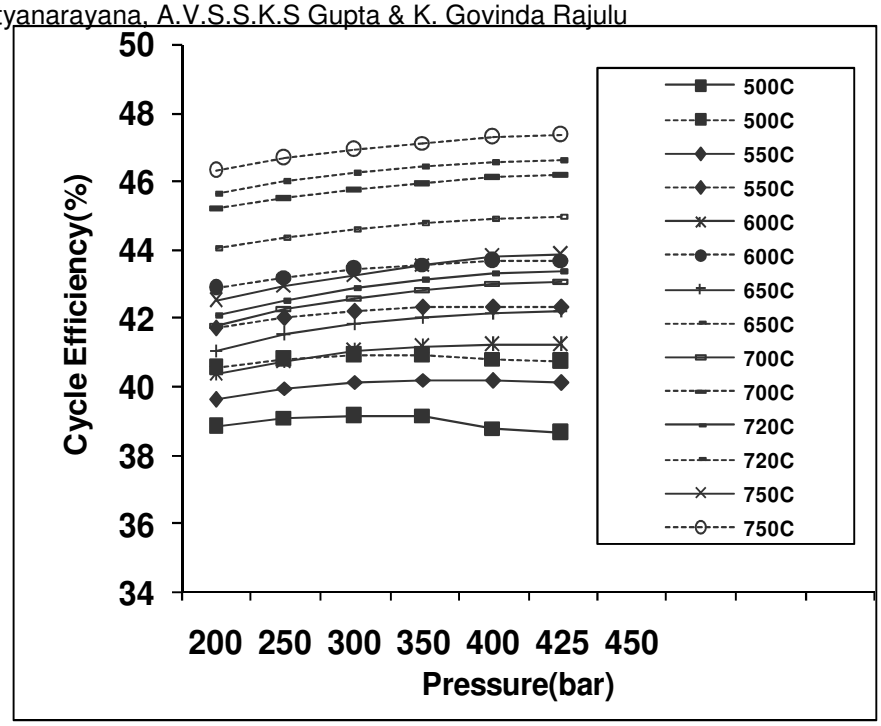

Fig.3. Variation of Cycle efficiency with P1 for Different values of T1 at P_c= 0.06 bar

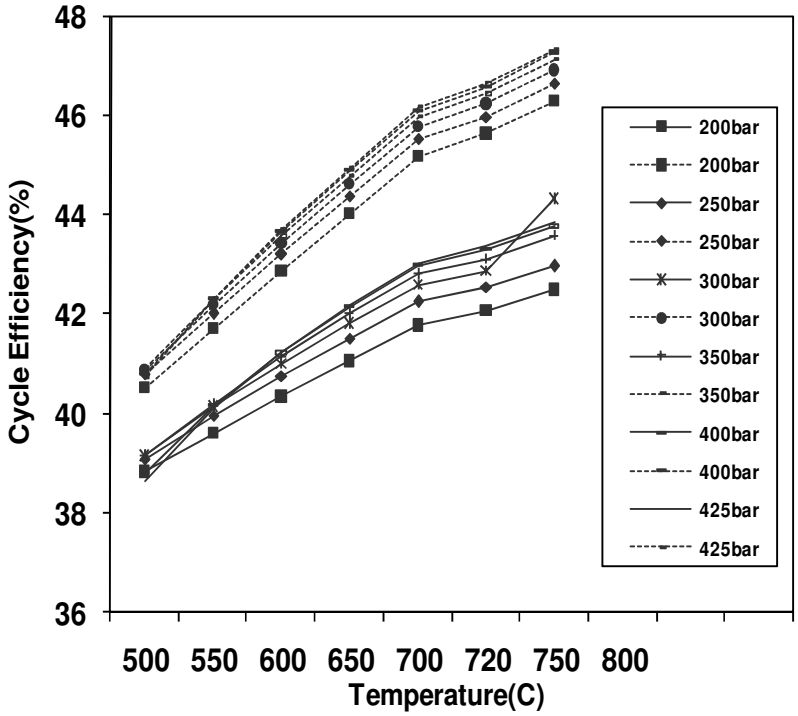

Fig.4. Variation of Cycle efficiency with T1 for Different values of P1 at P_c= 0.06 bar.

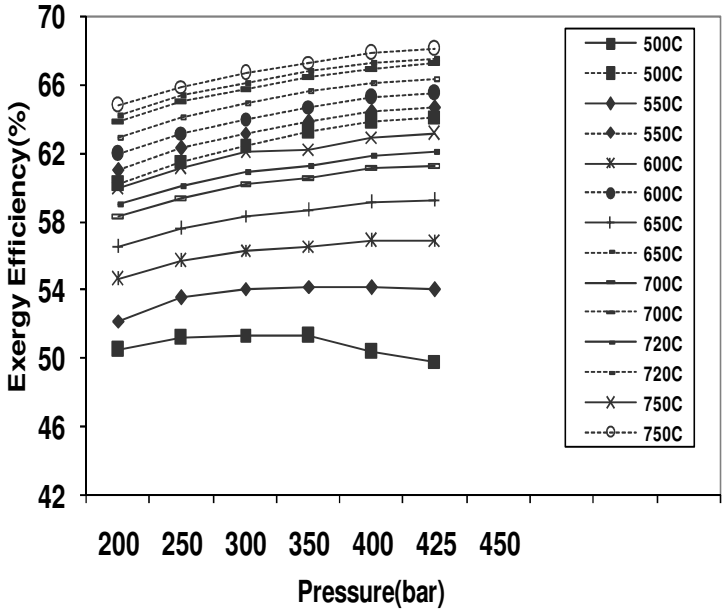

Fig5. Variation of Exergy efficiency with P1 for Different values of T1 at P_c= 0.06 bar.

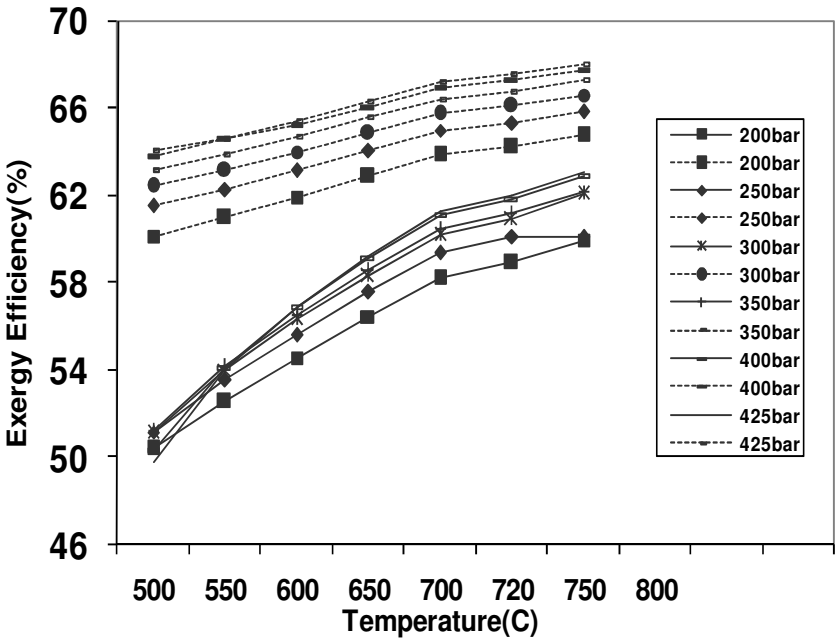

Fig 6. Variation of Exergy efficiency with T1 for Different values of P1 at P_c= 0.06 bar.

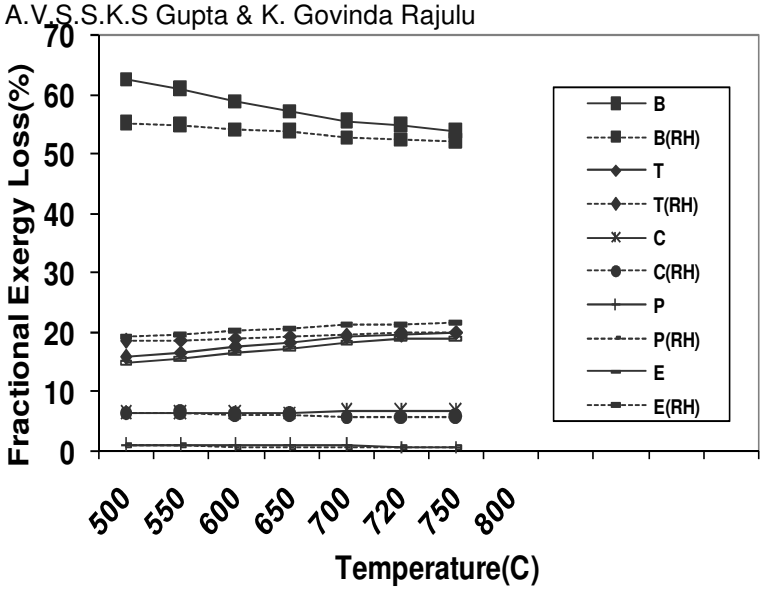

Fig 7. Effect of Temperature on Fractional Exergy loss of different components for P1=325bar

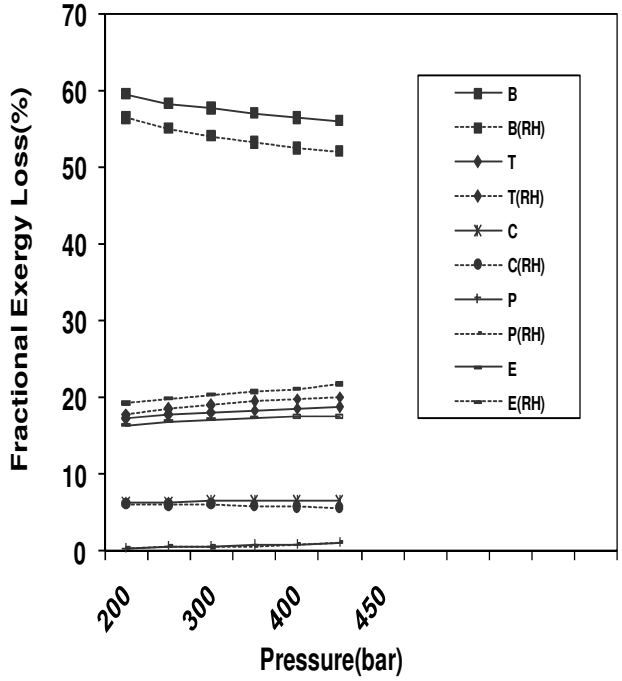

Fig 8. Effect of Pressure on Fractional Exergy loss of different components for T1=650^{0}C

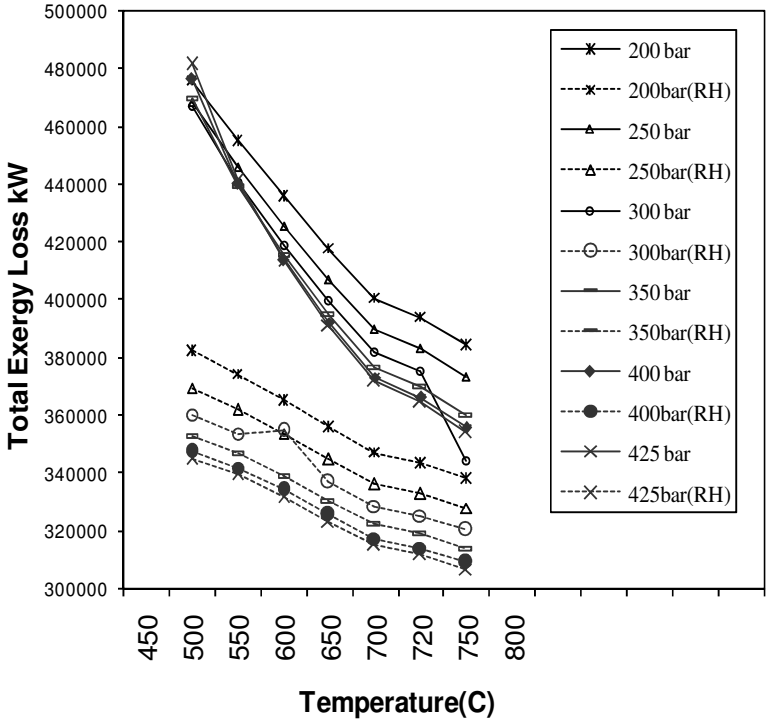

Fig 9. Variation of Total Exergy Loss with T1 for different values of P1

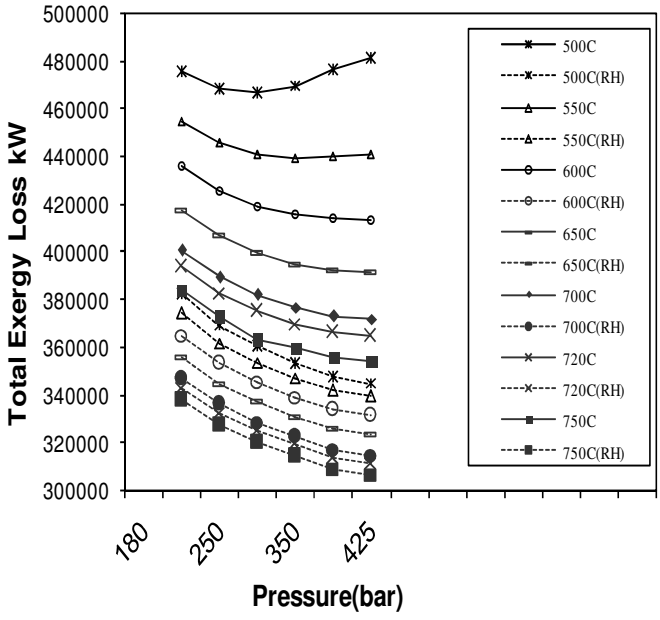

Fig 10 Variation of Total Exergy Loss with P1 for different values of T1

Figure 7shows the variation of fractional exergy loss of different components at different temperatures with and without reheating. It is observed that for a boiler the decrease in fractional exergy loss with increase in temperature is high for a cycle with reheating when compared to a cycle without reheating. At a Pressure/Temperature of 325bar/650^{0}C the decrease in fractional exergy loss in the boiler with reheating is nearly 6% when compared to a cycle without reheating. The fractional exergy loss is reduced nearly 5% in the turbine when compared with reheating.
Figure 8 shows the variation of fractional exergy loss of different components at different pressures with and without reheating. The fractional exergy loss in the boiler without reheat is 62.72% at 325bar/500^{0}C where as it is 53.73% at 325bar/750^{0}C. The fractional exergy loss with reheat at the same pressure at 500^{0}C is 54.92% and at 750^{0}C is 52.11%. The fractional exergy loss in the turbine is decreases with increase in temperature at particular pressure, but at higher temperature both fractional exergy loss is almost nearly same with and without reheating.

Figure 9 shows the variation of total exergy loss with temperature for different values of turbine inlet pressures with and without reheating. The total exergy loss is decreasing with increase of pressure and temperatures with and without reheating of the different components in the supercritical cycle. It is observed that total exergy loss is less with reheating when compared without reheating.

Fig 10 shows the variation of total exergy loss with pressure for different values of turbine inlet temperatures with and without reheating. The total exergy loss is decreasing with increase of temperature with and without reheating of the different components in the supercritical cycle. It is observed that total exergy loss is less with reheating when compared without reheating.

6. CONCLUSIONS:

This paper analyzes the supercritical cycle with and without reheat from both cycle efficiency, exergy efficiency. The energy and exergy analyzes of the cycle has been performed pressure range between 200bar to 425 bar and temperature range are 500^{0}C-800^{0}C. First law analysis and second law analysis has carried out throw with and withot reheat. The irreversibility and fractional exergy loss are determined for the cycle with and without reheat. It is found that the cycle efficiency is high in reheat than the non-reheat supercritical cycle. It is also conclude that exergy efficiency is high in reheat than non-reheat supercritical cycle. It is found that nearly 20-25% irreversibility is reduced by using single reheat in the boiler, where as it is 12-15% in the turbine than the without reheating. Fractional exergy losses of all the components in the cycle is determined and compared with and without supercritical cycle.

7. REFERENCES:

1. Bejan A., Tsatsaronis, G., and Moran A., 1996, Thermal Design and Optimization, Wiley, New York.
2. Nag, P.K. and Gupta, A.V.S.S.K.S, “Exergy analysis of Kalina cycle”, Applied Thermal Engineering Journal, Vol 18, No. 6, pp 427-439, 1998.
3. Kotas T.J., 1985, The Exergy method of Thermal Power analysis, Butterworth.
4. Kalina, I.A., “Combined-Cycle system with Novel Bottoming Cycle”, ASME Journal of Engineering for Gas Turbines and Power, Vol. 106, pp 737-742, 1984.
5. Milora, S.L., and Tester, J.W., “Geothermal Energy as a Source of Electrical Power”, MIT Press, 1977.
6. Y.M. El-sayed, and M. Tribus, “A Theoretical Comparision of Rankine and Kalina cycles, ASME publication, Vol. 1, 1995.
7. Kotas T.J., et al.,”Nomenclature for exergy analysis” ASME Journal of Power and Energy, Proc. Instn. Mech. Engrs Vol 209, pp 275-280.
8. Horlock J.H., et al., 2000, “Exergy Analysis of Modern Fossil-Fuel Power Plants”, J. of Engineering for Gas Turbines and Power, ASME , Vol.122 , pp 1-7

9. Nag P.K., Power plant engineering, 2nd Ed., Tata Mc Graw – Hill, New York, 1995.

10. R.H.Perry and D.Green, Perry's chemical Engineers Hand Book, 7th Ed., Mc Graw-Hill.

NOMENCLATURE:

h = enthalpy (kJ/kg)

P = Pressure (bar)

□̃ □Ambient temperature(^{0}C)

s = entropy (kJ/kg-K)

∑= Sum

m_s =Mass flow rate of steam(kg/s)

m_g = Number of moles of the flue gas

m_{cw} = Mass of cooling water (kg/s)

I = Irreversibility (kW)

T_o = Absolute Temperature (K)

C_{pw} = Specific heat at constant pressure (kJ/kg-K)

T_{wo} =Temperature of the cooling water out(^{0}C)

T_{wi} =Temperature of the cooling water in(^{0}C)

W_{net} = Net work done (kJ/kg)

G = Gibbs function (kJ)

Suffix:

rh = reheat

cw=cooling water

wi = water inlet

wo=water outlet

A = flue gas inlet

B = flue gas outlet

s*up= supplied*

ABRREVATIONS:

B = boiler

T = turbine

C = condenser

P = pump

E = exhaust

H.S = heat supplied

Interdisciplinary Automation and Control in a Programmable Logic Controller (PLC) Laboratory

Jack Toporovsky ytoporov@bridgeport.edu
Department of Electrical Engineering
University of Bridgeport
Bridgeport, CT, 06604, USA

Christine D. Hempowicz chemp@bridgeport.edu
Office of Sponsored Research
University of Bridgeport
Bridgeport, CT, 06604, USA

Tarek M. Sobh sobh@bridgeport.edu
Department of Computer Science and Engineering
University of Bridgeport
Bridgeport, CT, 06604, USA

Abstract

The University of Bridgeport's School of Engineering created a new PLC Industrial Control Lab to accommodate lab-based, hands-on training using different types of Programmable Logic Controllers (PLCs). The Lab and associated courses were designed to meet ABET's EC2000 standards and prepare students for the workforce.

Keywords: engineering education, interdisciplinary lab courses, programmable logic controllers, robotics.

1. INTRODUCTION/BACKGROUND

At the beginning of the new millennium, engineering education programs were challenged to meet the latest set of standards established by ABET, known as *Engineering Criteria 2000* (EC2000). EC2000 emphasized outputs, as expressed in 11 learning outcomes [1]. In particular, upon program completion, graduates should have acquired the knowledge and skills to solve problems, using techniques and tools of engineering practice in a collaborative setting.

This approach to engineering education is not entirely new. Early engineering education focused on skill acquisition through apprenticeships, practical training, and the like, until the end of World War I [2]. The emphasis on engineering science and mathematics in engineering curricula was not introduced until the mid-1950s. This had the effect of producing engineers who could analyze a problem but were less prepared to design and apply solutions [2]. EC2000 was, in part, a response to the need for engineering graduates to be able to seamlessly transfer classroom and laboratory knowledge and practice to the workplace. Engineering graduates must be "job ready" and practiced in working as part of an interdisciplinary team [3] and [4].

2. PROBLEM STATEMENT

The University of Bridgeport's School of Engineering (UBSOE) identified the need for a Programmable Logic Controller (PLC) Industrial Control Lab to support laboratory-based courses in which students could be educated in technological processes that are part of the field of automation control. Course curricula should support student outcomes outlined in EC2000's Criterion 3. Program Outcomes and Assessment, specifically 3a-e, j, and k. Further, course curricula should be interdisciplinary such that electrical

engineering and mechanical engineering students could enroll in the same course. Finally, students should have the opportunity to learn on leading PLC models in order to be best prepared to work in the private sector. The lab should be equipped, then, with Allen-Bradley and Mitsubishi PLCs since the former is widely used in the U.S. and the latter is widely used throughout Asia.

3. METHODOLOGY

UBSOE's existing Interdisciplinary Robotics, Intelligent Sensing, and Control (RISC) Laboratory was expanded to incorporate the new PLC Industrial Control Lab. The new PLC Lab was equipped with electrical cabinets and control panels outfitted with five Allen-Bradley and four Mitsubishi PLCs [5]-[12].

Two courses were developed: EE 463: Industrial Controls, and EE 464: Programmable Logical Controls. In EE 463, students learn basic concepts in pneumatic controls and different types of sensors used widely in industry, robotics, and vision concepts. In EE 464, students learn basic and advanced concepts and applications for PLC programming. In addition, students learn to integrate various components with PLCs, such as sensors, switches, vision cameras, variable speed drives, etc. Instructional design for each course is more focused on inquiry and problem-based learning within the context of classroom community, and less focused on lecture-style instruction. All are supported in the literature [13] and [14].

3.1 Equipment Design and Integration

In the PLC Industrial Control Lab, all control cabinets share the same local network with different types of PLCs and Human Machine Interfaces (HMIs), so students are able to communicate to any of them from the class computer stations.

A team of PLC students designed an integration of different brands of control components into one application. The components were: SLC5/03 Allen-Bradley PLC, Network Card 1761-NET-ENI, Mitsubishi Variable Frequency Drive, and Cutler Hammer PM1700 Touch Screen. For this project, students were involved in wiring, communications cable design, equipment programming, and troubleshooting.

Students produced the layout design and wiring diagrams for the project to integrate the SLC5/03 PLC with the Mitsubishi Variable Frequency Drive (VFD) and Cutler Hammer Touch Screen, and to establish a network to the PLC. The design layouts and wiring diagrams were created using AutoCAD. Students were able to build a control cabinet with output to an AC motor, programming of the PLC, VFD, touch screen, etc. (See Figure 1.)

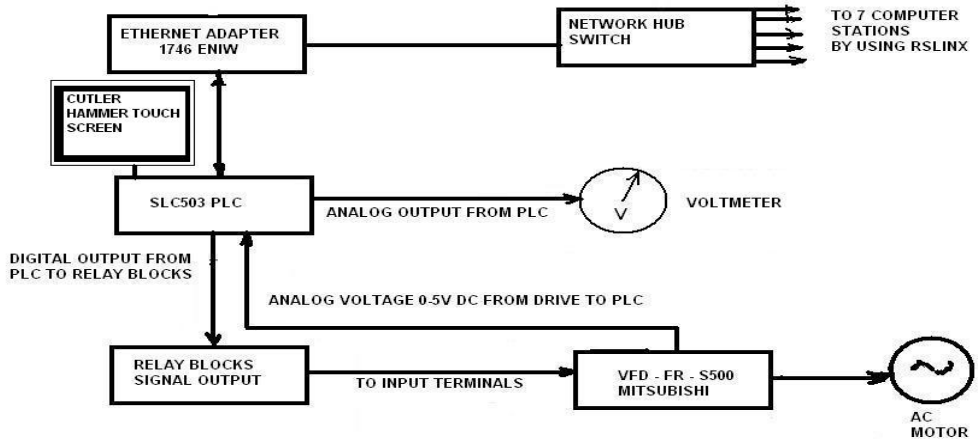

FIGURE 1: Any computer station can establish communication to the SLC5/03 PLC through the network hub switch and through the internet adapter (# 1746ENIW). At the same time, an AC motor (3-phase AC) runs commands from the PLC, transferring from the relay module to the Mitsubishi Variable Frequency Drive (VFD/FR/S500). The value of the frequency is converted to an analog voltage (0 to 5 volts) from the VFD; it is then read by an analog card. In this way, a closed-loop communication link is established between the PLC and the VFD.

During the project, students learned how to use the software FR Configurator to run the motor with different parameter sets and observe the effects. After the students decided which parameters were needed for the operation, they downloaded them into the VFD.

At the end of the project, different touch screen recipes for various applications had been created.

- **Recipe 1**
  Selector switch # 1 should be at the ON position. Press the start push button on the touch screen and select a value for the motor's speed. (The motor will run at one of three predetermined speeds.) The motor speed control parameter (expressed as voltage) is shown on the touch screen. Also shown is the motor's speed in RPM's.

FIGURE 2: Robotic arm is shown, controlling a conveyor line, with optical, proximity, and capacitive sensors. A Mitsubishi PLC is located on a shelf below the arm and to the right, and a Mitsubishi RV-M1 robotic unit is on the same shelf, to the left.

- **Recipe 2**
  Selector switch # 1 should in the OFF position. In this mode, the motor will run continuously, first at a low speed (typically 50 to 100 RPMs), then at a medium speed (approximately 100 to 300 RPMs), then at a high speed (300 to 500 RPMs), then back to low speed, medium speed, etc. The analog voltage drive speed and RPM are displayed on the touch screen.

- **Recipe 3**
  This mode is designed to control the jogging operation by pressing the jog-forward or jog-reverse push button or touching the jog-forward/reverse icon on the touch screen. The motor will rotate forward or reverse, depending on which jog button is pressed. The analog voltage drive speed and RPM are displayed on the touch screen.

- **Recipe 4**
  Establish motor control by reading the value potentiometer on the front panel. The speed can be increased from 0 RPM to a maximum of 500 RPM (as controlled by the PLC) by turning the potentiometer knob clockwise. To perform this test, the VFD parameter # 79 should have a value of 4.

3.2 PLC Programming and Robot Integration

The first author worked with a team of PLC students to design an automation conveyor line to implement closed-loop communications between the Mitsubishi robotic arm Roboware™ software and FX series Mitsubishi PLC. See Figure 2.

The major task of the project was to establish the communication and movements of the Robotics Arm using the Mitsubishi Movemaster RV-M1 series robotics kit. When the photo eye sensor detects the metal or plastic object on the loading area, the pneumatic cylinder then pushes the object to the part-detecting sensor (proximity sensor) (See Figure 3). If the object is plastic, the conveyor starts and stops at "position one," which is closer to the sensor. The robotic arm will move to pick up the plastic object and place it into "box one". If the object is metal, the conveyor stops when it is detected by the track sensor (see-through eye sensor) on the conveyor belt. The robotic arm moves to that position to pick up the object and place it into "box two".

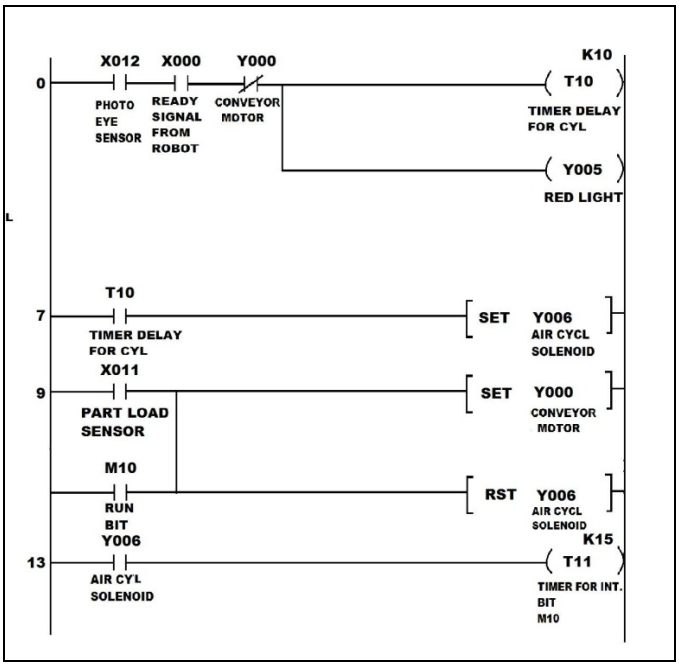

FIGURE 3: Controlling the belt movements (Y6), part present (X12), red light indicator (Y5) and ready signal from robot unit (X0), etc., presented in the ladder diagram. Constant communication between the robot controller and Mitsubishi PLC is provided through executing this program and running Roboware™ software.

The inputs and outputs are on the conveyor line, operated using the GX-Developer (Mitsubishi software). See Table 1.

Input	Address	Output	Address
Capacitive Proximity Sensor	X10	Conveyor Motor	Y00
Part Load Sensor (prox. sensor)	X11	Gear Motor	Y01
Photo Eye Sensor (loading area)	X12	Red Light	Y05
Track Sensor (end of the conveyor)	X13	Air Cylinder	Y06

TABLE 1: Programming of PLC and Robot

The command line to enter some commands such as MJ (Move Joint) is as follows:

Function: Turns each joint the specified angle from the current position. (Articulated interpolation)
(1) The least input increment of the turning angle is 0.1, e.g. specify 15.2 for 15.2.
(2) The open/close state of the hand does not change before and after the movement. Error mode II occurs before the axis motion if any turning angle entry exceeds the robot operational space.
(3) The default turning angle is 0.

The position data table for pick and place scenario loaded into robotic amplifier can be found in Table 2.

Robotic Arm Position Data (PD)					
1	+254.6	+427.2	+174.6	-46.9	+32.2
4	-259.0	+185.1	+212.0	-87.0	+32.2
5	-256.6	+187.2	+236.0	-87.0	+32.2
6	-259.0	+185.1	+199.0	-87.0	+32.2
7	-259.0	+185.1	+235.0	-87.0	+32.2
8	-259.0	+188.1	+192.0	-87.0	+32.2
9	-259.0	+185.1	+263.0	-87.0	+32.2
10	-317.4	-24.5	+263.0	-86.9	+32.2
11	-324.5	-25.1	+43.1	-89.0	+32.2
12	-324.5	-25.1	+36.1	-89.0	+32.2
13	-324.5	-25.1	+44.1	-89.0	+32.2
14	+299.1	+182.9	+233.8	-81.0	+145.1
15	+297.9	+179.1	+196.4	-86.0	+145.1
16	+302.5	+184.8	+258.3	-76.9	+145.1
17	+22.2	+353.8	+258.3	-76.9	+174.7
18	+23.3	+371.4	+58.8	-92.0	+174.7
19	+28.8	+397.2	+44.9	-87.0	+174.7
20	-14.4	+281.1	+515.6	-49.0	+179.9

TABLE 2: Robotic Arm Position Data (PD)

3.3 Assessment

Assessment of student understanding and ability to implement a PLC's interaction with sensors, motors, and other objects were performed for both short-term and long-term assessment. (1) Short-term

assessment took place within the timeframe of an individual course. Each student was assessed by performance on eight homework assignments (20 percent of course grade), an in-class, mid-term exam (30 percent of course grade) and an individual, open-ended project, in which each student was expected to incorporate codes, commands, and design functions (50 percent of course grade). (2) Long-term assessment is conducted after course completion and post-graduation. Each student is surveyed periodically to determine how each component of the lab course has helped the graduate in his or her professional employment and career.

4. RESULTS

Students who successfully complete a laboratory course are able to: understand and implement different types of software packages for the purpose of robot control (such as GX-Developer or Roboware™ for Mitsubishi products or RS-500 and RS-5000 and Factory-Talk for Allen-Bradley products); and program Human Machine Interface (HMI) screens to integrate them into PLC control automation lines. After graduation, they can perform the tasks listed above and communicate intelligently with members of a team of designers working on automating any industrial process.

5. CONCLUSIONS AND FUTURE WORK

UBSOE's PLC Industrial Control Lab will continue to provide critical laboratory education for graduate engineering students. Further, the authors envision that the Lab will assist local companies in hardware design and manufacturing and provide the necessary software programming for different applications in process automation.

6. ACKNOWLEDGEMENT

The authors acknowledge the equipment contributions by Gibson Engineering Company, Incorporated of Norwood, MA and HESCO of Rocky Hill, CT.

7. REFERENCES

[1] L.R. Lattuca, P.T. Terenzini, and J.F. Volkwein. "Engineering Change: A Study of the Impact of EC2000", ABET, Inc. Baltimore, MD (March, 2006).
[2] M. T. Huber and S. Morreale (Eds.). "Disciplinary Styles in the Scholarship of Teaching and Learning: Exploring Common Ground", Washington, DC: AAHE/ Carnegie Foundation for the Advancement of Teaching (2002).
[3] D. Richter. "Infusing an interdisciplinary automation experience in engineering technology education," in Proceedings of the 2007 American Society for Engineering Education Annual Conference & Exposition, Honolulu, HI, USA, 2007.
[4] T. Stiller and G. Johnson. "Constituent influences on engineering curricula," in Proceedings of the 2004 American Society for Engineering Education Annual Conference & Exposition, Salt Lake City, UT, USA, 2004.
[5] C. Mirman. "Educating future engineers requires teamwork". Automation Notebook, Fall Issue 12, 2008 [Online].
[6] "E-Designer for the E1000-series Reference Manual", Mitsubishi Electric, MA 00759A, 2005-03.
[7] "MicroLogix 1100 Programmable Controllers, Bulletin 1763, Instruction Set Reference Manual", Rockwell Automation, Inc., Publication 1763-RM001B-EN-P (April 2007).
[8] "FX Series Programmable Controllers Programming Manual", Mitsubishi Electric, Manual number JY992D88101, Manual revision D (April 2003).
[9] "Roboware™ Programming/Control Software for Mitsubishi Robots Ver 2.xx User Manual", KakeWare©, RV-M1 & RV-M2 Models.
[10] "Melsoft FR Configurator Instruction Manual VFD Software", Mitsubishi Electric, FR-SW2-SETUP-WE.
[11] "Logix 5000 Controllers Common Procedures Programming Manual", Rockwell Automation, Inc., Publication 1756-PM001I-EN-P (January 2007).
[12] "SLC 500 Instruction Set Reference Manual", Rockwell Automation, Inc., Publication 1747-RM011E-EN-P (January 2006).

[13] K.C. Bower, T.W. Mays, and C.M. Miller, “Small group, self-directed problem based learning development in a traditional engineering program,” in 34th ASEE/IEEE Frontiers in Education Conference, Savannah, GA, USA, 2004.
[14] S.M. Lord and M.M. Camacho, “Effective teaching practices: Preliminary analysis of engineering educators, in *37th* ASEE/IEEE Frontiers in Education Conference, Milwaukee, WI, USA, 2007.

Extraction of Satellite Image using Particle Swarm Optimization

Er.Harish Kundra
Assistant Professor & Head hodcseit@rayatbahra.com
Rayat Institute of Engineering & IT , Railmajra,
Punjab,India.

Dr. V.K.Panchal
Director, vkpans@hotmail.com
DTRL,DRDO,
Delhi,India.

Sagar Arora
B.Tech Student touch_sagar@yahoo.com
Rayat Institute of Engineering & IT
Punjab,India.

Karandeep Singh
B.Tech Student karanatter@gmail.com
Rayat Institute of Engineering & IT, Railmajra
Punjab,India

Himashu Kaura
B.Tech Student himanshu.kaura21@yahoo.com
Rayat Institute of Engineering & IT, Railmajra
Punjab,India.

Abstract

Of all tasks in photogrammetry the extraction of cartographic features is the most time consuming. Fully automatic acquisition of features like roads and buildings, however, appears to be very difficult. The extraction of cartographic features form digital satellite imagery requires interpretation of this imagery. The knowledge one needs about the topographic objects and their appearances in satellite images in order to recognize these objects and extract the relevant object outlines is difficult to model and to implement in computer algorithms. This paper introduces Particle Swarm Optimization based method of object extraction from Google Earth image (satellite image). This paper deals with the land cover mapping by using swarm computing techniques. The motivation of this paper is to explore the improved swarm computing algorithms for the satellite image object extraction.

KEYWORDS - Objects extraction, Google Earth image, Unsupervised Learning PSO algorithm

1. INTRODUCTION

Natural or man-made objects extracted from Google earth has been used for many different purpose, e.g.. military, map publishing, transportation, car navigation, etc. Automatic natural objects (road, building, forest, water body etc.) extractions are a challenging problem, and no

existing software is able to perform the task reliably. Since manual extraction of natural objects from imagery is very time consuming, automatic method have the potential to improve the speed and utility for military and civil application and are therefore highly desirable. Google Earth is a virtual globe, map and geographic information program that were originally called Earth Viewer. Google Earth provides satellite images of any area. In this paper, Google earth's image is used for implementation of extraction natural or man-made object from satellite image.Simultaneously there is a new wide range of computational algorithms that have emerged from the behaviour of social insects. Social insects are usually characterized by their self organization and with the minimum communication or the absence of it. Every social insect individually is self-autonomous. They can obtain information about environment and interact with the remote insects or environment indirectly, by stigmergy. All these features characterize Swarm Intelligence . We can found these features in nature such as ant colonies, bird flocking, animal herding, fish schooling etc. The two most widely used swarm intelligence algorithms are Ant Colony Optimization (ACO) and Particle Swarm Optimization (PSO).

We are presenting here the usage of PSO (Particle Swarm Optimization) algorithms applied to Google earth's image for the extraction of natural or man-made object. The activities for the development of this paper are organized in four sections.

In section 1, a high- resolution satellite image (Google earth), including scenes of highways, forest, buildings, were formed and how particle swarm optimization, unsupervised learning technique are used. In section 2, using the collected image form section 1, PSO algorithm to detect and extract the natural or man-made objects was developed.In section 3, algorithms to detect, extract and classify natural or man-made objects (road, building, forest, barren land etc.) were implemented.In section 4, the feasibility of using this image and the results are presented.

2. SECTION 1: USAGE OF IMAGE FROM GOOGLE EARTH AND APPLICATION OF PARTICLE SWARM OPTIMIZATION AND UNSUPERVISED LEARNING

Google Earth

Google Earth is used to get number of satellite images. Google Earth is a virtual globe, map and geographic information program that was originally called Earth Viewer, and was created by Keyhole, Inc, a company acquired by Google. To collect image from Google Earth and implementing PSO algorithm for extracted natural or man-made object from satellite image (Google Earth). Google Earth displays satellite images of varying resolution of the Earth's surface, allowing users to visually see things like cities and houses etc. The degree of resolution available is based somewhat on the points of interest and popularity, but most land (except for some islands) is covered in at least 15 meters of resolution.

A few Google Earth images :

A)

B)

Figure 1. Enlarge Google earth images (A,B)

Particle Swarm Optimization

Particle swarm optimization (PSO) is a swarm intelligence based algorithm to find a solution to an optimization problem in a search space, or model and predict social behavior in the presence of objectives.

Particle swarm optimization is a stochastic, population-based computer algorithm for problem solving. It is a kind of swarm intelligence that is based on social-psychological principles and provides insights into social behavior, as well as contributing to engineering applications. The particle swarm optimization algorithm was first described in 1995 by James Kennedy and Russell C. Eberhart. The techniques have evolved greatly since then, and the original version of the algorithm is barely recognizable in current ones.

Social influence and social learning enable a person to maintain cognitive consistency. People solve problems by talking with other people about them, and as they interact their beliefs, attitudes, and behaviors change; the changes could typically be depicted as the individuals moving toward one another in a socio-cognitive space.

The particle swarm simulates this kind of social optimization. A problem is given, and some way to evaluate a proposed solution to it exists in the form of a fitness function (4).

The swarm is typically modeled by particles in multidimensional space that have a position and a velocity. These particles fly through hyperspace and have two essential reasoning capabilities: their memory of their own best position and knowledge of the global or their neighborhood's best. So a particle has the following information to make a suitable change in its position and velocity:

a. A global best that is known to all and immediately updated when a new best position is found by any particle in the swarm.
b. Neighborhood best that the particle obtains by communicating with a subset of the swarm.
c. The local best, which is the best solution that the particle has seen.

Unsupervised Learning

In unsupervised learning, all the observations are assumed to be caused by latent variables, that is, the observations are assumed to be at the end of the causal chain. In practice, models for supervised learning often leave the probability for inputs undefined. This model is not needed as long as the inputs are available, but if some of the input values are missing, it is not possible to infer anything about the outputs. If the inputs are also modeled, then missing inputs cause no problem since they can be considered latent variables as in unsupervised learning.

In unsupervised learning, the learning can proceed hierarchically from the observations into ever more abstract levels of representation. Each additional hierarchy needs to learn only one step and therefore the learning time increases (approximately) linearly in the number of levels in the model hierarchy.

3. SECTION 2: DEVELOPMENT OF PSO ALGORITHM TO DETECT AND EXTRACT NATURAL AND MAN MADE OBJECTS

Natural or man-made object Extraction.

Object extraction of image procedures is to automatically categorize all pixels in an image into roads, forest, barren land, water bodies and settlements. In this paper we extract the objects from the images using PSO algorithm. To do this, appropriate threshold values have to be computed, and then segmentation is performed. To compute the appropriate threshold values several problems had to be analyzed. In this phase, an algorithm for the extraction of objects from Google earth's image was developed. This test image is presented various conditions under which the performance of our algorithm was evaluated. In the following section the proposed algorithm is described.

The Algorithm: Detection of Objects

The algorithm is based on global threshold (average) using PSO. To obtain the desired results, the

histograms of several of the scenes in the database containing Objects, were analyzed. From the analysis, we divided the histogram in five main regions in the basis of Unsupervised learning. Figure drawn below shows these regions. Region I start from the lowest intensity values to half of the midway of average intensity. For most of the cases, the intensity values on this region cover water bodies. Region II covers intensities that go from approximately half of the midway of the average intensity to midway of average intensity, and typically covers trees. Region III goes from midway of average intensity, to average intensity and covers bright gray objects such as highways. Region IV goes approximately from average intensity to midway of highest intensity and generally covers bright objects like buildings, road dividers, etc. Region V goes approximately from midway of highest intensity to highest intensity and generally covers barren land(6).

Figure 2: Google's Earth Image

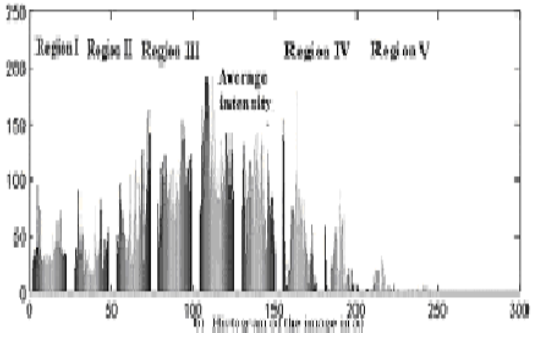

Figure 3: Histogram of the Image (2)

Morphological Operations

Morphology is a technique of image processing based on shapes. The value of each pixel in the output image is based on a comparison of the corresponding pixel in the input image with its neighbours. By choosing the size and shape of the neighbourhood, you can construct a morphological operation that is sensitive to specific shapes in the input image.

4. SECTION 3: IMPLEMENTATION OF ALGORITHMS TO GET THE DESIRED RESULT

Computing the Threshold T using PSO

To evaluate the threshold values, we created ten agents which scan their respective regions assigned to them from the image. Every agent scans the image row wise to find local best values for each row and eventually evaluates its global best for the assigned region. Among these regional global bests the agents select the most suitable candidate solution by communicating with each other. This is known as the Threshold value or the Global best.

Pseudo code for Object Extraction

The process comprises of following steps:

1. Preprocessing: e.g. Atmospheric, correction, noise suppression, band ration, principal component analysis etc.
2. Selection of the particular feature which best describes the object.
3. Decision: Choice of suitable fitness function for comparing the image patterns with the target patterns.
4. Assessing the accuracy of the object extraction

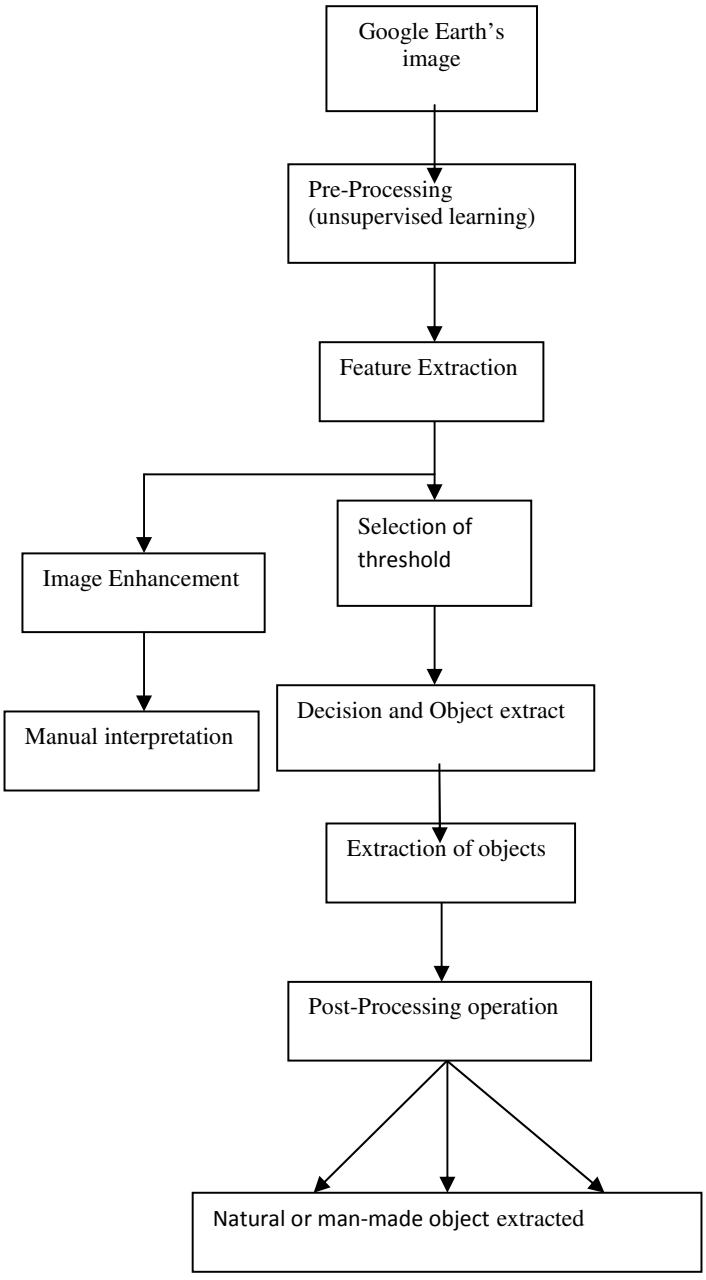

Figure 4: Flowchart for feature extraction

```
Main Program
Iteration =100
Particle= 10
While fitness value= threshold value
For each iteration
  For each particle in the swarm
     Initialize each particle randomly respective regions
     If particle finds best local best value (best object)
         Then update particle position and velocity
Else
Not updated
End for
Find best global best particle (fitness function)
End for
End while
End Program Loop
```

Pseudo code: Implementation of algorithm

5. SECTION 4: RESULTS

Figure 5 shows natural or man-made objects which we extract from Google earth image.
To extract Water, Barren land, Road, Settlement, Tree etc. objects in the image which are following:

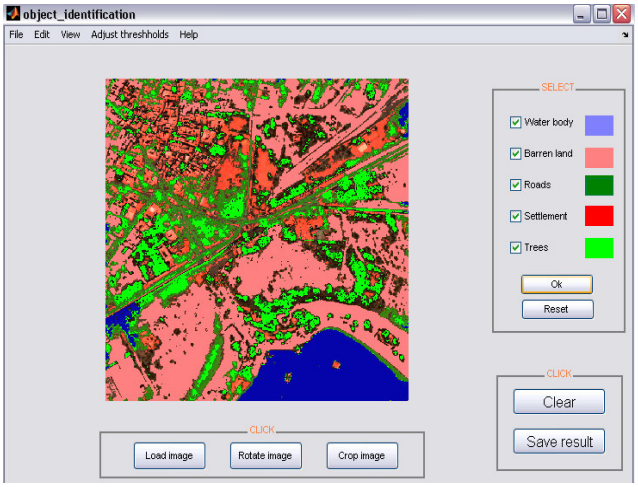

Figure 5: Natural or Man-made Object Extraction image.

6. CONCLUSION

In this paper, a new approach for natural or man-made object extraction in urban areas from high resolution satellite image (Google Earth) is proposed. By combining the spectral information and shape measures we may to find natural objects from the image. These objects may further be used for urban planning, ground water estimation, GIS mapping etc. The experimental results on

real Google Earth imagery demonstrate that it is an effective way to detect objects by learning from object's features. It is fully depend on unsupervised earning. The results prove that proposed approach effectively extracts the major objects from the Google Earth's image.

7. REFERENCES

1. Campbell, J.B. (1987) *Introduction to Remote Sensing.* The Guilford Press, New York.
2. Tso Brandt and Mather Paul, *Classification Methods for Remotely Sensed Data*, Taylor and Francis, London & New York.
3. T.M. Lillesand and R.W. kiefer "*Remote Sensing & Image Interpretation*", 3rd edition, 1994.
4. Swarm intelligence - James Kennedy
5.GoogleEarth
6. Er. Aashima,Er.Harish Kundra, Er.Monika Verma *"Filter for Removal of Impulse Noise By Using Fuzzy",* International Journal of Image Processing (IJIP),Vol 3 Issue 5, Pages:184-25

Transient Stability Assessment of a Power System by Mixture of Experts

Reza Ebrahimpour ebrahimpour@ipm.ir
Department of Electrical Engineering
Shahid Rajaee University
Tehran, P.O.Box 19395-5746, Iran

Easa Kazemi Abharian e63kazemi@gmail.com
Department of Electrical Engineering
Shahid Rajaee University
Tehran, Iran

Seyed Zeinolabedin Moussavi Smoussavi@srttu.edu
Department of Electrical Engineering
Shahid Rajaee University
Tehran, Iran

Ali Akbar Motie Birjandi motiebirjandi@srttu.edu
Department of Electrical Engineering
Shahid Rajaee University
Tehran, Iran

Abstract

Recent blackouts in different countries have illustrated the very importance and vital need of more frequent and thorough power system stability. Therefore transient stability investigation on power system have became in focus of many researchers in the field. We have tried to introduce a new model for transient stability prediction of a power system to add a contribution to the subject. For this reason we applied so called, Committee Neural Networks (CNNs) methods as tools for Transient Stability Assessment (TSA) of power system. We use the "Mixture of Experts" (ME) in which, the problem space is divided into several subspaces for the experts, and then the outputs of experts are combined by a gating network to form the final output. In this paper Mixture of the Experts (ME) is used to assess the transient stability of power system after faults occur on transmission lines. Simulations were carried out on the IEEE 9-bus and IEEE 14-bus tests systems considering three phase faults on the systems. The data collected from the time domain simulations are then used as inputs to the ME in which is used as a classifier to determine whether the power systems are stable or unstable.

Keywords: Transient Stability Assessment, Committee Neural Networks, Mixture of the Experts, Time domain simulation method.

1. INTRODUCTION

This paper presents a novel method of using a neural network to predict transient stability. The security assessment of a power system requires analysis of the dynamic system behavior under a prescribed set of events known as contingencies. Conventionally this is done by simulating the system nonlinear equations. Since the stability limits cannot be determined from a single simulation. More than one simulation is required. The large size of the system adds to the complexity [1-3]. This method consists of simulating during and post-fault behaviors of the system for a given disturbance, observing its electromechanical angular swings during a few seconds. It is usually used to estimate stability status and to provide detailed operation information of the faulted systems as a benchmark. However, the simulation method is infeasible for on-line TSA mainly due to its time-consuming computation [2].

Problem of transient stability prediction has been treated by the flowing methods such as application of numerical routines or state space techniques [4,5], decision trees [6] , fuzzy neural networks [7,8], Multi Layer Perceptrons (MLPs) neural networks [3,9], radial base function neural networks[10-12], Probabilistic Neural Network (PNN) [13]. In a accordance to [2, 3] we proposed use of Committee Neural Networks (CNNs) for TSA.

By predicting transient stability status of power system, proper control actions can be taken. For instance, use can be made of this prediction to initiate important relay operations such as out-of-step blocking and tripping, or other control actions such as fast-valve control of turbines, dynamic braking, superconducting magnetic energy storage system, system switching, modulation of high voltage direct current (HVDC) link power flow and load shedding [6,7]. Moreover, by means of these predictions, the system planners can identify weak points of their power system (from transient stability viewpoint) for future developments [2].

N. Amjadi et al. in [2] uses non-trainable static combiners CNNs. They proposed a new hybrid intelligent system for transient stability of power system. In this method interpreter combine the response of neural networks in a voting procedure to determine the transient stability by status of the power system. The initiative work [3] we use stacked generalization model that it is trainable static combiners in CNNs. In this paper, we return our keen focus to dynamic combiners by the employment of mixture of experts. The result is a powerful and reliable method for transient stability assessment of power systems.

The actions of transient stability assessment using ME are explained and the performance of the CNNs is more efficient comparing with the stacked generalization model and the MLPs.

2. Mathematical Model of Multi-machine Power System

These The differential equations to be solved in power system stability analysis using the time domain simulation method are the nonlinear ordinary equations with known initial values. Using the classical model of machines, the dynamic behavior of an n-generator power system can be described by the following equations:

$$M_i \frac{d^2\delta_i}{dt^2} = P_{mi} - P_{ei} \quad (1)$$

It is known that,

$$\frac{d\delta_i}{dt} = \omega_i \quad (2)$$

By substituting (2) in (1), therefore (1) becomes

$$M_i \frac{d\omega_i}{dt} = P_{mi} - P_{ei} \quad (3)$$

Where:

. δ_i = rotor angle of machine i

. ω_i = rotor speed of machine i

. P_{mi} = mechanical power of machine i

. P_{ei} = electrical power of machine i

. M_i = moment of inertia of machine i

A time domain simulation program can solve these equations through step-by-step integration by producing time response of all state variables.

3. Mixture of Experts

Mixture of experts is the most famous method in the category of dynamic structures of classifier combining, in which the input signal is directly involved in actuating the mechanism that integrates the outputs of the individual experts into an overall output [16].
The combination of experts is said to constitute a committee machine**.** Basically, it fuses knowledge acquired by experts to arrive at an overall decision that is supposedly superior to that attainable by any one of them acting alone. Committee machines are universal approximations. They may be classified into two major categories:

1. Static structures. In this class of committee machines, the responses of several predictors (experts) are combined by means of a mechanism that does not involve the input signal, hence the designation "static."This category includes the following methods:
Ensemble averaging**,** where the outputs of different predictors are linearly combined to produce an overall output.
Boosting, where a weak learning algorithm is converted into one that achieves arbitrarily high accuracy.

2. Dynamic structures. In this second class of committee machines, the input signal is directly involved in actuating the mechanism that integrates the outputs of the individual experts into an overall output, hence the designation “dynamic”. Here we mention two kinds of dynamic structures:

- Mixture of experts, in which the individual responses of the experts are nonlinearly combined by means of a single gating network.
- Hierarchical mixture of experts, in which the individual responses of the experts are nonlinearly combined by means of several gating networks arranged in a hierarchical fashion [14].

In this paper we used mixture of experts by a single gating network that shows in fig 1.The first model’s network architecture is the well-known “mixture of experts” (ME) network.
The ME network contains a population of simple linear classifiers (the “experts”) whose outputs are mixed by a “gating” network [15].
In a revised version of “mixture of experts” model, to improve the performance of the expert networks, we use MLPs instead of linear networks or experts in Fig.1. The application of MLPs in the structure of expert networks calls for a revision in the learning algorithm. In order to match the gating and expert networks, the learning algorithm is corrected by using an estimation of the posterior probability of the generation of the desired output by each expert. Using this new learning method, the MLP expert networks’ weights are updated on the basis of those estimations and this procedure is repeated for the training data set. It should be mentioned that we do not use the notation of [15 & 16] to formulize the learning rules of the modified ME, but we follow the one which is described of [12], since it’s clear explanation of learning rules makes its extension easier for our purpose (the learning algorithm of the mixture structure with linear classifiers as experts is described in [16]).
Each expert is an MLP network with one hidden layer that computes an output O_i as a function of the input stimuli vector, x, and a set of weights of hidden and output layers and a sigmoid activation function. We assume that each expert specializes in a different area of the input space. The gating network assigns a weight g_i to each of the experts’ outputs, O_i. The gating network determines the g_i as a function of the input vector x and a set of parameters such as weights of

its hidden and output layers and a sigmoid activation function [16]. The g_i can be interpreted as estimates of the prior probability that expert g_i can generate the desired output y. The gating network is composed of two layers: the first layer is an MLP network, and the second layer is a soft max nonlinear operator. Thus, the gating network computers O_g, which is the output of the MLP layer of the gating network, then applies the soft max function to get:

$$g_i = \frac{\exp(O_{gi})}{\sum_{j=1}^{N} \exp(O_{ji})} \qquad i=1,2,3,\ldots,N \qquad (4)$$

Where N is the number of expert networks. So the g_i is nonnegative and sum to 1. The final mixed output of the entire network is:

$$O_T = \sum_i O_i g_i \qquad i=1,2,3,\ldots,N \qquad (5)$$

The weights of MLPs are learned using the error back-propagation, BP, algorithm. For each expert i and the gating network, the weights are updated according to the following equations:

$$\Delta w_y = \eta_g h_i (y - O_i)(O_i(1 - O_i))O_{hi}^T \qquad (6)$$

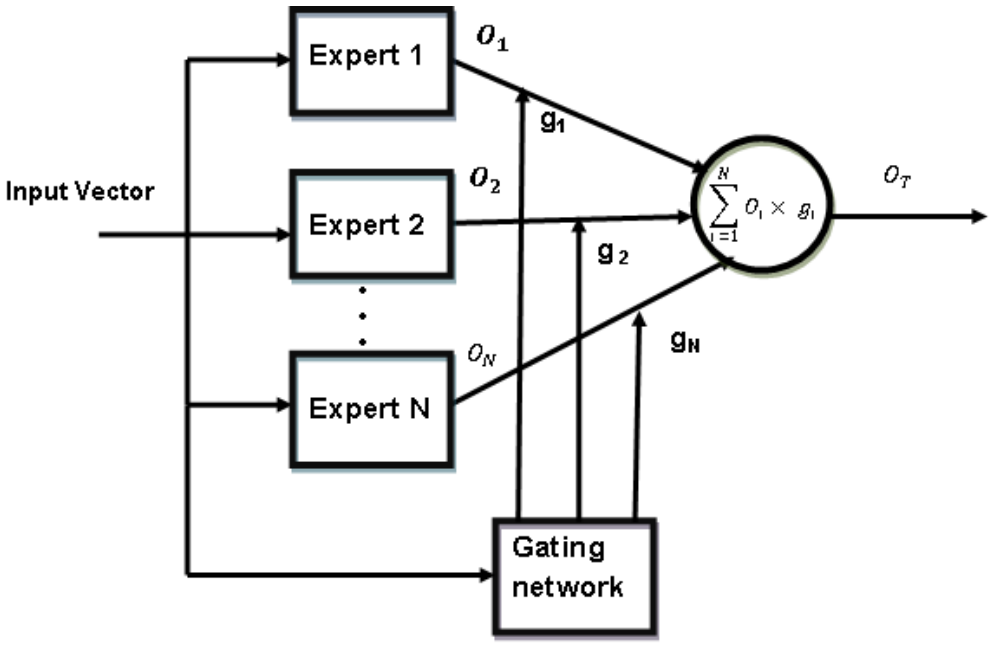

FIGURE 1: Mixture of experts is composed of expert networks and a gating network. Each expert is a feed forward network and all experts receive the same input and have the same number of outputs. The gating network is also feed forward, and typically receives the same input as the expert networks.

$$\Delta w_h = \eta_e h_i w_y^T (y - O_i)(O_i(1 - O_i))O_{hi}(1 - O_{hi})x_i \qquad (7)$$

$$\Delta w_{yg} = \eta_g (h-g)(O_g(1-O_g))O_{hg}^T, \quad (8)$$

$$\Delta w_{hg} = \eta_e w_{yg}^T (y-O_i)(O_g(1-O_g))O_{hg}(1-O_{hg})x_i \quad (9)$$

Where η_e and η_g are learning rates for the expert and the gating networks, respectively. w_y and w_h are the weights of input to hidden and hidden to output layer, respectively, for experts and w_{hg} and w_{yg} are the weights of input to hidden and hidden to output layer, respectively, for the gating network. O_{hg}^T and O_{hi}^T are the transpose of O_{hi} and O_{hg}, the outputs of the hidden layer of expert and gating networks, respectively. h_i is an estimate of the posterior probability that expert i can generate the desired output y:

$$h_i = \frac{g_i \exp(-\frac{1}{2}(y-O_i)^T(y-O_i))}{\sum_j g_j \exp(-\frac{1}{2}(y-O_i)^T(y-O_i))} \quad (10)$$

As pointed out by Dailey and Cottrell [15], in the network's learning process, ''the expert networks 'compete' for each input pattern, while the gate network rewards the winner of each competition with stronger error feedback signals. Thus, over time, the gate partitions the input space in response to the expert's performance''.
In this paper, we use 3 experts that experts are MLPs which are 10 neurons in hidden layer and gating network is a MLP which is 4 neurons in hidden layer.
Learning rate for gating network is $\eta_g = 0.01$ and learning rate for experts networks are $\eta_e = 0.28$ and numbers of epoch for training are 100 epochs.

4. Methodology

For validation and verification of the ME method in transient stability assessment we use the IEEE 9-bus and IEEE 14-bus power systems. Before the ME implementation, time domain simulations considering several contingencies were carried out for the purpose of gathering the training data sets. Simulations were done by using the MATLAB-based PSAT software [20].
Time domain simulation method is chosen to assess the transient stability of a power system because it is the more accurate method compared to the direct method. In PSAT, power flow is used to initialize the states variable before commencing time domain simulation. The differential equations to be solved in transient stability analysis are nonlinear ordinary equations with known initial values. To solve these equations, the techniques available in PSAT are the Euler and trapezoidal rule techniques. In this work, the trapezoidal technique is used considering the fact that it is widely used for solving electro-mechanical differential algebraic equations [6].
The type of contingency considered is the three-phase balanced faults created at various locations in the system at any one time. When a three-phase fault occurs at any line in the system, a breaker will operate and the respective line will be disconnected at the Fault Clearing Time (FCT) which is set by the user. The FCT is set randomly by considering whether the system is stable or unstable after a fault is cleared. According to [18], if the relative rotor angles with respect to the slack generator remain stable after a fault is cleared, it implies that FCT < CCT and the power system is said to be stable but if the relative angles go out of step after a fault is cleared, it means FCT>CCT and the system is unstable[5].

5. Transient Stability Simulation on the Test Systems:

Figure 2 shows the IEEE 9-bus system in which the data used for this work is obtained from [3, 6, and 20]. The system consists of three Type-2 synchronous generators with AVR Type-1, six transmission lines, three transformers and five loads.

By using data IEEE 9-bus system and applied data to PSAT software step time responses in Fig. 4 are resulted. By observing results stable and unstable cases come be clearly classified. A three phase fault is said to occur at time t=1 second on tree phase lines between bus 7 and 5. In Fig. 4(a), the FCT is set at 1.083 second while in Fig. 4(b) the FCT is set at 1.3 second. Fig. 4(a) shows that the stable relative rotor angles of the second and third generators oscillation compared to the first relative rotor angles generator. Figure 4(b) shows that the relative rotor angles of the generators that go out of step after a fault is cleared and inconsequence system is unstable.

Figure 3 shows the IEEE 14-bus system in which the data used for further investigation in this research work is obtained from [6]. The system consists of five Type-2 synchronous generators with AVR Type-1, 20 transmission lines and eleven loads. Figure 5 shows examples of the time domain simulation results illustrating stable and unstable cases.

A three phase fault is assumed to occur at time t=1 second between bus 4 and 2. In Figure 5(a), the FCT is set at 1.083 second while in Figure 5(b) the FCT is set at 4 second.

Name of input features	No. of features
Relative rotor angles $(\delta_i - 1)$	2
Generator speed (ω_i)	3
P_{gen} & Q_{gen}	6
P_{line} & Q_{line}	12
P_{trans} & Q_{trans}	6
Total number of feature	29

Table 1: Input feature selected for IEEE 9-bus system

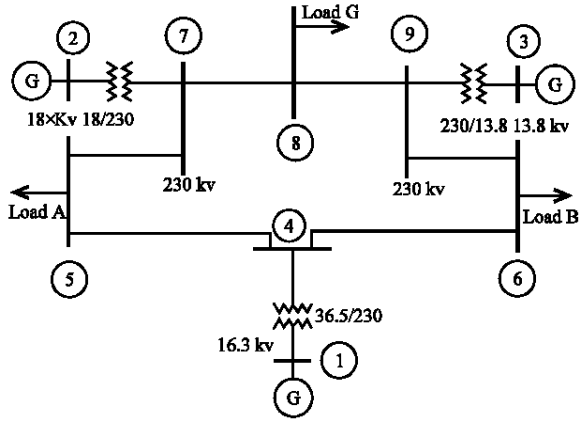

FIGURE 2: IEEE 9 bus System

Name of input features	No. of features
Relative rotor angles $(\delta_i - 1)$	4
Generator speed (ω_i)	5
P_{gen} & Q_{gen}	10
P_{line} & Q_{line}	40
P_{trans} & Q_{trans}	48
Total number of feature	107

Table 2: Input feature selected for IEEE 14-bus system

6. Data Preprocessing

The simulation on the system for a fault at each line runs for five seconds at a time step Δt , set at 0.05 sec. The fault is set to occur at one second from the beginning of the simulation. Data for each contingency is recorded in which one steady state data is taken before the fault occurs and 21 sampled data taken for one second duration after the fault occurs.

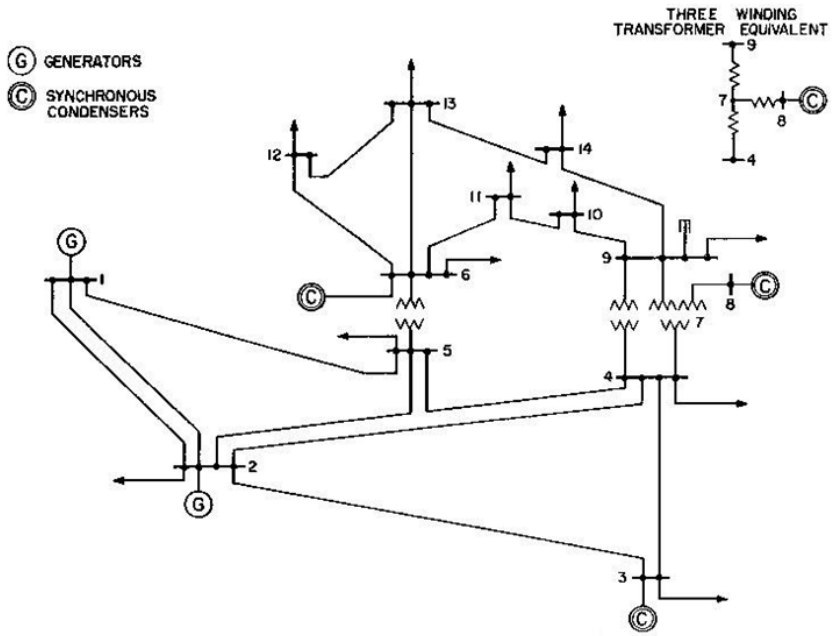

FIGURE 3: IEEE 14 bus System

There are 25 contingencies simulated on the IEEE 9-bus system and this gives a size of 25×21 or 525 data collected. The collected data were reduced to 468 after eliminating of data redundancy. There are 39 contingencies simulated on the IEEE 14-bus system and this gives a size of 39×21 or 819 data collected. Next, the repetitions are due to the faults that occur on the same line. For IEEE 9-bus systems, the FCT of the same line are set at four different times, two for stable cases and two for unstable cases.

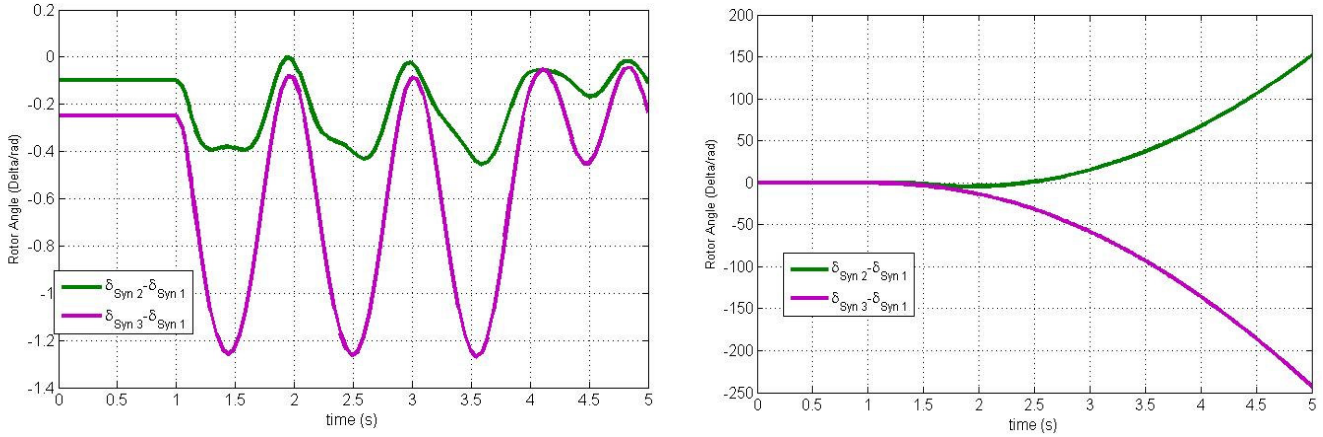

FIGURE 4: - Relative rotor angle bents of generators for a) stable and b) unstable cases for the IEEE 9-bus

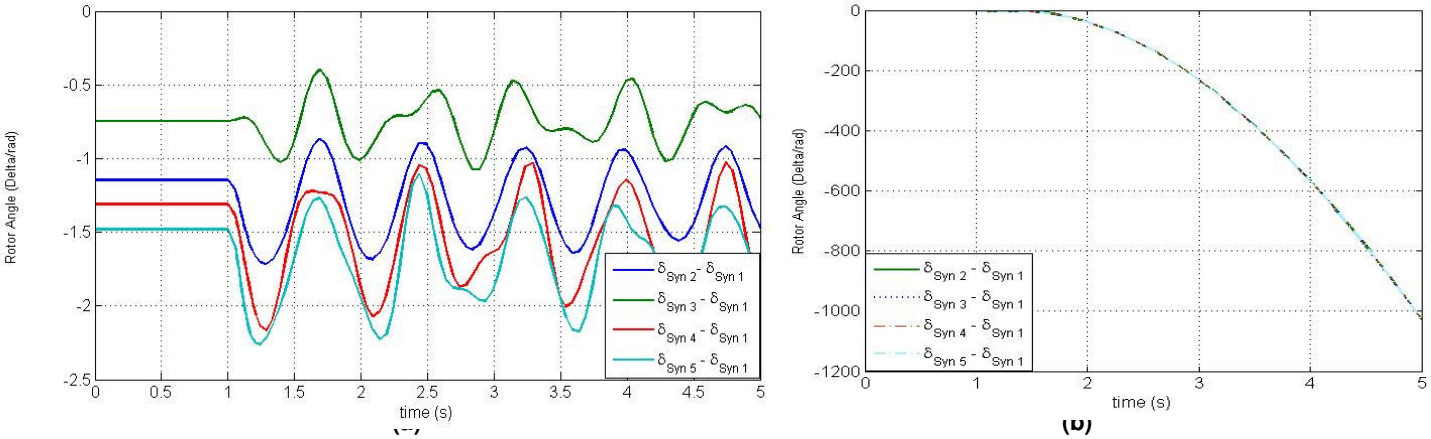

FIGURE 5: Relative rotor angle bents of generators for a) stable and b) unstable cases for the IEEE 14-bus system

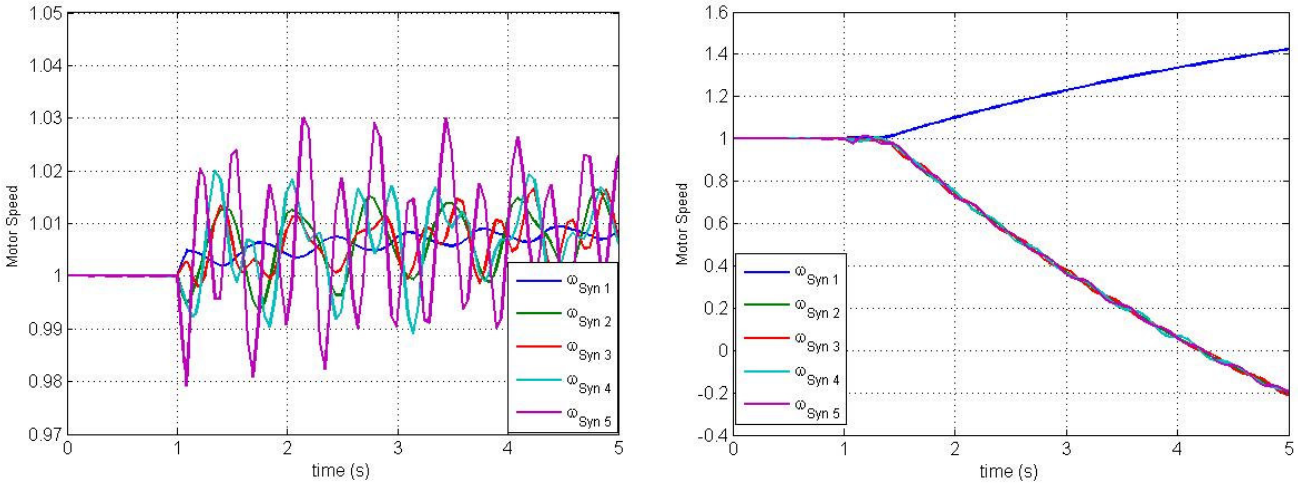

FIGURE 6: Relative angle speed bents of generators for a) stable and b) unstable cases for the IEEE 14-bus system

Model	Number of input features	Mean error	Misclassification(%)
MLP	107	53.2	370 (56.97%)
ME	107	0	0%

Table 3: The result of for IEEE 14-bus system

Model	Number of input features	Mean error	Misclassification(%)
MLP	29	0.0253	4 (3.42%)
CNN	29	0.0085	1(0.85%)
ME	29	0	0%

Table 4: The result of for IEEE 9-bus system

Methods	Mean error	Misclassification(%)
N.Izzri et al. [13]	1.71	1.71
R.Ebrahimpour et al. [3]	0.85	0.85
S.Kirishna et al. [11]	2.29	1.64
L. S. Moulin et al. [33]	4.8	4.8
N.Amjadi et al. [2]	0. 28	
A.G. Bahbah et al. [12]	0.025	
The proposed method	**0**	**0**

Table 5: Comparisons of the presented method with the related (%)

7. Input Features Selection in IEEE 9-bus system:

The selection of input features is an important factor to be considered in the ME implementation. The input features selected for this work are relative rotor angles (δ_{i-l}),generator angle speed(ω_i), generated real and reactive powers (Pgen , Qgen), real and reactive power flows on transmission line (P_{line} ,Q_{line}) and the transformer powers (P_{trans} , Q_{trans}). Overall there are 29 input features to the ME for IEEE 9-bus systems shown in table 1. Out of the (468) data collected from simulations, a quarter of the data which is (117) data are randomly selected for testing and the remaining (351) data are selected for training the neural networks. For IEEE 14-bus system a new feature namely voltage buses is consider too. In this case, there are 107 input features to the ME shown in table 2. Similarly 150 data out of 800 are randomly selected for testing and remaining data used as training.
ME results using 29 input features for IEEE 9-bus and 107 feature for IEEE 14-bus are given respectively in the tables 3&4.

8. Performance evaluation:

In the proposed method, three experts and one gating network are used which we consider it as MLPs. For MLPs evaluation we used : Learning rate for gating network is $\eta_g = 0.01$ and learning rate for experts networks are $\eta_e = 0.28$ and the number of iteration reaches 100. After training all the neural networks are trained with same input features which are parameters of transient stability assessment.
Performance of the developed ME can be gauged by calculating the error of the actual and desired test data. Firstly, error is defined as,

$$\text{Error}, E_n = \left|(\text{Desired output})_n - (\text{Actual output})_n\right| \quad (11)$$

Where, n is the test data number. The desired output is the known output data used for testing the neural networks. Meanwhile, the actual output is the output obtained from testing on the trained networks.

From equation (12), the percentage mean error, ME (%), can be obtained as:

$$\text{Percentage of Mean Error, Me}(\%) = \sum_{n=1}^{N} \frac{E_n}{N} \times 100 \quad (12)$$

Where N is the total number of test data.
The percentage classification error, CE (%), is given by,

$$\text{CE}(\%) = \frac{\text{No of misclassfied of the test data}}{N} \times 100 \quad (13)$$

We compare assessment methods in table 3&4 where we showed zero mean error and zero percent miss classification in ME method for both IEEE 9-bus and IEEE 14-bus systems.
Table 3&4 show ME testing results using the 29 & 107 input features the total error of misclassification and the mean error are both (0%).The MLPs result for transient stability assessment according to table 3 with IEEE 14-bus system, the total error of misclassification is 370 (56.97%and the mean error (53.2%) , too, with IEEE 9-bus, total error of misclassification is 4 (3.42%) , the mean error (0.0253) and the CNN result for transient stability assessment according to table 4 with IEEE 9-bus system the total error of misclassification is 1 (0.85%) and the mean error (0.0085).
Table 5 shows very suitable performance of the proposed method over other reported methods. The error rate of the proposed method reached to (0%) , which is a very demand improvement compared with other methods.

9. Conclusion

We should announce that ME proposed method in transient stability assessment has a very high reliability. When we compared with others methods namely MLP and CNN, the proposed ME method shows zero mean error and zero percent miss classification for IEEE 9-bus and IEEE 14-bus power systems, which assures very greats performance.

10. REFERENCES

1. Kundur , P. , Paserba ,J., Ajjarapu ,V., Anderson, G., Bose,A., Canizares ,C., Hatziargyriou ,N., Hill, D. tankovic ,A.,Taylor , C., Cutsem,T. , and Vittal, V. "*Definition and classification of power system stability"*, IEEE Trans.Power Syst., 3,(19): 1387–1401, 2004

2. Amjady , N. ,and Majedi ,S.F. "*Transient Stability Prediction by a Hybrid Intelligent System*", IEEE Trans. Power Syst, 3, (22):1275-1283, 2007.

3. Ebrahimpour, R., and Kazemi Abharian,E."*An Improved Method in Transient Stability Assessment of a Power System Using Committee Neural Networks*", IJCSNS, 9, (1):119-124, 2009

4. Bai , X., Jiang, T., Guo, Z.,Yan, Z., and Ni, Y. "*A unified approach for processing unbalanced conditions in transient stability calculations*", IEEE Trans. Power Syst., 21, (1): 85–90 , 2006

5. Amjady, N., and Ehsan, M. "*Transient stability assessment of power systems by a new estimating neural network"*, Can. J. Elect. Comp.Eng, 22, (3): 131–137,1997

6. Rovnyak, S., Kretsinger, S., Thorp, J. , and Brown, D. *"Decision trees for real-time transient stability prediction"* ,IEEE Trans. Power Syst., 9,(3) :1417–1426,1994

7. Liu, C.W., Su, C.W., Tsay ,S. S., and Wang,Y. J. "*Application of a novel fuzzy neural network to real-time transient stability swings prediction based on synchronized phasor measurements"*, IEEE Trans .Power Syst 14,(2): 685–692,1999.

8. Amjady , N. "*Application of a new fuzzy neural network to transient stability prediction"*,in Proc. IEEE PES Summer Meeting, San Francisco, CA, pp 69–76 ,Jun. 2005

9. Krishna, S. and Padiyar, K.R.*"Transient Stability Assessment Using Artificial Neural Networks"*, Proceedings of IEEE International Conference on Industrial Technology, pp.627-632, 2000.

10. Boudour, M., and Hellal, A. "*Combined Use Of Supervised And Unsupervised Learning For Power System Dynamic Security Mapping*", Engineering Applications Of Artificial Intelligence, 18, (6): 673-683, 2005

11. Sawhney, H., and Jeyasurya, B. "*On-Line Transient Stability Assessment Using Artificial Neural Network*", Large Engineering Systems Conference on Power Engineering, pp.76-80, 2004

12. Bahbah, A.G., and Girgis, A. A. *"New Method for Generators' Angles and Angular Velocities Prediction for Transient Stability Assessment of Multi machine Power Systems Using Recurrent Artificial Neural Network"*, IEEE Trans. Power Syst. ,2004, 19,(2):1015-1022, 2004

13. Abdul Wahab,N.I, Azah ,M., and Aini, H.*"An Improved Method in Transient Stability Assessment of a Power System Using Probabilistic Neural Network*, JAS R, 3,(11):1267-1274, 2007

14. Haykin, S. "Neural Networks: A Comprehensive Foundation", Prentice-Hall , 2nd edition, (1999)

15. Dailey, M.N., and Cottrell, G.W. *"Organization of face and object recognition in modular neural network models"*, Neural Networks, 12 , pp. 1053–1073, 1999

16. Ebrahimpour, R., kabir, E., and Yuosefi, M.R. *"Teacher-directed learning in view-independent face Recognition with mixture of experts using Single-view eigenspaces"*, Journal of the Franklin Institute 345 , pp. 87–101 ,2008

17. Racz, L.Z., and Bokay,B. *"Power System Stability"*, New York: ElsevierScience, (1988)

18. Milano, F.: 'Documentation for Power System An a l y s is T o o l b o x (P S A T)', http://www.power.uwaterloo.ca/~fmilano/downloads.htm. accessed 2008

19. Kundur,P. "Power System Stability and Control' , in The EPRI Power System Engineering Series ,McGraw Hill, (1994)

20. Mihrig, A. M. , and Wrong, M. D. "Transient stability analysis of multimachine power systems by catastrophe theory", Proc. Inst. Elect. Eng. C, 136, (4): 254–258 ,1989

21. Liu, C. W., Su, M. C., Tsay, S. S., and Wang, Y. J. "Application of a novel fuzzy neural network to real-time transient stability swings prediction based on synchronized phasor measurements", IEEE Trans.Power Syst., 14,(2): 685–692,1999

22. Amjady, N. "*Application of a new artificial neural network in transient stability assessment*", in Proc. IEEE Lescope Conf., pp. 126–132, , Halifax, NS, Canada, 1999

23. Sanyal, K. K., *"Transient Stability Assessment Using Neural Network"*. IEEE International Conference on Electric Utility Deregulation, Restructuring and PowerTechnologies, Hong Kong, pp. 633-637, 2004

24. Silveira, M.C.G., Lotufo, A.D.P., and Minussi, C.R. "*Transient stability analysis of electrical power systems using a neural network based on fuzzy ARTMAP*", Proc. IEEE Power Conference, Bologna, 2003

25. Wolpert,D.H., *"Stacked generalization"*, Neural Networks, 5, (2):241–2591992

26. Smyth, P., and Wolpert, D. H. *"Stacked Density Estimation"*, Neural Information Processing Systems 10, MIT Press, 1998

27. Michael, Y. H., and Tsoukalas, K. *"Explaining Consumer choice through neural networks: The stacked Generalization approach"*, European Journal of Operational Research 146,:650–660, 2003

28. Anderson, P.M. and Fouad, A.A. *"Power System Control and Stability"*, IEEE Press, 2nd Ed., USA, 2003

29. Ebrahimpour, R., kabir, E., and Yuosefi , M.R. *"Teacher-directed learning in view-independent face recognition with mixture of experts using overlapping eigenspaces"*, Computer Vision and Image Understanding , 111, pp 195–206, 2008

30. Gu'ler, I., and U'beyl˙, E.D. "*A mixture of experts networkstructure for modelling Doppler ultrasound blood "ow signals*" ", Computers in Biology and Medicine pp.1-18, 2004

31. Goodband, J.H. , Haasa, O.C.L., and Mills, J.A.: *"A mixture of experts committee machine to design compensators for intensity modulated radiation therapy",* Pattern Recognition, 39 ,pp. 1704 – 1714,2006

32. Jacobs, R.A., Jordan, M.I., Nowlan, S.E., and Hinton, G.E. *"Adaptive mixture of expert"*, Neural Comput, 3, pp.79–87, 1991

33. Moulin, L. S., Alves da Silva, A. P., El-Sharkawi, M. A., and Marks II, R. J.*"Support vector machines for transient stability analysis of large scale power systems"*, IEEE Trans. Power Syst., 19,(2):818–8252004

CALL FOR PAPERS

International Journal of Engineering (IJE) is devoted in assimilating publications that document development and research results within the broad spectrum of subfields in the engineering sciences. The journal intends to disseminate knowledge in the various disciplines of the engineering field from theoretical, practical and analytical research to physical implications and theoretical or quantitative discussion intended for both academic and industrial progress.

Our intended audiences comprises of scientists, researchers, mathematicians, practicing engineers, among others working in Engineering and welcome them to exchange and share their expertise in their particular disciplines. We also encourage articles, interdisciplinary in nature. The realm of **International Journal of Engineering (IJE)** extends, but not limited, to the following:

- Aerospace Engineering
- Agricultural Engineering
- Biomedical Engineering
- Chemical Engineering
- Civil & Structural Engineering
- Computer Engineering
- Control Systems Engineering
- Education Engineering
- Electrical Engineering
- Electronic Engineering
- Engineering Mathematics
- Engineering Science
- Environmental Engineering
- Fluid Engineering
- Geotechnical Engineering
- Industrial Engineering
- Manufacturing Engineering
- Materials & Technology Engineering
- Mechanical Engineering
- Mineral & Mining Engineering
- Nuclear Engineering
- Optical Engineering
- Petroleum Engineering
- Robotics & Automation Engineering
- Telecommunications Engineering

CFP SCHEDULE

Volume: 4
Issue: 2
Paper Submission: March 31 2010
Author Notification: May 1 2010
Issue Publication: May 2010

CALL FOR EDITORS / REVIEWERS

CSC Journals is in process of appointing Editorial Board Members for ***International Journal of Engineering (IJE)***. CSC Journals would like to invite interested candidates to join **IJE** network of professionals/researchers for the positions of Editor-in-Chief, Associate Editor-in-Chief, Editorial Board Members and Reviewers.

The invitation encourages interested professionals to contribute into CSC research network by joining as a part of editorial board members and reviewers for scientific peer-reviewed journals. All journals use an online, electronic submission process. The Editor is responsible for the timely and substantive output of the journal, including the solicitation of manuscripts, supervision of the peer review process and the final selection of articles for publication. Responsibilities also include implementing the journal's editorial policies, maintaining high professional standards for published content, ensuring the integrity of the journal, guiding manuscripts through the review process, overseeing revisions, and planning special issues along with the editorial team.

A complete list of journals can be found at http://www.cscjournals.org/csc/byjournal.php. Interested candidates may apply for the following positions through http://www.cscjournals.org/csc/login.php.

Please remember that it is through the effort of volunteers such as yourself that CSC Journals continues to grow and flourish. Your help with reviewing the issues written by prospective authors would be very much appreciated.

Feel free to contact us at coordinator@cscjournals.org if you have any queries.

Contact Information

Computer Science Journals Sdn BhD
M-3-19, Plaza Damas Sri Hartamas
50480, Kuala Lumpur MALAYSIA

Phone: +603 6207 1607
+603 2782 6991
Fax: +603 6207 1697

BRANCH OFFICE 1
Suite 5.04 Level 5, 365 Little Collins Street,
MELBOURNE 3000, Victoria, AUSTRALIA

Fax: +613 8677 1132

BRANCH OFFICE 2
Office no. 8, Saad Arcad, DHA Main Bulevard
Lahore, PAKISTAN

EMAIL SUPPORT
Head CSC Press: coordinator@cscjournals.org
CSC Press: cscpress@cscjournals.org
Info: info@cscjournals.org

COMPUTER SCIENCE JOURNALS SDN BHD
M-3-19, PLAZA DAMAS
SRI HARTAMAS
50480, KUALA LUMPUR
MALAYSIA